EFFECTS OF EPISODIC DROUGHTS AND FIRE ON THE CARBON CYCLE OF AMAZONIAN VEGETATION: FIELD RESEARCH AND MODELING OF A NEAR-TERM FOREST DIEBACK

By

PAULO MONTEIRO BRANDO

A DISSERTATION PRESENTED TO THE GRADUATE SCHOOL
OF THE UNIVERSITY OF FLORIDA IN PARTIAL FULFILLMENT
OF THE REQUIREMENTS FOR THE DEGREE OF
DOCTOR OF PHILOSOPHY

UNIVERSITY OF FLORIDA

2010

To my parents, my brother, and my friends

ACKNOWLEDGMENTS

I am most thankful to my advisor for his major influence on my intellectual development during my PhD. I also thank Daniel Nepstad for challenging every finding, word, and result I present here. Most of all, I thank all of those that rendered this thesis a synthesis of years of collaborative field research and modeling efforts. Among this very special group of people from several research groups I want to name a few: Eric Davidson, Mike Coe, David Ray, Britaldo Soares-Filho, Rafaella Silvestrini, Herman Rodrigues, Paul Lefebvre, Paulo Moutinho, Pieter Beck, Alessandro Baccini, Oswaldo Carvalho, Claudia Stickler, Scott Goetz, Wendy, Kingerlee, Marcos Costa, Ane Alencar, Adilson Coelho, Osvaldo Portella, Oswaldo Carvalho, Raimundo Quintino, Val, Osmar, Wanderley Rocha, William Riker, Darlisson Nunes, Bati, Sandro, Bibal, Marcia Macedo. Especial thanks to Ben Bolker, Mary Christman, Leda Kobziar, Wendell Cropper, Ted Schuur, Yadvinder Malhi, Scott Saleska, and Jennifer Balch for their various contributions to my dissertation. I thank Allie Shenkin, Fay Ray, and all my friends in Gainesville for their support during all these years and helping to make my experience in the United States an enjoyable one. The Instituto de Pesquisa Ambiental da Amazonia (IPAM) and Woods Hole Research Center (WHRC) provided essential institutional support for my PhD.

TABLE OF CONTENTS

page

LIST OF TABLES

LIST OF FIGURES

Abstract of Dissertation Presented to the Graduate School
of the University of Florida in Partial Fulfillment of the
Requirements for the Degree of Doctor of Philosophy

EFFECTS OF EPISODIC DROUGHTS AND FIRE ON THE CARBON CYCLE OF AMAZONIAN VEGETATION: FIELD RESEARCH AND MODELING OF A NEAR-TERM FOREST DIEBACK.

By

Paulo Monteiro Brando

August 2010

Chair: Francis Edward Putz
Major: Interdisciplinary Ecology

Climate change may cause decreased rainfall in Amazonia and move forests to large-scale dieback events. To inform debates about this issue, I evaluated the impacts of drought and fire on Amazonian vegetation. Using a throughfall exclusion experiment, I found that wood production was the most sensitive component of above-ground net primary productivity to drought and that aboveground carbon stocks declined by 32.5 Mg ha^{-1} over 6 years of the treatment. These results indicate that severe droughts can substantially reduce forest C stocks in the Amazon.

Based on a process-based model (CARLUC) that incorporates results from that partial throughfall exclusion experiment, I showed that total C stocks tended to increase between 1995-2004 (dry season) over the Amazon, corresponding to increases in photosynthetic active radiation. These results could partially explain the increases in biomass observed in the field over decades in the Amazon.

To clarify how the gross productivity of Amazonian is influenced by drought, I used improved MODIS-enhanced vegetation index measurements (EVI) to show that in densely forested areas of the Amazon, no climatic variable tested contributed to

explaining the high EVI inter-annual variability. Instead, I found evidences that suggest that production of new leaves could play an important role in the inter-annual EVI variability, but not necessarily in changes in vegetation productivity. These findings suggest that it still is unclear whether EVI can be employed as a tool to measure the vulnerability of tropical forests to drought.

Finally, I studied the mechanisms associated with fire-induced tree mortality in a tropical forests in the southern Amazon. I found that the presence of water in the bark reduced the differential in temperature between the fire and vascular cambium due to boiling water in the bark. Also, I show that experimental fires influenced mortality through several processes unrelated to cambium insulation, suggesting that several plant traits that reduce the negative and indirect effects of fire should also be considered in the assessments of tropical forests' vulnerability to fire.

In conclusion, I found evidence that droughts and fires exert strong influences on the terrestrial carbon cycling, but no evidences for imminent regime shifts in the region driven by climate change alone.

CHAPTER 1
INTRODUCTION

There is an urgent need for in-depth assessments of tropical forest vulnerability to global changes, a critical step for understanding and predicting ecological trajectories in the near future. Currently, it is clear that human-induced climate change are likely to cause dramatic changes in the world's tropical forests (Christensen et al. 2007). Many climate models predict that moderate to intense climate change will lead to large-scale dieback of forests by the end of the 21st Century (e.g., Cox et al. 2004). Large scale deforestation and widespread forest fires could exacerbate the negative effects of climate change on ecosystem services of Amazonian forests (e.g., water cycling) (Nepstad et al. 2008), causing the dieback of large portions of these forests much earlier than currently predicted.

The question of how much climate change is too much for the maintenance of tropical forest integrity remains unanswered (Malhi et al. 2008) but in my dissertation, I provide some of the information needed. Because global climate change coupled with deforestation is predicted to cause reductions in rainfall over portions of the Amazon (Malhi et al. 2008), I studied the effects of experimentally reduced rainfall on the aboveground net productivity (i.e., how much carbon is fixed by plants) of an eastern Amazonian forest in Chapter 2 of my dissertation. Although shortage of soil water availability will ultimately reduce the abilities of trees to fix carbon, based on currently available science, the thresholds at which reductions in soil water availability will cause major changes in forest functioning are not at all clear, nor are the mechanisms associated with disruption in forest functioning (e.g., carbon allocation to different parts of plants, tree mortality, soil respiration).

In Chapter 3, I modify an ecosystem model to include forest responses to drought that were observed in field experiments, but that are lacking in most (if not all) models employed to predict future trajectories of Amazonian forests (e.g., Cramer et al. 2001, Foley et al. 1998). For example, droughts are expected to alter allocation of C among leaves, trunks, and roots, which, in turn, can influence forest capacity to cycle carbon or to cope with drought-induced stress. But we know very little how this process will influence C-cycling during periods of severe droughts in the Amazon. Also, while most models assume that droughts will affect C assimilation only via reduced photosynthesis, there is strong evidences that episodic, severe droughts kill trees. After evaluating how these two processes may affect carbon C stocks in the Amazon, I evaluate the potential responses of Amazonian vegetation to climate oscillations during 1995-2005, in an attempt to reconcile field-based measurements (Phillips et al. 2009) and model predictions.

Given the report that the Amazon became “greener” during one of the strongest droughts over the last century and the consequent inferences about forest vulnerability to drought (Saleska et al. 2007), I found that there was a need to investigate what 'greener' means in terms of forest functioning. In Chapter 4 of my dissertation, I evaluated how a vegetation index used to measure the greening of the Amazon, derived from satellite-based measurements, correlated with variations in vegetation dynamics as measured by leaf area index, litterfall, vegetation phenology, and several climatic variables. I then investigated how this vegetation index varied across the Amazon and how these variations were associated with oscillations in climate.

The likelihood of trees being exposed to fire is increasing in the tropics due to synergistic interactions among droughts, forest degradation and fragmentation, and increased fire ignition (Alencar et al. 2006, Aragao et al. 2007, Nepstad et al. 2008), yet little is known about the characteristics that determine which trees survive and which succumb to understory fires. For example, while bark thickness appears to be the most important plant trait in preventing fire-induced damage (Barlow et al. 2003), its importance in preventing fire-induced tree mortality has not been widely tested for tropical forest trees and may be modulated by several other traits. In Chapter 5 of my dissertation, I use field experiments and model-based analyses to evaluate the influences of bark traits, plant size, and wood density on tree mortality following recurrent understory fires of varying intensity in a transitional forest of Mato Grosso.

While the Amazon may experience severe degradation due to synergistic interactions between drought and fire, the extent of these degradations is still poorly understood. Thus, the field experiments, data analyses, and model simulations run across different scales I employ in this dissertation should help to clarify how the Amazon region responds to drought and fire and how these responses will be expressed in the future under increasing drought conditions.

CHAPTER 2
DROUGHT EFFECTS ON LITTERFALL, WOOD PRODUCTION, AND BELOWGROUND CARBON CYCLING IN ANAMAZON FOREST: RESULTS FROM A PARTIAL THROUGHFALL REDUCTION EXPERIMENT.

Introduction

The fate of approximately 86-140 Pg of carbon contained in the forests of the Amazon (Saatchi et al. 2007) will depend, in part, upon the effect of drought episodes on the amount and allocation of forest biomass production. Several lines of evidences suggest that Amazon drought episodes may be more common and more severe in a warming world (Li et al. 2006).

One of the most important ways in which severe droughts influence tropical forest carbon stocks is through tree mortality. Droughts associated with ENSO events elevated tree mortality in East Kalimantan from a background of 2% to 26% yr^{-1} (Van Nieuwstadt and Sheil 2005), in central Amazonia from 1.1% to 1.9% (Williamson et al. 2000), Panama from 2% to 3% (Condit et al. 1995), and Sarawak from 0.9% to 4.3-6.4% (Nakagawa et al. 2000). (In one Panama forest, ENSO had no effect on tree mortality (Condit et al. 2004)). Experimentally-induced drought in one hectare of an east-central Amazonian forest permitted the identification of a threshold of declining plant-available soil moisture and cumulative canopy water stress beyond which canopy tree mortality rose from 1.5% to 9% (Nepstad et al. 2007).

Responses of net primary productivity (NPP) and its allocation during drought may have important influences on carbon stocks, but remain poorly understood in moist tropical forests (Houghton 2005). Seasonal and inter-annual variation in the NPP of moist tropical forests is controlled mostly by changes in light and soil moisture (Clark and Clark 1994). Hence, NPP increases during ENSO events, when reduced cloud

cover increases photosynthetically-active radiation without provoking soil moisture deficits large enough to inhibit photosynthesis. When soil moisture is in short supply, NPP may decline and its relative allocation among leaves, stems and roots may be affected, but our understanding of these responses is poor. Stem growth is expected to be the most sensitive component of NPP to drought because it is low on the carbon allocation hierarchy (Chapin et al. 1990).

The response of root production to drought is less clear, in part because of substantial methodological challenge of mensuration (Trumbore et al. 2006). Soil respiration, which integrates CO_2 production from all belowground sources, including root respiration and leaf litter decomposition, tends to be lower in the dry season compared to the wet season (Davidson et al. 2004, 2000, Saleska et al. 2003); this is probably due largely to seasonal variation of heterotrophic respiration in the litter layer. Responses to long-term drought treatments may also include changes in root production.

A seven-year, partial throughfall exclusion experiment was conducted in east-central Amazonia to examine forest responses to a 35-41% effective reduction in annual rainfall. I quantified forest LAI litterfall, wood production, soil respiration, and the $\delta^{13}C$ and $\Delta^{14}C$ composition of CO_2 emitted from the soil in one-hectare treatment and control plots to test the following predictions: wood production is the most responsive component of aboveground NPP to drought, declining rapidly with the onset of drought stress; litterfall increases initially through drought-induced leaf shedding, then declines to below non-treatment levels as LAI stabilizes at a lower level; and, soil CO_2 efflux is

affected by responses of multiple processes of heterotrophic and autotrophic respiration, which could have either accumulating or canceling effects.

Methods

Site Description and Treatment Design

The experiment was carried out in the Tapajós National Forest, Pará, Brazil (2.897^{o}S,54.952^{o}W). Annual precipitation ranges from 1700-3000 mm and averages ~ 2000 mm, with a 6 mo dry season (Jul-Dec) when rainfall rarely exceeds 100 mm mo^{-1}. Mean annual temperature is 28^{o} C (min 22^{o}C, max 28^{o}C). The soil is deeply weathered Haplustox. The depth to water table at a similar site 12 km away was >100 m, which means that the stocks of soil water availability to trees is recharged by rainfall.

The throughfall exclusion experiment was carried out in two structurally and floristically similar one-ha plots: an 'exclusion plot' (treatment) and a 'control plot'. In the exclusion plot, approximately 34-40% of annual incoming precipitation was diverted from the soil (70% of throughfall) during the 6-mo wet season from 2000 to 2004. Details of the experimental design can be found in Nepstad et al. (2002). Please see (Hurlbert 1984) for more information on large-scale unreplicated experiments.

Soil water to 11-m depth was measured monthly in five deep soil shafts per plot between 1999 and 2005 using time domain reflectometry (TDR; (Jipp et al. 1998)) . Here I present volumetric water content (VWC) for two depth intervals: 0-200 cm (upper soil profile); and 200-1100 cm (deep soil profile).

Aboveground NPP, Tree Mortality, and Soil CO_2 Efflux

Dendrometer bands were installed on trees ≥ 10 cm dbh (diameter at 1.3 m or above buttresses) and vines > 5 cm dbh in the exclusion (342 individuals) and control plots (409 individuals). Diameter increment was monitored monthly between 2000 and

2005 using an electronic caliper from which relative stem diameter growth was calculated. Wood production at the plot-level was calculated by summing biomass estimates for trees and lianas determined using the allometric equations from (Chambers et al. 2001) and (Gerwing and Farias 2000), respectively. I also calculated individual annual stem growth averaged for small (10 to 20 cm dbh (trees) and 5 to 20 cm dbh (lianas)) and large (>20 cm dbh) stems. Ingrowth stems were added as they exceeded the lower dbh threshold. Mortality of stems > 10 cm dbh in both plots was assessed on an individual basis monthly between 1999 and 2005 and is described in (Nepstad et al. 2007). Litterfall was collected bi-weekly from 1999 to 2005 from ~ 64 mesh traps (0.5 m^2) on a systematic grid in the understory of both plots. Leaf area index (LAI) was estimated indirectly monthly at these same points using two LiCor 2000 Plant Canopy Analyzers (LI-COR, 1992) operating in differential mode. Above-ground NPP was calculated as the sum of wood production and litterfall biomass in each year of the study (2000 to 2005) according to the methodology of Clark et al. (2001). A manual dynamic chamber system was used to measure soil CO_2 efflux on 18 chambers per treatment per date, as described by Davidson et al. (2004). Carbon isotope measurements were determined for soil respiration on 5 occasions from 2000 to 2005.

Statistical Analysis

I used a repeated measures design to test for year-to-year differences between plots for stem growth (using initial dbh as a covariate), LAI, litterfall, and soil CO_2 efflux. Changes in mortality were assessed using a generalized linear model with binomial errors. The relationships among, VWC, ANPP, and LAI, were tested using linear regressions.

Results

Soil Water

Prior initiation of treatment, VWC was 25 and 62 mm lower in the exclusion plot than the control plot for the upper (0-200 cm) and deeper (200-1100 cm) soil profiles, respectively (Figs. 2-1, 2-2). After three periods of partial throughfall exclusion (2002), VWC was 97 and 272 mm lower in the exclusion plot than the control plot in the upper and deeper soil profiles, respectively. The difference in VWC between plots did not continue to increase in 2003 for two reasons. First, natural precipitation was well below normal that year (Fig. 2-2), so that soil water was not fully recharged in the control plot. Second, drought-induced mortality in 2003 (see Mortality and Necromass section below) may have reduced transpiration in the exclusion plot.

Mortality and Necromass

From 2000 to 2005, the annual mortality rate of individuals ≥ 10 cm dbh was significantly higher in the exclusion plot (5.7% yr^{-1}) than in the control plot (2.4% yr^{-1}); 2001 was an exception to this general trend (Fig. 2-3A). The most dramatic treatment effects were observed in 2002 and 2003, when the annual rate of mortality in the exclusion plot reached 7.2% yr^{-1} and 9.5% yr^{-1}, respectively, as reported in Nepstad et al. 2007. Mortality was also significantly higher in the exclusion (7.2 yr^{-1}) than the control plot (3.1% yr^{-1}) after the termination of the experimental throughfall exclusion, in 2005.

The spike in treatment induced mortality in 2002 and 2003 led to a 25% reduction in above-ground live biomass (AGLB) in the exclusion plot relative to the control plot (Fig. 2-3B), a difference which remained stable after the exclusion treatment was terminated in August 2004 and through the end of 2005. From 2000 through 2005,

47 Mg ha^{-1} more necromass [dead biomass] was produced in the exclusion compared to the control plot (Fig. 2-4D).

Stem Growth and Wood Production

The treatment caused a reduction in relative stem diameter growth of large individuals ($P<0.001$) yet had no effect on smaller stems (Fig. 2-5A,B,C), which were growing less in the exclusion plot than the control plot before the treatment was applied ($P=0.322$; Fig. 2-5B). Later, following the pulse in mortality of large trees in 2003, I observed increased stem growth in small individuals in the exclusion plot relative to the control plot ($P<0.001$). During this same period (2004 to 2005), stem growth was declining in the control plot (Fig. 2-5A,B,C), perhaps as a lagged response to low annual precipitation in 2003 (Figs. 2-1C, 2-2).

Total wood production during the first exclusion period (2000) was 13% lower in the exclusion (4.87 Mg ha^{-1} yr^{-1}) than in the control plot (5.61 Mg ha^{-1} yr^{-1}). This difference increased over the treatment period to 46%, 63%, and 58% in 2001, 2002, and 2003, respectively (Fig. 2-4B). After the drought treatment was removed in 2005, the difference in biomass production between plots declined to 23% due to an increase in individual tree growth (mostly small trees) in the exclusion plot and a decrease in growth in the control plot.

Litterfall and Carbon Dynamics

The drought treatment also reduced LAI over time (Fig. 2-6A; $P<0.001$). Differences between plots in LAI were small during the two first years of the study, followed by a larger drop in 2002 and remaining 21% to 26% lower than the control-plot through 2005.

Litterfall, which was higher in the exclusion plot than the control prior to the initiation of the treatment, declined in the exclusion plot compared to the control. However, it was lower in the exclusion plot than the control plot only in 2003 (23%, $P<0.001$; Fig. 2-4A). During the last year of the treatment (2004) differences in litterfall between plots were reduced to 10%, and, after the drought stress was removed (2005), litterfall was 2% higher in the exclusion plot than the control plot, indicating a relative increase in litterfall in the exclusion plot compared to the control ($P<0.001$).

ANPP

ANPP progressively declined in the exclusion plot relative to the control from 2000 to 2003: 12%, 30%, and 41% lower in 2001, 2002, and 2003, respectively (Fig. 2-4C). In the last year of the treatment (2004) and in 2005, when the exclusion treatment was removed, ANPP differences between plots were diminished to 30% and 10% of the control, respectively. The average reduction in ANPP from 2000 to 2005 was 21%, corresponding to a cumulative difference between plots of 17 Mg ha^{-1}.

Correlates of ANPP and LAI

Annual variations in VWC in the upper soil profile (0-200 cm) explained 51% of the variation in ANPP over the 6-yr study period (Fig. 2-7A). Annual average LAI showed a strong positive linear relationship with VWC (R^2: 92%; $P<0.001$; Fig. 2-7B), and with ANPP (R^2: 49%; $P=0.006$; $\ln(ANPP) = -0.9995 + 0.8362 * \ln(LAI)$).

Soil CO2 Efflux

The effect of throughfall exclusion treatment on soil CO_2 efflux was not consistent among years or seasons. Although there was a significant treatment-by-year interaction ($p < 0.001$), the treatment-by-year-by-season interaction was not significant ($p = 0.65$). When large pulses were measured, which were probably related with recent wetting

events, they tended to be higher in the control plot (Fig. 2-8A). The exclusion plot had somewhat higher CO_2 efflux rates on most of the other dates during the exclusion treatment years. These differences largely cancelled, resulting in nearly identical estimates of average annual CO_2 efflux from the two plots during the 5-year exclusion period (12.8 ± 1.0 Mg C ha^{-1} yr^{-1} in the exclusion plot and 12.8 ± 1.3 Mg C ha^{-1} yr^{-1} in the control plot).

The ^{13}C signature of the soil CO_2 efflux revealed a divergence between treatments in 2004, when the $^{13}CO_2$ increased (became less negative) in the exclusion plot (Fig. 2-8B). A similar difference in foliar $\delta^{13}C$ had been observed for some species in 2002 (J. Ometto and J. Ehleringer, pers. comm.). I also observed a similar difference in $\delta^{13}CO_2$ measured within the soil profile in 2003 (not shown), which would reflect allocation of fractionated C substrates to root respiration.

There were no differences between treatment plots in $^{14}CO_2$ signatures on any date (Fig. 2-8C), which suggests that the relative age of respired C substrates was not altered by the exclusion treatment. These radiocarbon values are 10-25 ‰ greater than values for CO_2 in ambient air sampled at the same time. This indicates that the C being respired is a mixture of modern C substrates with substrates that are 5-40 years old and are more enriched in ^{14}C due to the signal of atmospheric testing of nuclear weapons in the 1950s and 1960s (Trumbore et al. 2006).

Discussion

Response and Recovery of ANPP

The most striking result of this study was the differential response of wood production and litterfall to throughfall exclusion. Wood production in the exclusion plot was 13 to 62% below that of the control plot during each of the five treatment years,

while litterfall was substantially lower than the control plot (23%) only during the year of lowest rainfall, in 2003. The allocation of ANPP to wood and litterfall was therefore highly sensitive to soil moisture availability. At the beginning of the experiment (2000) wood and litterfall comprised 40 and 60%, respectively, of the total ANPP, while in the third year of the exclusion (2002), they were 29 and 71% of the ANPP, respectively. This finding provides an important exception to the widely-held assumption of drought-insensitive allocation of ANPP between litterfall and wood, as represented in many ecosystem models (e.g., Hirsch et al. 2004, Potter et al. 2001, Tian et al. 1998). These results also run contrary to the positive response of LAI to short-term drought that has been postulated for Amazon forests based upon remotely-sensed (MODIS) estimates of LAI (Huete et al. 2006, Myneni et al. 2007, Saleska et al. 2007). If such a positive response is real and widespread, it may be overridden as drought severity grows. However, it is important to remember that our throughfall exclusion treatment did not simulate the higher radiation that is typically associated with lower rainfall.

Litterfall and wood production recovered rapidly following cessation of the drought. Despite the death of 9% of all trees ≥10 cm dbh in 2003, litterfall recovered fully during the first post-treatment year (2005) and wood production, which was 42% of the control plot in 2003, climbed to 77% that of the control plot in 2005. This rapid recovery is partially explained by the positive growth responses observed for residual, surviving trees following the death of neighboring individuals, perhaps attributable to reduced competition for light and soil moisture resources. LAI declined in the exclusion plot in 2003 and 2004, increasing light availability in the understory; the difference in VWC between exclusion and control plots also diminished, in part because of reduced

transpiration associated with tree mortality . A second litterfall recovery mechanism was the establishment of fast-growing trees in the exclusion plot understory (P. Brando, D. Nepstad, unpublished data). Increased soil nutrient availability associated with tree mortality may have also contributed to the accelerated growth of surviving trees and the establishment of fast-growing trees.

The rapid recovery of litterfall in 2004 and after the treatment ended in 2005 was, surprisingly, not accompanied by a recovery of LAI. The relationship between LAI and litterfall was similarly unexpected throughout the experiment since litterfall remained high, with a small decline in 2003, despite the sharp, sustained decline of LAI beginning in the third year of the treatment (2002). LAI declined in response to drought with little effect on litterfall either through a lower specific leaf area or through a shortening of leaf longevity or both.

Drought-induced tree mortality and reductions in wood production resulted in a 63 Mg ha^{-1} reduction in AGLB that persisted through the first post-treatment year. The long-term recovery of pre-treatment AGLB will depend upon the balance between wood production and tree mortality. The latter declined to the level of the control plot during the post-treatment year, and could decline further if the drought treatment accelerated the death of trees that were already senescent and prone to die in the near future. Post-treatment, tree-level increases in stem diameter growth contributed to an acceleration of wood production that, if it continued, could also reduce the time required to recovery pre-treatment AGLB.

In sum, the experimental drought caused a rapid and drastic reduction in aboveground wood production, while litterfall was less strongly affected. By the third

year of the exclusion treatment in 2003, a reduction in litterfall coincided with increased mortality of large trees in the exclusion plot relative to the control plot, suggesting that available soil water had fallen below a minimum threshold required to sustain minimal physiological processes (Nepstad et al. 2007). Although the response of plants to soil water depletion may have been initially delayed due to the several coping strategies plants use to avoid or tolerate drought (Oliveira et al. 2005), increased mortality and reductions in forest growth resulted in a 24% reduction in ANPP by the end of the experiment, which was highly correlated with a decline in volumetric water content and LAI.

Belowground Carbon Accumulation

Heterotrophic soil respiration can be inhibited by drought either directly through microbial drought stress or indirectly through substrate limitation (Davidson et al. 2006), which is consistent with observations of lower soil CO_2 efflux rates during the dry season in Amazonian forests (Davidson et al. 2000, 2004; Saleska et al. 2003). On the other hand, it is also possible that increased allocation of C to fine roots could be an adaptation to explore for deep water resources (Nepstad et al. 1994), which might increase belowground inputs of C as a response to drought. The depletion of soil moisture proceeds from the litter and upper mineral soil layers, where root systems are concentrated, to deeper (>8 m in about 1/3 of the Amazon) soil layers (Jipp et al. 1998; Nepstad et al. 1994). New root growth therefore occurs at progressively deeper soil layers during drought episodes and may be inhibited near the soil surface by the lack of available moisture. These plausible responses that differ in sign may help explain the lack of a consistent and significant treatment effect on soil CO_2 efflux. Either there were no changes in belowground C cycling processes, or the changes that did occur

cancelled with respect to CO_2 production, thus resulting in nearly identical average annual CO_2 efflux rates.

The isotope data shed some light on these possibilities. First, the ^{13}C data demonstrate that C fixed by drought-stressed leaves, which is more enriched (less negative) in ^{13}C than in the control plot, was transported to the soil and/or forest floor by litterfall and/or root respiration and root inputs. Hence the heavier ^{13}C signatures of C respired in 2004 could reflect the decomposition of enriched-^{13}C leaf litter produced the 1-2 years previously, a contribution of heavier ^{13}C in root respiration reflecting drought stress effects on photosynthetic fractionation, or both. However, the two-year lag between fractionation of fresh foliage in 2002 and the first detection of that isotopic signal in surface CO_2 efflux in 2004 suggests that decomposition of aboveground litterfall rather than root respiration (which would reflect the isotopic signature of current year's photosynthate) dominates the surface CO_2 efflux.

The ^{14}C data demonstrate that there was no significant shift in the relative age of respired CO_2 as a result of the drought treatment. In other words, the relative contributions of respiration from young substrates (root respiration and microbial respiration of exudates and fresh leaf and root litter) and older substrates (root, leaf, and wood litter and soil organic matter that has persisted 5 years) did not change appreciably. Rhizosphere respiration typically has a ^{14}C signature that matches the atmospheric $^{14}CO_2$ of the same year, so that an increase in allocation to roots in an amount necessary to offset a reduction in CO_2 derived from older litter decomposition in the exclusion plot would have reduced ^{14}C values overall. Likewise, had there been significant changes in decomposition rates of soil carbon stocks with higher ^{14}C values

(leaf and root litter and soil organic matter; Trumbore et al. 2006), we should have detected a change in the radiocarbon signature. Hence, we see little evidence of significant changes in belowground C cycling processes induced by the drought treatment. Responses to natural seasonal droughts, which temporarily reduce respiration (Saleska et al. 2003), should not be confused with responses to longer-term droughts, which may or may not alter annual rates of C inputs to and turnover times within the soil. These results highlight the danger of extrapolating short-term metabolic responses to longer-term ecosystem level responses that potentially involve changes in C allocation, mortality, and growth.

Carbon Stock Accumulation and Forest Recovery

Partial throughfall exclusion induced reduction in AGLB points to the potential for severe and intense droughts predicted for the Amazon basin to increase carbon emissions to the atmosphere. Even mild droughts, such as those induced during the first year of exclusion, can inhibit wood production and, hence, the long-term pattern carbon storage in this forest ecosystem. This finding has important implications regarding reports that many Amazon forest appear to be undergoing net carbon uptake (Baker et al. 2004, Grace et al. 1995, Phillips et al. 1998, Phillips et al. 2009)— a finding that has been met with some skepticism (Clark 2002, Saleska et al. 2003). Reductions of rainfall in regions of strong seasonal drought, comprising nearly half of the Amazon's forests (Nepstad et al. 2004), may reduce wood production, diminishing or reversing the net uptake of carbon from these ecosystems.

The long-term effect of the 63 Mg ha^{-1} reduction in AGLB on aboveground carbon stocks will depend upon the complex balance between ABLG regrowth and the rate at which trees killed by the drought decompose. Many factors influence ABLG re-

accumulation, including tree mortality rate, wood production rate, and the wood density of the trees that eventually replace those killed by drought stress. Forests recovering from slash-and-burn agriculture in the Venezuelan Amazon required approximately two centuries to recover pre-disturbance carbon stocks in part because of shifts in species composition (Saldarriaga et al. 1988). The decline of LAI and AGLB observed in this study also suggest that the positive feedback between drought and fire may be stronger than previously hypothesized (Nepstad et al. 2001), which could have large long-term implications for carbon storage. Hence, even this relatively long-term, 5-year experimental manipulation was not long enough to investigate the full effects of climate change on carbon stocks of Amazonian forests. Nevertheless, we have demonstrated that multi-year drought induced substantial losses of aboveground biomass and productivity.

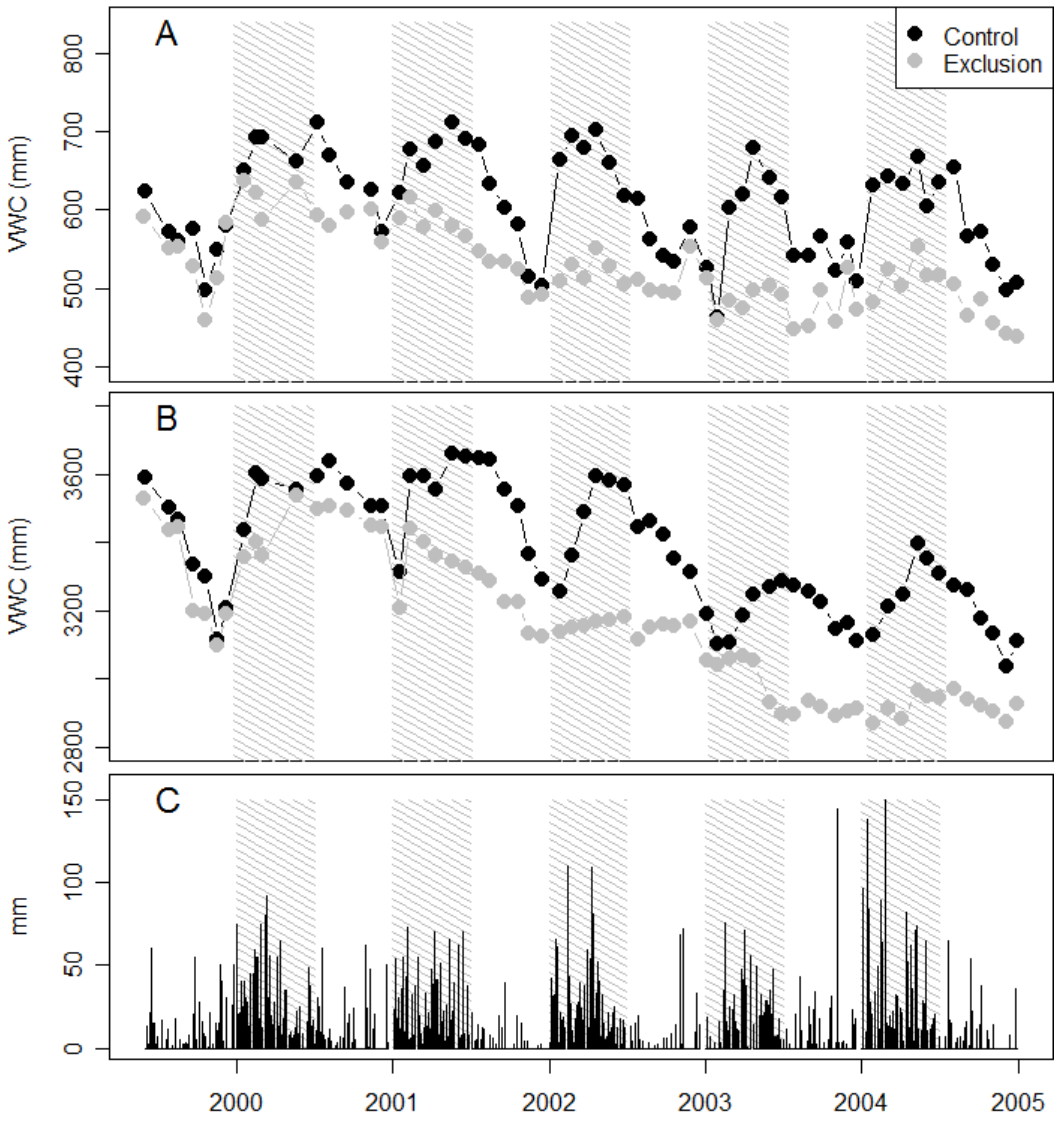

Figure 2-1. Soil volumetric water content (VWC) integrated from 0 to 200 cm (A) and from 200 to 1100 cm (B) and daily precipitation (C). Measurements were taken from August 1999 to December 2004.

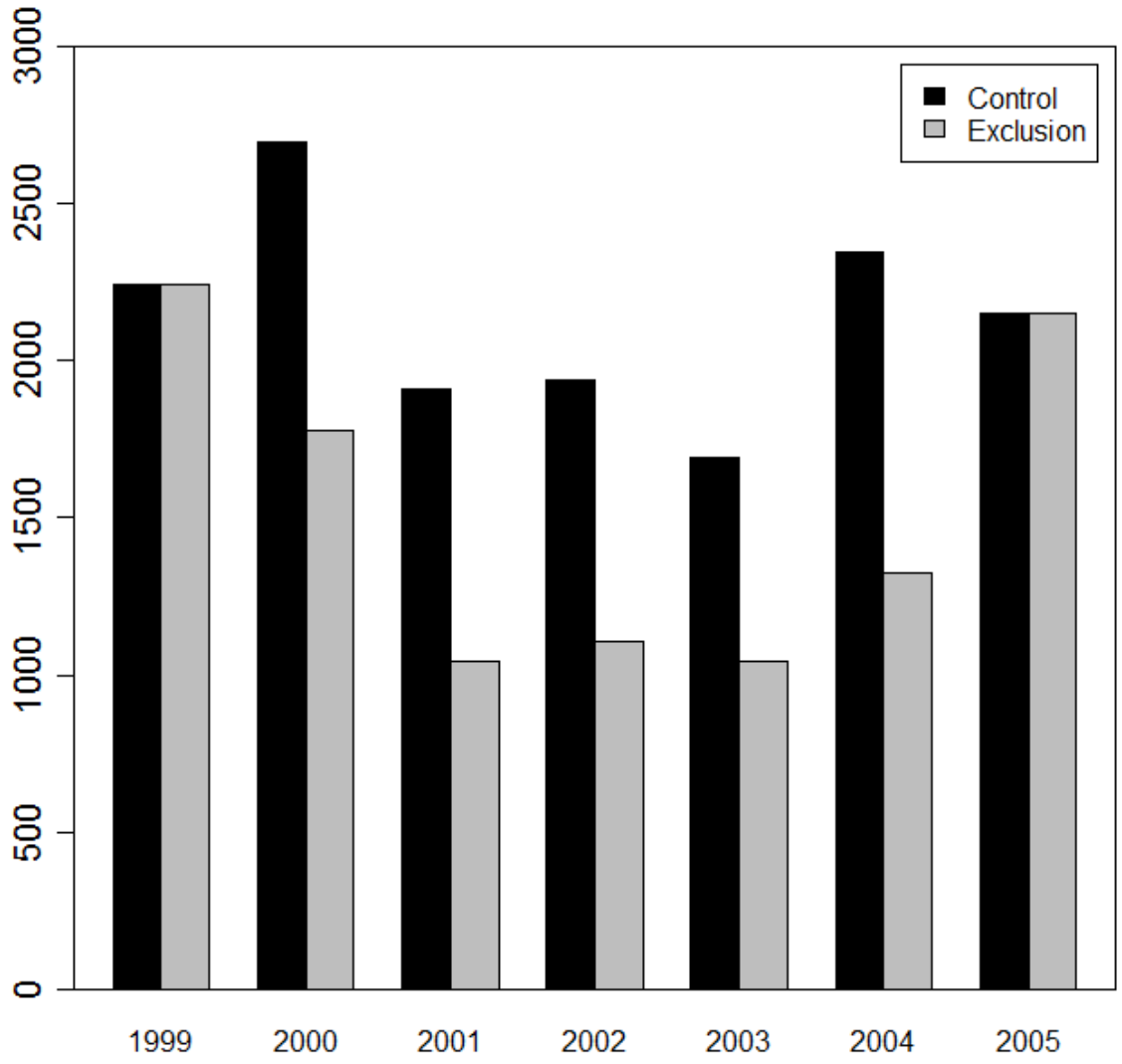

Figure 2-2. Annual rainfall (control plot) and effective rainfall (annual rainfall minus water excluded by the plastic panels during the wet season). The partial throughfall exclusion treatment was carried during the six-month wet season each year beginning in January 2000 and ending in August 2004.

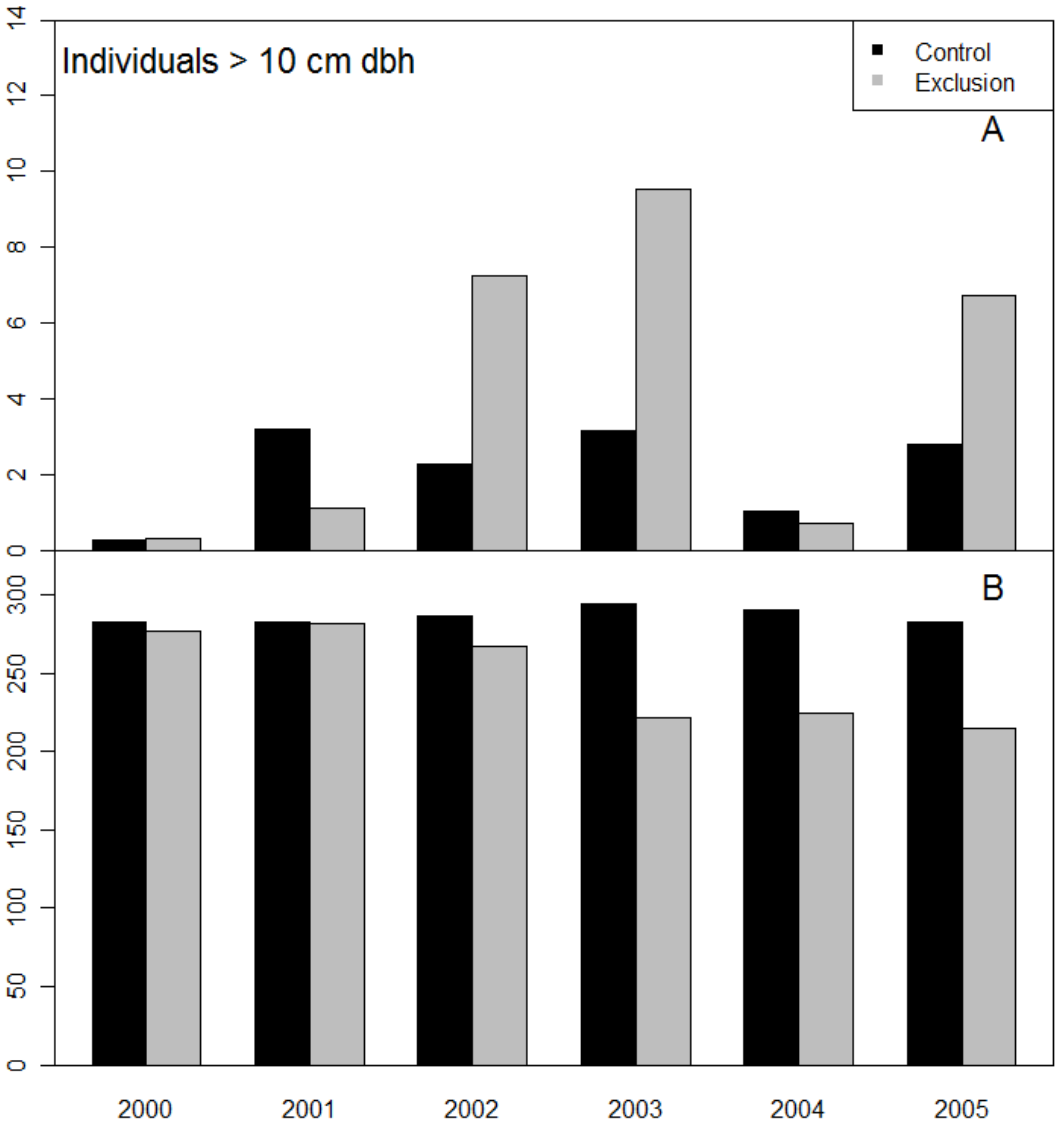

Figure 2-3. Upper panel: annual percent of mortality measured on an individual basis for all individuals ≥ 10 cm dbh in the exclusion and control plots from December 2000 to December 2005. Lower panels: above-ground standing live biomass (AGB Live) of all individuals ≥ 10 cm dbh for the exclusion and control plots during the same period.

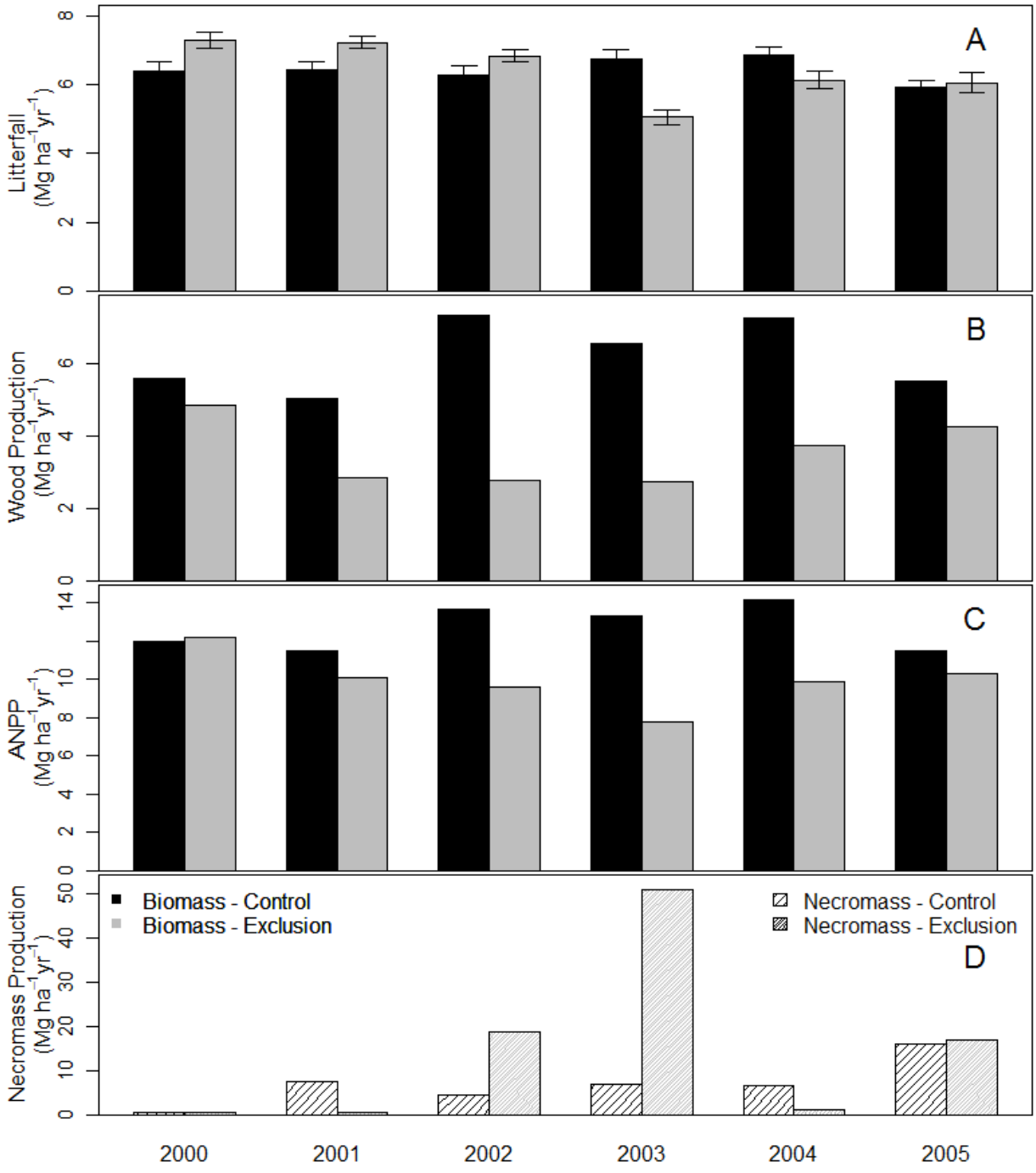

Figure 2-4. Annual trends in the exclusion and control plots of: A) litterfall; B) wood production; C) above-ground net primary productivity (ANPP); and D) necromass production. Measurements were taken from January 2000 to December 2005. Units are Mg ha^{-1} yr^{-1}. Error bars (± 1 SE) are presented only for litterfall.

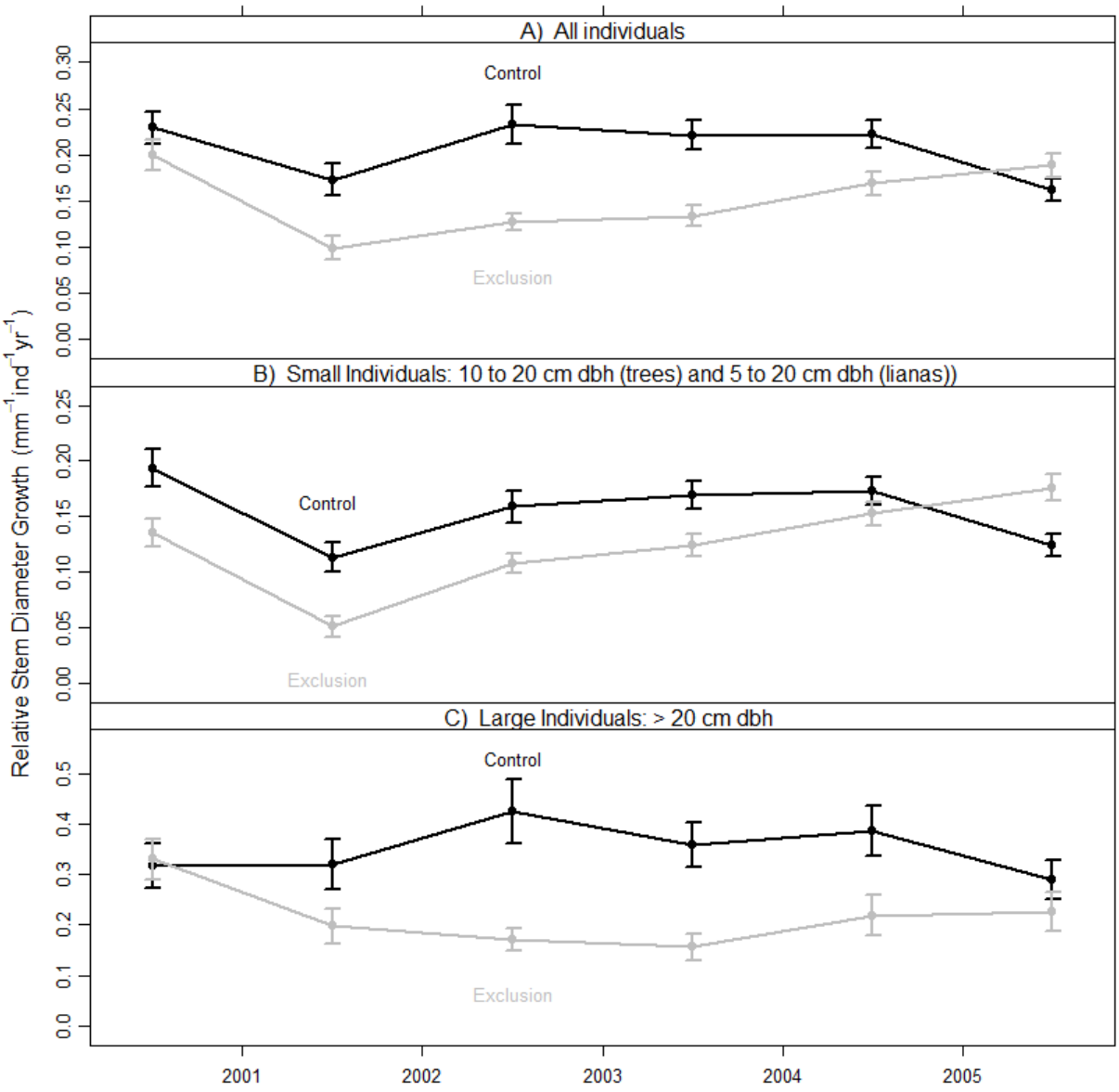

Figure 2-5. Stem growth of individuals in the exclusion and control plots by different size classes: A) > 20 cm dbh; B) between 5 (lianas) 10 (trees) and 20 cm dbh; and C) > 5 cm dbh (lianas) and > 10 cm dbh (trees). Error bars indicate ± SE (N is given by the number individuals). Measurements were taken from December 1999 to December 2005. Annual stem growth was calculated as the difference in dbh measured between two sampling intervals (December of each year).

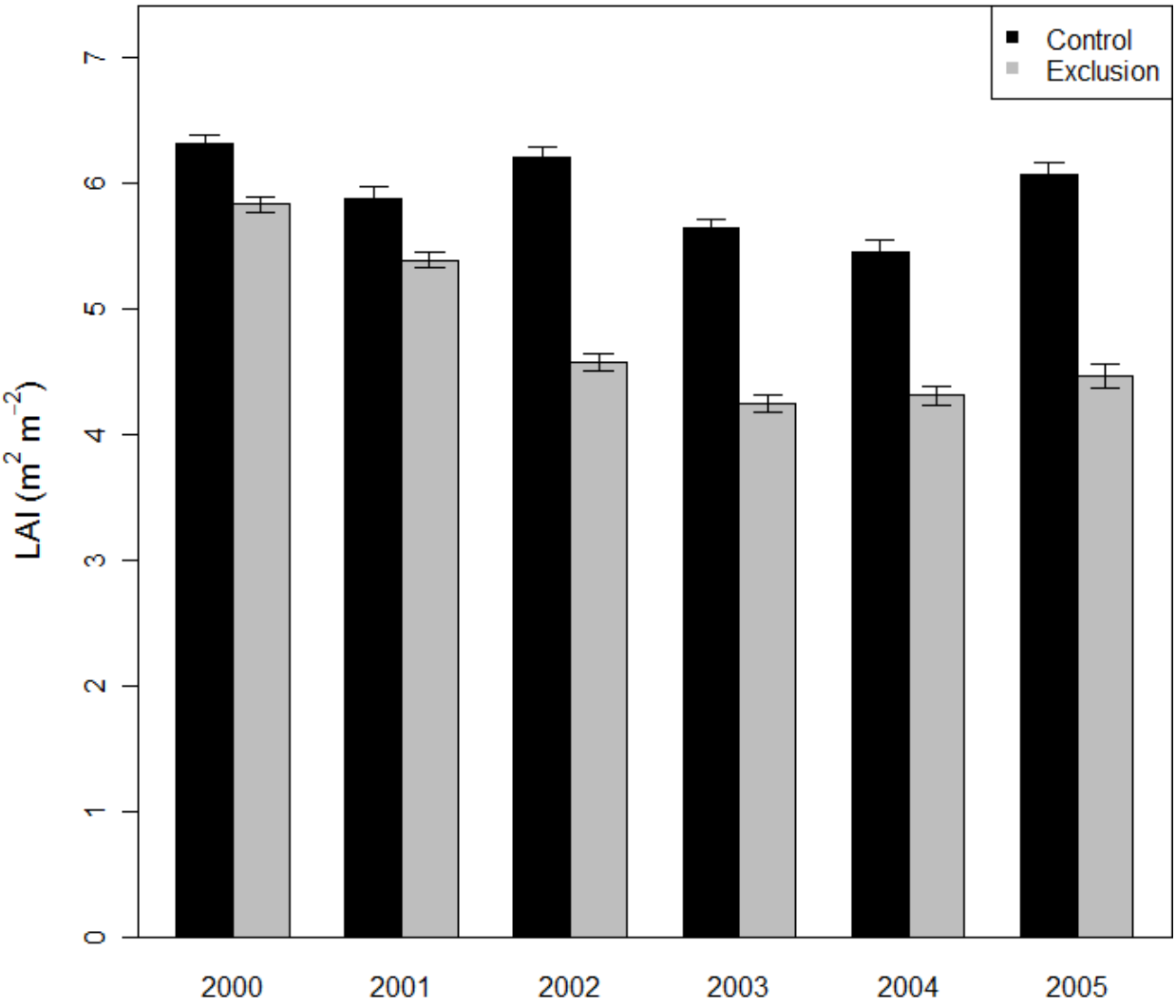

Figure 2-6. Annual trends in the exclusion and control plots of leaf area index (LAI). Measurements were carried out from January 2000 to December 2005. Error bars for LAI indicate ± SE.

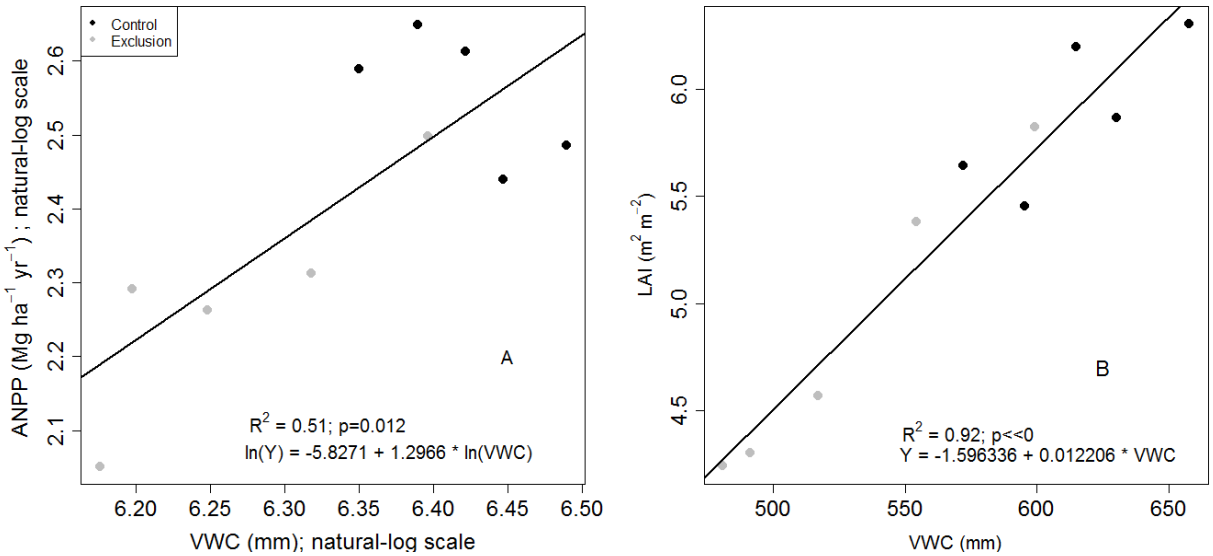

Figure 2-7. Relationships between annual mean VWC measured in the upper soil profile (0 – 200 cm) and A) above-ground net primary productivity (ANPP) and B) leaf area index (LAI). Data represents annual means from January 2000 to December 2004.

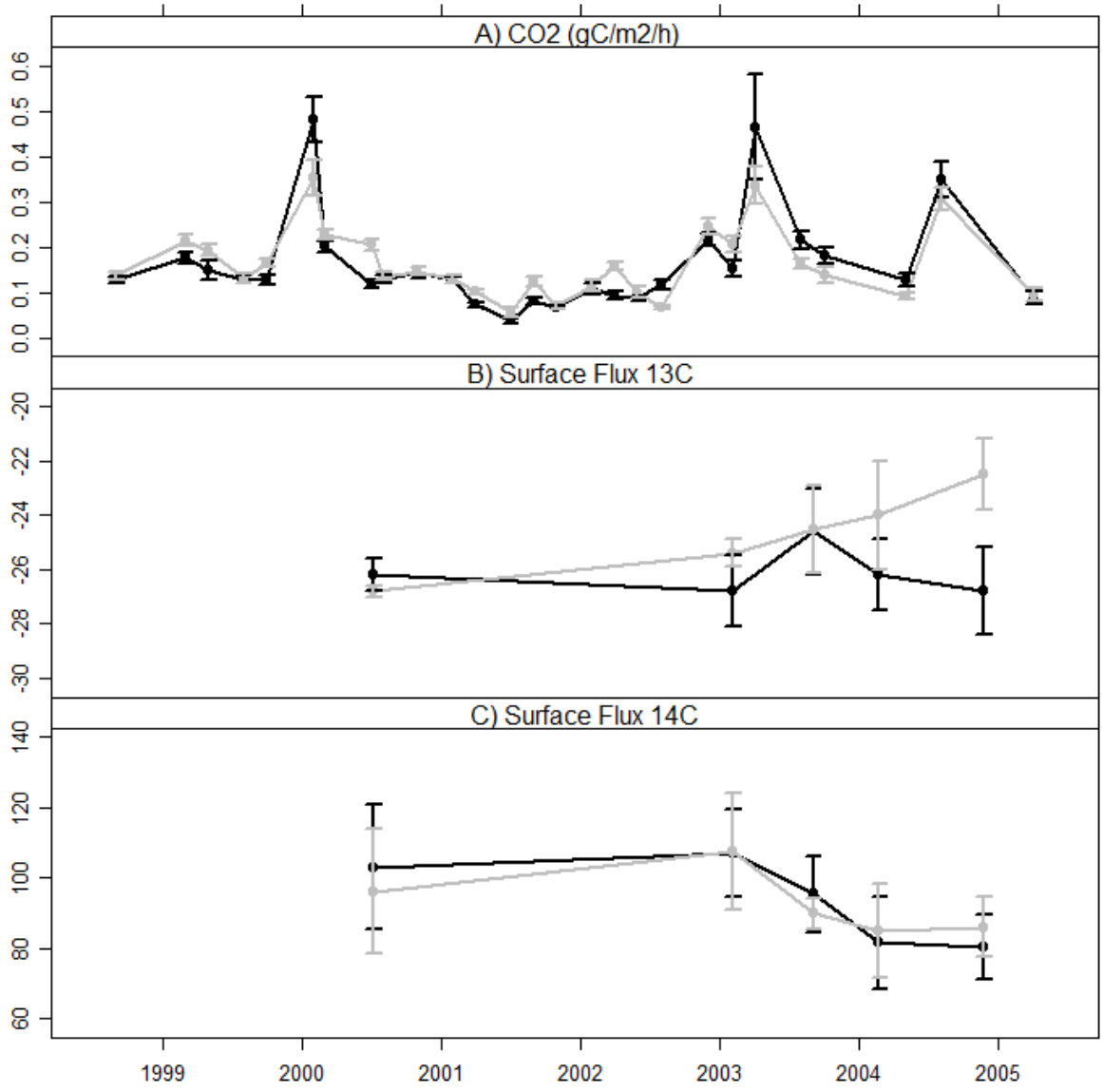

Figure 2-8. Measurements of surface flux of carbon dioxide, $\delta^{13}C$, and $\Delta^{14}C$ in the exclusion (grey) and control plots (black). The error bars represents standard errors of the mean.

CHAPTER 3
EVALUATING THE RELATIONSHIPS BETWEEN INTERANNUAL CLIMATIC VARIABILITY AND ABOVEGROUND CARBON STOCKS IN AMAZONIA

Introduction

Climate change is projected to have major impacts on tropical forest metabolism and carbon stocks (Bonan 2008). In Amazonia, increases in atmospheric CO_2 concentrations may stimulate vegetation productivity (Lloyd & Farquhar, 2008), but the drier and warmer conditions resulting from these increases may ultimately render the region susceptible to late-century diebacks, according to predictions of climate-dynamic vegetation global models (Cox et al. 2000, Cramer et al. 2001, Nobre et al. 1991). If predicted diebacks do occur, a large amount of the 80-120 Gt of C stored in forests of the Amazon will be released to the atmosphere (Betts et al. 2004, Cox et al. 2004). Moreover, this occurrence may lead to a positive feedback loop, hastening further climate warming and drying (Costa and Foley 2000).

The responses of Amazonian forests to drier and warmer climatic conditions remains controversial. One outstanding issue relates to the large uncertainties about the the intensity of drought needed to provoke widespread forest dieback across the Amazon Basin (Malhi et al., 2009). While field-based studies have shown that episodic droughts associated with climatic cycles are capable of causing increased mortality of large trees in the tropics (Condit et al. 1995, Nakagawa et al. 2000, Van Nieuwstadt and Sheil 2005, Williamson et al. 2000), recent satellite-based studies suggest that Amazonian forests could be more drought resistant than previously thought (Saleska et al. 2007). Indeed, there is strong evidence that forest photosynthesis (gross primary productivity, GPP) increases at least during early stages of drought because of higher

photosynthetically active radiation, but decreases when thresholds in plant available soil moisture cause increased tree mortality and reduced tree growth (Poulter et al. 2009).

Findings from two throughfall exclusion experiments carried out in moist tropical forest systems of the Brazilian Amazon (Tapajos and Caxiuana National Forests) have helped identify drought thresholds that could cause major changes in vegetation metabolism and structure (Fisher et al. 2007, Meir et al. 2009, Nepstad et al. 2002). In both experiments, net primary productivity (NPP), light saturated photosynthetic rates, and leaf area index (LAI) all declined in response to drought treatment (i.e., 50% wet-season throughfall exclusion) of 2-3 years. Following protracted water stress, substantial increases in tree mortality rates were observed, corresponding to reductions in plant available water (Brando et al. 2008, Nepstad et al. 2007). If the general responses of Amazonian forests to drought are similar to those observed in the Caixuana and Tapajos Forests, a drier future climate is likely to have major effects on the physiology and carbon stocks.

In 2005, the southwestern Amazon experienced one of the most severe droughts of the last century (Aragao et al. 2007, Marengo et al. 2008, Zeng et al. 2008). This exceptionally dry and hot period, caused by an anomalously warm tropical North Atlantic, provided an opportunity to observe forest resistance to severe drought at a large-scale, similar to those predicted in the future. Based on results from a network of permanent plots spread across the Amazon, Phillips et al. (2009) found that several Amazonian forests were sensitive to the 2005 drought , with mortality increasing at rates that were high enough to reverse a trend in C accumulation of 0.45 PgC yr-1 to a -1.2-1.6 PgC annual net emissions. Although the results of this study have received some

criticism because of the limited number of plots (Chambers et al. 2009), Gloor et al. (2009) suggest that the RAINFOR plot network capture most of the variation in tree mortality and, hence, on short-term, inter-annual oscillations in C stocks.

Here I evaluate the potential responses of Amazonian vegetation to drought from 1995 to 2005 using a process-based, ecosystem model, CARLUC (Carbon Land Use Change; Hirsch et al. 2004). In particular, I estimate the effects of climate variability on total carbon stocks and fluxes of Amazonian vegetation across the Basin and of forests where permanent plots from RAINFOR are located (Phillips et al. 2009). Based on previous findings of increased rates of carbon accumulation over the tropics (Baker et al. 2004, Phillips et al. 1998), I expect CARLUC simulations to describe C accumulation over the Amazon from 1998 to 2004, but C losses during the 2005 drought.

Given that CARLUC was parameterized using data from a rainfall exclusion experiment representing a small area in Tapajos National Forest (TNF), it has limitations in reproducing vegetation patterns in other regions. Despite this limitation, simulations using CARLUC should provide insights into forest vulnerability to oscillations in climate, given that it integrates four representative climatic variables of NPP into a single predictor, potential carbon stocks.

Methods

Model Description

I assessed the effects of climate on carbon stocks of Amazonian forests between 1995 and 2005 using the CARLUC ecosystem model (described in detail in Hirsch et al. 2004), which borrows its basic structure from the 3-PG model (Landsberg and Waring 1997). Briefly, CARLUC is a process-based, dynamic model that estimates net primary productivity based on characteristics of the vegetation [quantum efficiency (*qe*), and

carbon use efficiency (*fnr*)] and on climatic variables [vapor pressure deficit (VPD), temperature (TEMP), photosynthetic active radiation (PAR), and plant available water (PAW)] (Fig. 3-1). As the leaf area index increases, NPP saturates according to the light- extinction function derived from Beer's law (eq. 1; note that all climatic variables were scaled to range from 0 to 1). In the version of the model presented here, the allocation of NPP to leaves, stems, and roots is represented as a function of PAW and based on results from the TNF throughfall exclusion experiment (Fig. 3-2). Tree mortality is modeled as being dependent on soil water availability: as PAW declines to ≤ 40%, the fraction of live biomass declines exponentially with PAW (Fig 3-2). As for 3-PG, CARLUC was designed to integrate process-based phenomena with empirical relationships derived from field experiments.

$$NPP = fnr \cdot qe \cdot PAR \cdot TEMP \cdot \min(PAW, VPD) \cdot \left(1 - e^{-0.7 \cdot SLA c_{leaf}}\right) \quad (3\text{-}1)$$

Input Data

The model was initiated using interpolated meteorological climate data (~280 stations spread across the Amazon Basin) at a resolution of 2 km x 2 km (described in detail in Nepstad et al. 2004). Because PAR was not available from these meteorological stations, estimates were obtained using the GOES-8 satellite product (Nepstad et al., 2004). The external variable PAW (i.e., independent from vegetation dynamics) was generated based on the difference between soil field capacity (SW_{fc}) and wilting point (SW_{pwp}). Briefly, texture data samples collected in the field were combined with empirical relationships between soil texture and SW_{fc} and SW_{pwp}. Equations relating soil texture and carbon content to field capacity and permanent wilting point were developed by Tomasella and Hodnett (1998) using soil water versus

matric potential curves for Amazon soils. Following, estimates of PAW_{max} (in mm) were generated for each meter of the soil horizon from 0 to 10; PAW_{max} among horizons were summed to estimate PAW_{max} for the entire sampled profile.

Experimental Runs

I performed four simulations to evaluate the potential effects of drought on the carbon stocks of Amazonian forests.

- The mortality and NPP allocation functions were held constant by keeping PAW fixed at 100% (see Fig. 3-2).
- The mortality and NPP allocation functions were allowed to vary spatially and temporally with PAW.
- The mortality function was allowed to vary with PAW, while the NPP allocation function was held fixed.
- The mortality function was held fixed according to PAW, while the NPP allocation function was allowed to vary with PAW.

Analysis

Based on the runs of CARLUC in which mortality and NPP allocation were allowed to vary as a function of PAW, I assessed spatial-temporal carbon stocks across the Amazon as follows:

- First, I extracted CARLUC-predicted aboveground stocks only for the TNF and compared these predictions with field measured data from Brando et al. (2008).
- Second, I summed all 13 carbon pools from CARLUC for each of the 132 months of the simulations. In this analysis I evaluated intra- and inter-annual variability in C pools (referred as "Total C stocks").
- Third, I chose three regions of to represent three different levels of dryness (i.e., PAW), and averaged the aboveground carbon pools for each region to evaluate temporal patterns in C storage.
- Fourth, I evaluated the average aboveground carbon stocks of Amazonian forests from 1995 to 2005 where field permanent plots are located (Phillips et al. 2009) to

assess how CARLUC predictions relate to field-plot measurements (referred as "Field Plots").

Results

CARLUC Predictions for TNF

At the Tapajos National Forest, predicted average aboveground carbon stocks (140 MgC ha^{-1}) were within ranges observed in the field. The temporal dynamics of simulated C, however, diverged from on-site measurements. While predicted average annual leaf carbon stocks (Cleaf) tended to increase from 2000 to 2005 at a rate of 0.0055 kgC ha^{-1} $year^{-1}$ (± 0.001; p=0.0038) (Fig. 3-3), Brando et al. (2008) observed minor reductions in LAI from 2000 to 2004 (with the exception of 2002, when LAI was higher than average, Brando et al. 2008). In 2005, however, both predicted Cleaf and observed LAI were above the 2000-2004 average. Whereas predicted C stocks in stems (Cstem) also tended to increase from 2002 to 2005, these increases were relatively low when compared to total standing stocks (Fig. 3-3), which is in agreement with field measurements of aboveground C stocks up to 2004. In 2005, however, there was an decrease in biomass observed in the field, probably resulting from a lag-response of vegetation to reduced plant available water, while an increase in predicted C stocks in Cstems.

Experimental Runs: Tree Mortality and NPP Allocation

Carbon stocks predicted by CARLUC for the entire Amazon Basin indicated vegetation sensitivity to drought as expressed by the effects of PAW on tree mortality. Whereas CARLUC runs with PAW having no effect on mortality reached equilibrium at 108 Gt (total stocks for the entire Amazon), this equilibrium was reached at ~ 100 Gt when PAW affected both mortality and NPP allocation. This result suggests a potential

interaction between the functions representing mortality and NPP allocation, given that increased mortality may have reduced NPP. In contrasts, when PAW was allowed in the model to affect either mortality or NPP allocation alone, CARLUC reached equilibria at 107 and 105 Gt, respectively.

Specific Regions and Field Plots

Given that simulated C stocks in CARLUC were sensitive to PAW (when mortality and NPP allocation were allowed to vary as a function of PAW), drier regions of the Amazon not only tended to reach equilibrium at lower C stocks, but also showed greater temporal variability in C stocks than wetter regions (Fig. 3-4). For instance, monthly analyses of C stocks in three regions of the Amazon (low, medium, and high levels of PAW) showed that the driest region was predicted to lose carbon in 2004-2005, while aboveground live C pools were predicted to increase in all three regions from 1995 to 2003. These predicted losses suggest that thresholds in PAW were crossed in drier regions of the Amazon between 2004 and 2005.

CARLUC simulations of carbon stocks from regions where permanent plots are located (e.g., Phillips et al. 2009) (Fig. 3-4) carried out on a monthly basis revealed little change C pools over time (Figure 3-5). From 1995 to late 2003, live aboveground biomass increased, but non-significantly, and then began to increase at low rates in late 2003.

Total Carbon Stocks

Based on temporal analyses among years and between seasons for the entire Amazon Basin using CARLUC, I found that total wet season carbon stocks tended to increase between 1995-1998 but to decrease subsequently, from 1999 to 2005 (Fig. 3-5). In contrast, during the dry seasons, C stocks declined between 1995-2000, and

then increased between 2001-2004. During the major drought of 2005, there was a minor shift in this trend of increments at the Basin scale, with an overall net reduction of 0.06 GtC $year^{-1}$. In sum, these contrasting wet and dry season behaviors resulted in a net increase in C stocks between 1995 and 2004. Patterns of between season increases and decreases in C stocks were associated with contrasting temporal patterns in climate over the Basin. Whereas increases in dry season PAR contributed positively to vegetation productivity after 2000, decreases in PAW (associated with lower wet-season PPT and higher VPD) reduced productivity during the wet seasons, particularly after 1998.

Climate and Carbon Pools

Although CARLUC indicated that PAW accounted for most variability in C stocks, PAR had important effects in some cases as well. In regions with no soil water deficits, higher PAR led to higher C stocks. It follows that by dividing the Amazon into the relatively drier East and wetter West (following methodology in Malhi et al. 2009), there was a clear difference in PAR, temperature, and VPD between these two regions (higher in the East than the Western Amazon). In other words, where PAR was high and PAW high enough to prevent mortality, productivity tended to be higher (Figs 3-6, 3-7).

Discussion

Based on the process-based coupled vegetation-atmosphere model CARLUC, I evaluated the potential effects of climate variability on carbon dynamics of Amazonian vegetation from 1995 to 2005. Predicted C stocks in leaves showed a slight trend of increase from 1995 to 1998 (during the wet seasons) and from 1999 to 2003 (during dry seasons), which suggest favorable weather conditions for forest growth from 1995 to 2003 (i.e., higher NPP) due to increasing PAR over time. These findings are partially

supported by results from Hashimoto et al. (2009), whose study on vegetation responses to climate variability in the western Amazon (during 1984-2002) showed that increases in NDVI were associated with increases in short-wave radiation between August and December.

Despite the apparently favorable weather condition for C accumulation, I observed a steady decrease in wet-season precipitation (and hence PAW) subsequent to the drought of 1998. These reductions tended to lower predicted-C pools during the wet seasons, exacerbating differences between dry and wet seasons over time. This conspicuous seasonal pattern may be because portions of the Amazon reached levels of PAW that were low enough to cause tree mortality (most variability in CARLUC-based predictions of C stocks was associated with tree mortality). Note, however, that this interpretation is based on the assumption that all forests of the Amazon would respond to drought in ways similar to the site in Tapajos National Forest on which the drought-induced tree mortality function was developed.

Losses of standing stocks of C were also observed following the drought of 2005. In this year, there was a reversal in C accumulation compared to 2004 (shown in the Basin-wide analysis), with a small net loss of C. While the general trend of increasing C pools during the dry season until 2004, followed by a reduction in 2005, corroborates the findings of Phillips et al. (2009), the magnitude of the reduction observed here was less pronounced than in their study. At least four explanations may account for this difference between studies. First of all, because CARLUC predicted modest increases in C pools for RAINFOR plots whereas Phillips et al. (2009) reported actual reductions for the same plots based on field measurements, it is reasonable to infer that the

Tapajos Forest (where the mortality function in CARLUC was developed) was more resistant to drought than RAINFOR forests on average. This potential difference in sensitivity of Amazonian forests to drought is probably a result of long-term adaptations to cope with periods of low soil moisture. These results reinforce the need for long-term, large-scale measurements of tree response to oscillations in climate.

Second, PAW driving CARLUC may have been overestimated, reducing predicted drought-induced tree mortality. For example, CARLUC has no representation of feedbacks between PAW and vegetation canopy cover or photosynthesis; PAW is an external variable. Therefore, any potential increase in evapotranspiration in 2005 associated with vegetation dynamics (e.g., increased photosynthesis) could have no effect on modeled PAW (see Nepstad et al., 2004 for more details on PAW calculations). As a result, the model may have overestimated PAW, which could explain the lower predicted C losses here compared to Phillips et al. (2009). In addition, PAW was modeled based on the assumption that the top 2 m of the soil profile represented depths down to 10 m at which point roots are exceedingly scarce (Nepstad et al. 1994). In contrast, the scant available data on soil physics below 2 m (Jipp et al. 1998) indicate that PAW maximum declines with depth (probably only for regions with very deep water table); hence the estimates used to run CARLUC may have been overestimated. On the other hand, higher drought-induced tree mortality in 2005 could have lowered ET, thus increasing modeled PAW compared to actual PAW.

The plot network used by Phillips et al. (2009) to infer C patterns over the Amazon Basin may not represent the climatic variability over the region. Although RAINFOR plots are widely distributed, there are very few plots located between Peru and Manaus,

a region that CARLUC predicted to have had high productivity in 2005. Therefore, this high productivity, associated with high levels of PAR and low mortality, could counter balance C losses from mortality occurring in other parts of the Amazonia . Note, however, that while the climate data used here are from 280 widely distributed stations, there are still several large geographical gaps.

Finally, CARLUC does not represent some intrinsic processes in vegetation dynamics that are captured in field-based studies. CARLUC is an envelope of climatic variables alone used to predict carbon stocks; hence, interspecific competition and other important ecosystem processes are missing. These intrinsic dynamics, which are difficult to capture in in models that do not represent competition among individuals or species (e.g., 'big-leaf' models), could explain the differences between the model and the field-based data.

While predictions suggest that droughts may become more common and intense in the near future, apparently no model used to predict future vegetation trajectories in the Amazon has yet incorporated the effects of drought-induced tree mortality on carbon stocks; instead, droughts are assumed to have affect only photosynthesis (e.g., Foley et al. 1996). Similarly, the allocation of NPP to different plant parts is often ignored, which contrast with results from a partial throughfall exclusion experiment in which aboveground wood production was drastically reduced in response to the throughfall exclusion, while litterfall and soil CO_2 efflux showed minor or no response to the throughfall exclusion, respectively (Brando et al. 2008). Without field-based, large-scale data on carbon fluxes and stocks across the region measured over time, it is still difficult

to evaluate the future of forests of the Amazon at the basin scale under different climate change scenarios.

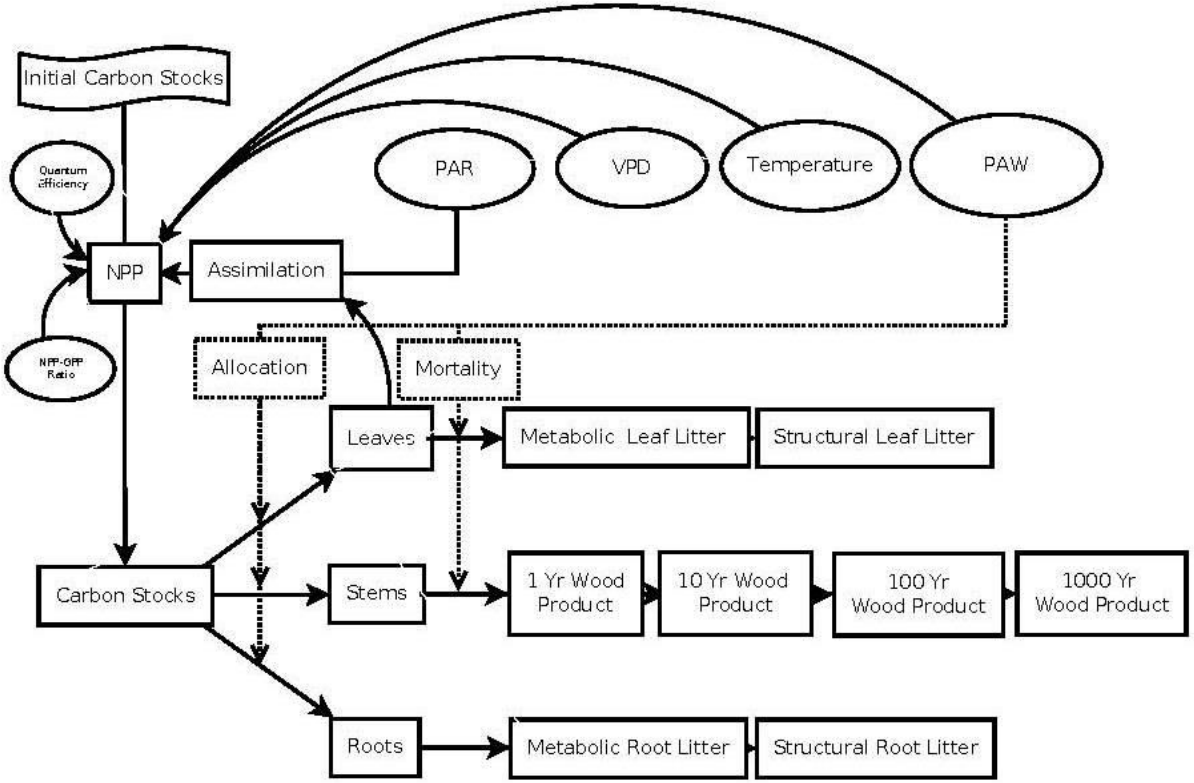

Figure 3-1. Conceptual diagram of the CARLUC ecosystem model. Carbon pools are controlled by climate (via its effects on NPP) and PAW (via its effects on NPP, mortality, and NPP allocation). Once tissue dies, part of the carbon is transferred to pools with low and high residence times. The other portion of the carbon resulting from dead tissues is transferred directly to the atmosphere.

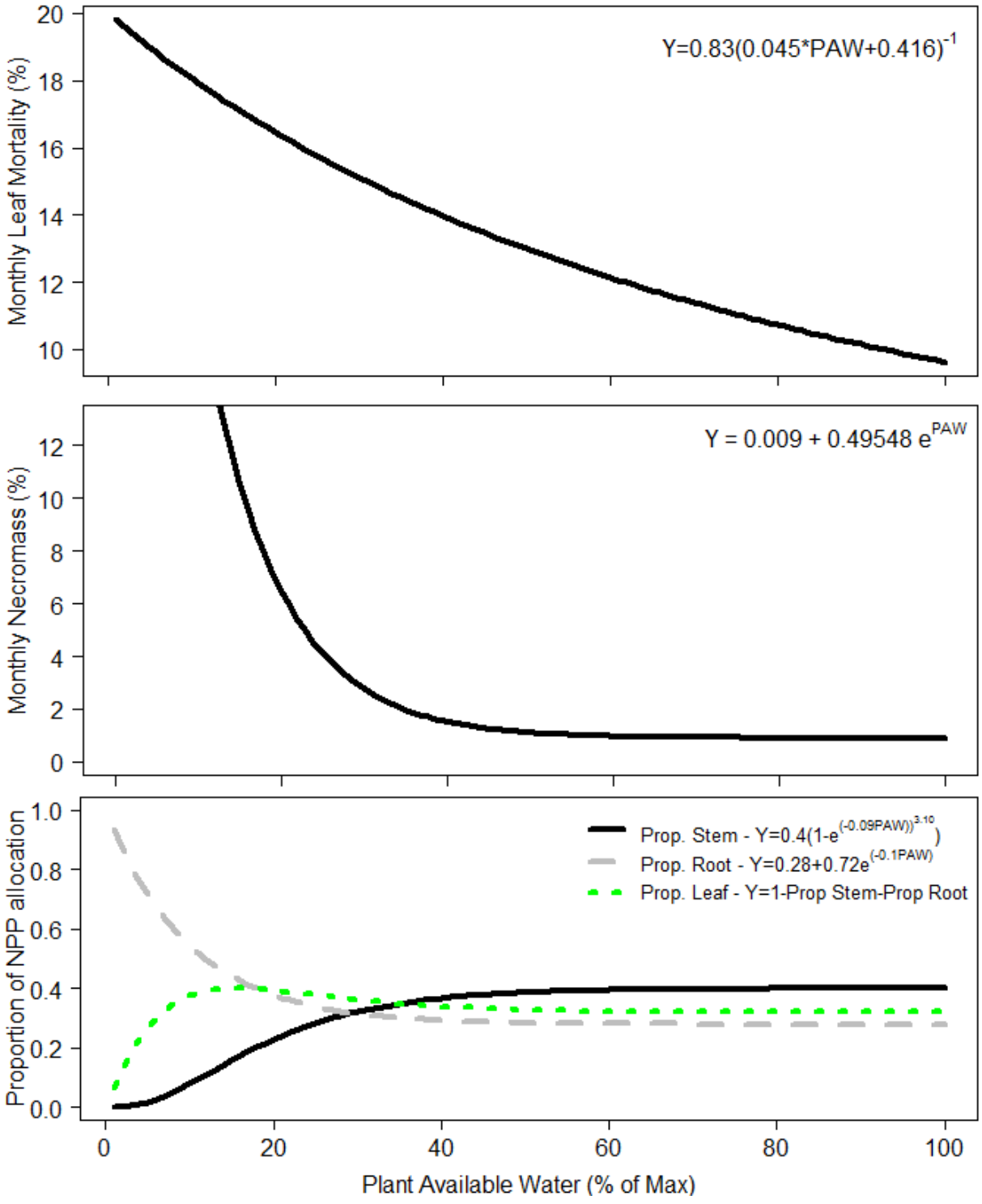

Figure 3-2. Annual rates of leaf mortality (top panel), stem mortality (mid panel), and NPP allocation (lower panel) as a function of PAW. These relationships were derived from data from a large-scale partial throughfall exclusion experiment (Nepstad et al. 2002, 2007; Brando et al. 2008).

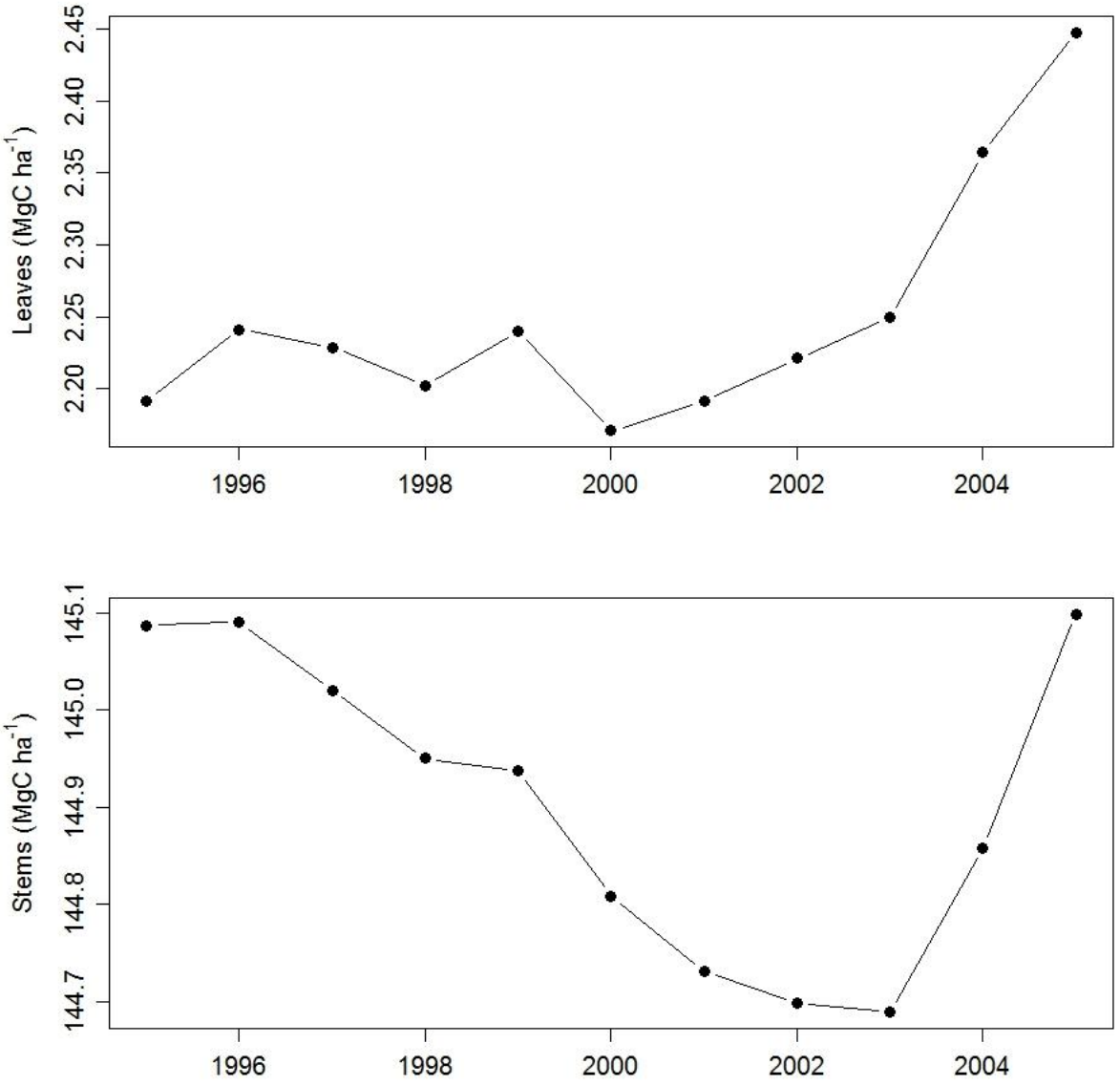

Figure 3-3. Temporal patterns in carbon stocks predicted by CARLUC in leaves (upper panel) and stems (lower panel) for the Tapajos National Forest.

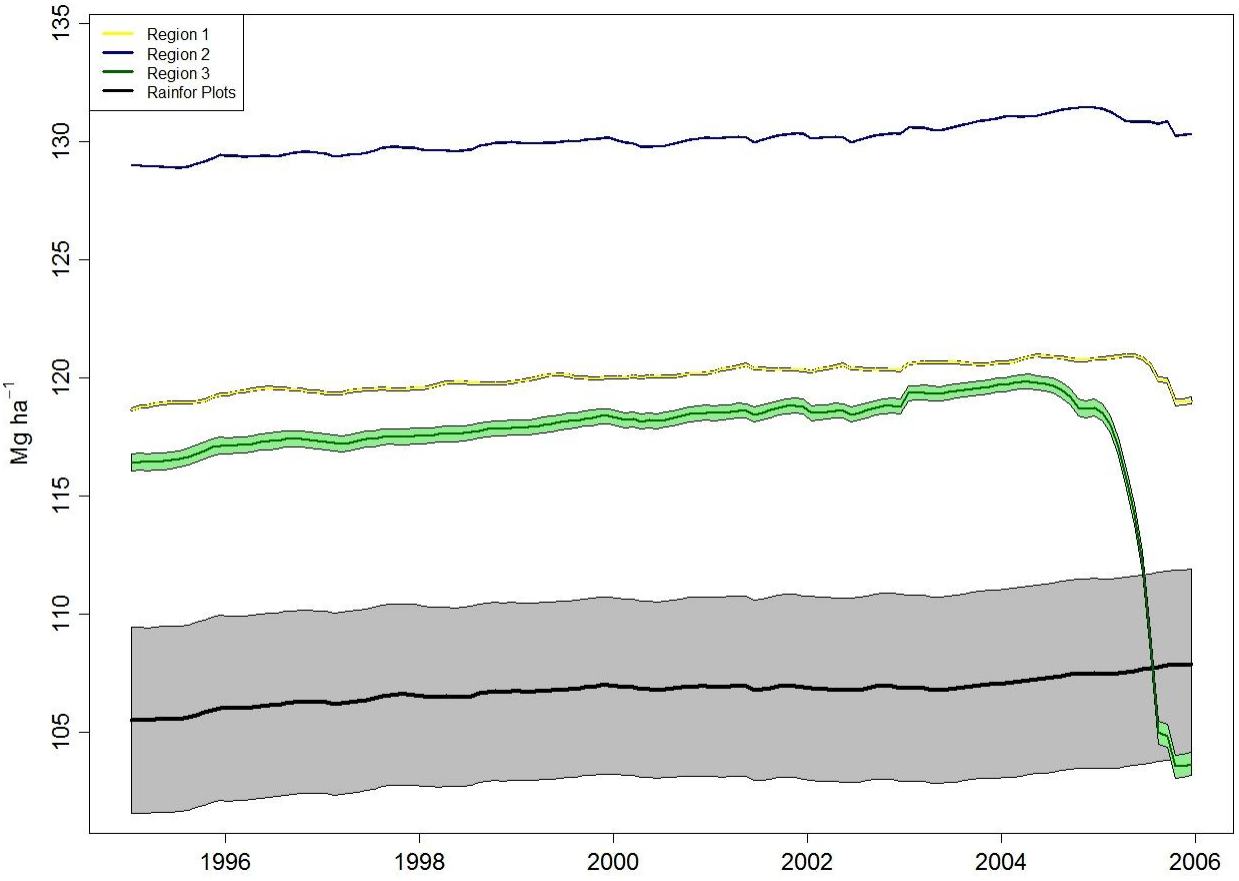

Figure 3-4. Temporal patterns in average aboveground C stocks in regions with low, medium and high levels of PAW. The black line represents C behavior estimated by CARLUC in regions where permanent plots are used to infer about aboveground carbon dynamics.

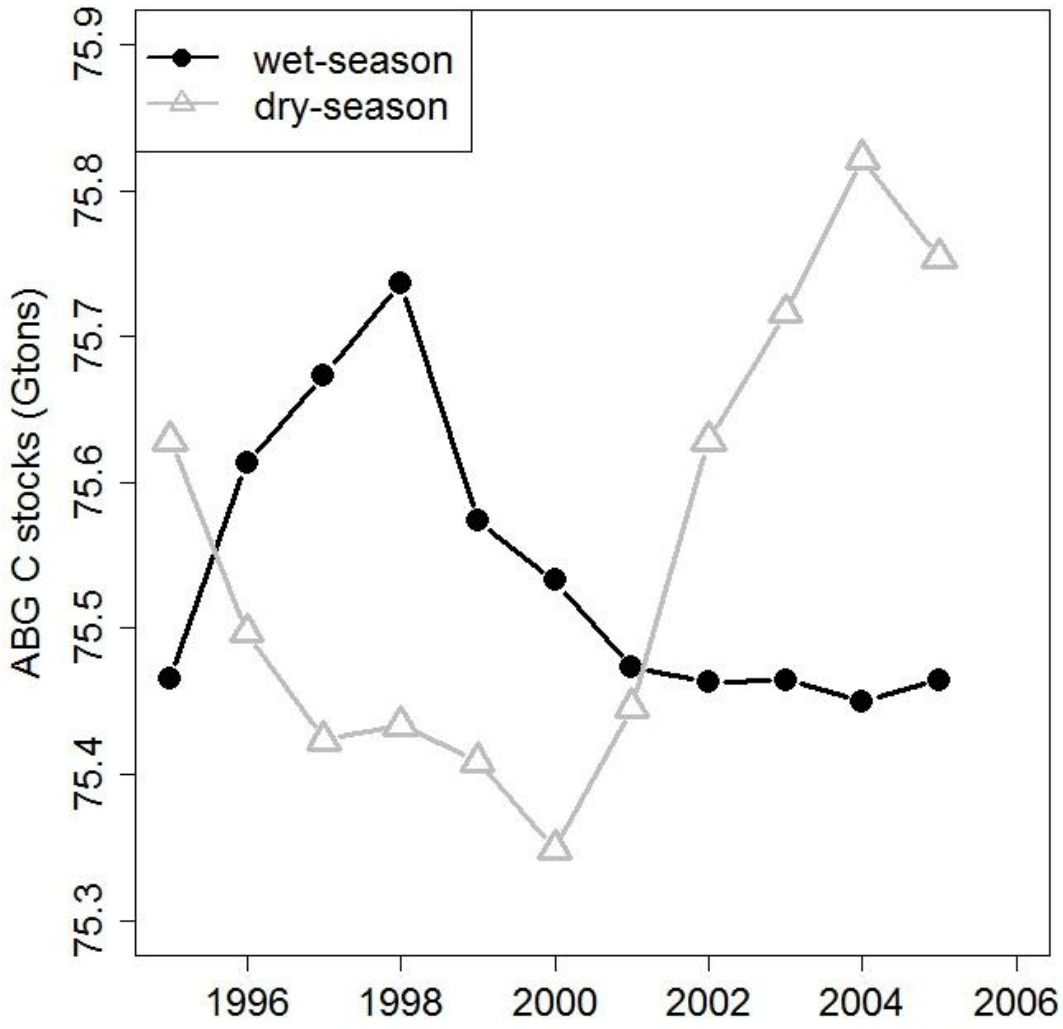

Figure 3-5. Temporal patterns in total aboveground carbon stocks averaged by dry and wet season and per year. The dry season was represented by the months August, September, and October, while the wet season by the months between January and May. Note that the CARLUC run with both mortality and NPP allocation varying as a function of PAW were used to generate the pools of C.

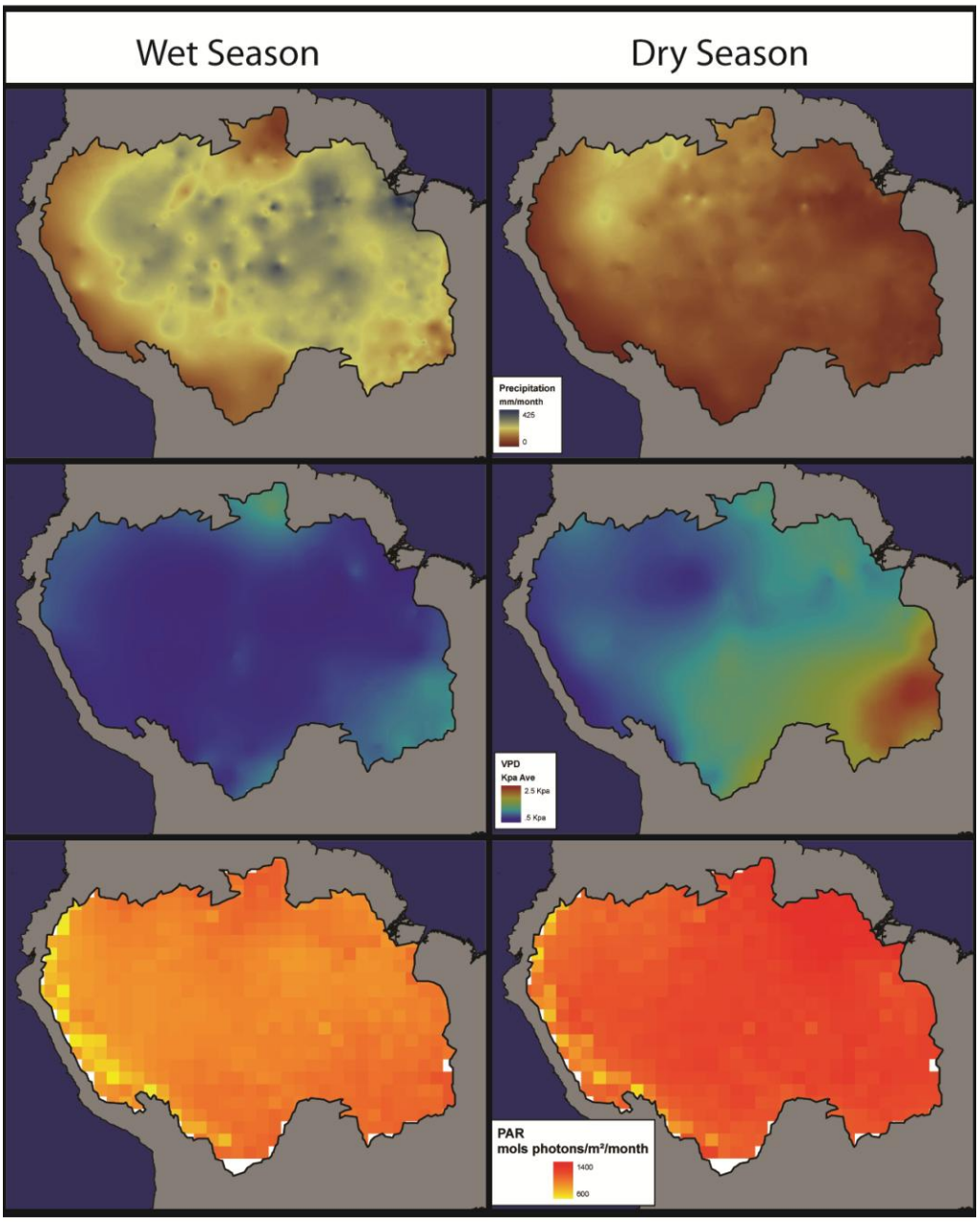

Figure 3-6. Climate patterns during the dry (July-October) and wet (January-April) seasons. Each climatic variable was averaged per season from 1995 to 2005.

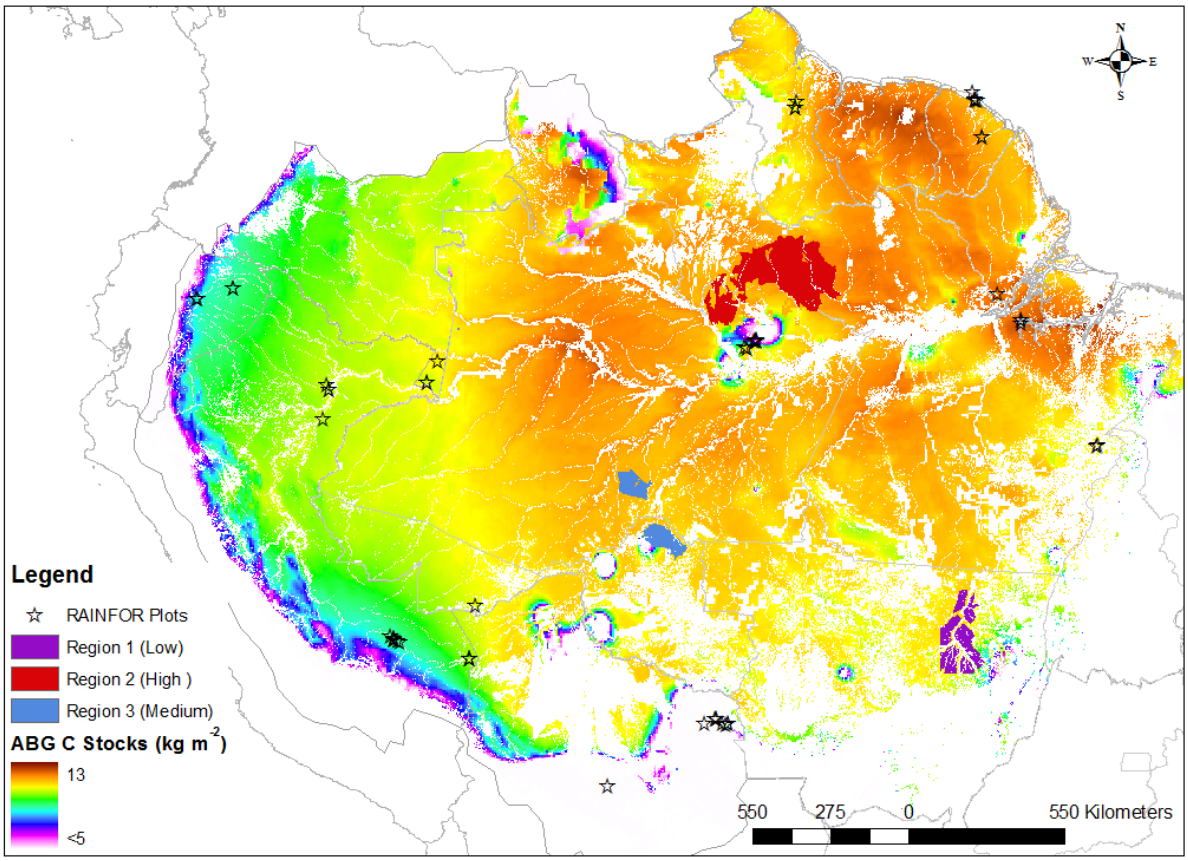

Figure 3-7. Total aboveground carbon stocks simulated by CARLUC for the entire Amazon and for three regions of varying PAW. Stars represent RAINFOR sites. Note that in this simulations the functions representing drought-induced change in NPP allocation and mortality varied according to oscillations in PAW.

CHAPTER 4
SEASONAL AND INTERANNUAL VARIABILITY OF CLIMATE AND VEGETATION INDICES ACROSS THE AMAZON

Introduction

The accumulation of heat-trapping gases in the atmosphere may subject large areas of the Amazon Basin and other tropical forest formations to a greater frequency and severity of drought in the coming decades (Christensen et al. 2007, Malhi et al. 2008). This trend may interact synergistically with regional inhibition of rainfall driven by deforestation (Costa and Foley 2000, Nobre et al. 1991, Werth and Avissar 2002) and more frequent sea surface temperature anomalies (e.g., El Nino Southern Oscillation and North Atlantic Tropical Oscillation) (Cox et al. 2008, Marengo et al. 2008, Nepstad et al. 2004) to move these tropical forest regions toward large-scale forest dieback events. Drier and warmer climate in the region favors the persistence of grasses and shrubs over trees, in a process that is reinforced by recurring fire (Nepstad et al. 2008). Large scale forest diebacks would transfer to the atmosphere a substantial fraction of the 250 Gt C contained in tropical forest trees (Christensen et al. 2007).

It is difficult to assess the drought thresholds beyond which forest dieback might occur in part because of conflicting evidence regarding the response of forest photosynthesis to drought (Fisher et al. 2006, Betts et al. 2008, Huntingford et al. 2008, Mayle and Power 2008, Lloyd and Farquhar 2008). Some studies suggest that forest photosynthesis (gross primary productivity, GPP) increases during the early stages of drought because of higher photosynthetically active radiation (PAR) (Graham et al. 2003, Hutyra et al. 2007, Saleska et al. 2003). In contrast, two partial throughfall exclusion experiments conducted in the Amazon region found that proxies of forest productivity all declined under mild drought conditions, with tree mortality increasing

under high cumulative canopy water stress resulting from limited plant available water (PAW) [reviewed by (Meir et al. 2009)]. These impacts were observed only after 2-3 years of simulated drought, with the lag probably due to plant adaptations to reduced soil water availability (Oliveira et al. 2005) .

The apparently contradictory findings about drought effects on plants are particularly striking in 2005, when the most severe drought of the last 100 years affected the southwestern Amazon (Marengo et al. 2008c) . This dry and warm period, linked to an anomalously warm tropical North Atlantic, provided an opportunity to evaluate forest resistance to drought over a greater spatial extent than the partial throughfall experiments noted above. Two studies reporting on this drought event diverged in their findings. Phillips et al. (Phillips et al. 2009) found evidence that intact forests of the Amazon Basin were drought-sensitive, accumulating 1.2-1.6 Pg less carbon during the drought period of 2004-2005 than in previous years, and concluded that Amazonian forests were negatively affected by the drought of 2005. Conversely, Saleska et al. (Saleska et al. 2007) found that intact Amazon forests experiencing anomalously low precipitation (PPT) in 2005 had higher photosynthetic activity, as indicated by the enhanced vegetation index (EVI), a canopy reflectance metric developed to minimize the attenuating influences of background and atmospheric effects and thus remain effective even in areas of high biomass and chlorophyll content (Huete et al. 2002). The authors of the latter study concluded that these forests were more drought-resistant than previously thought. A possible resolution of this conflict was provided by a recent paper by Samanta et al. (2010) that suggested that the higher EVI observed in 2005 by

Saleska et al. (2007) could be attributable to atmospherically induced variations associated with aerosol loadings.

We conducted a study to better understand the responses of tropical forests to climate extremes, particularly the processes that permit forests to sequester carbon during drought conditions. First, we evaluated the temporal patterns of climatological variables from 280 meteorological stations (1995-2005), PAR from GOES, and an improved MODIS EVI data set over the dry seasons of 2000-2008 across the Amazon Basin. Second, we examined statistical relationships between EVI during the dry season (July to September) and three integrative climate variables (VPD, PPT, and modeled PAR). We analyzed the EVI – climate variable relationships for both the entire Amazon Basin (intra-annually) as well as just for the densely forested areas (inter-annually). For the Basin-wide analysis, we predicted that EVI within a given year would demonstrate greater sensitivity to drier climatic conditions (e.g., high VPD and low PPT) across a gradient of increasing canopy closure. In densely forested areas (≥70% canopy cover), we predicted that inter-annual EVI variability would be positively correlated with modeled PAR in sites with high precipitation history (i.e., average monthly dry-season precipitation for 1995-2005 > 100 mm). We also predicted that EVI would be negatively correlated with VPD in locations with low PPT history (< 100 mm per dry season month), where dry-season VPD is likely to limit productivity, thus reducing leaf production and leaf area. Finally, using data at relatively high spatial (0.25 km^2) and temporal resolution, we evaluated the EVI relationships not only on the basis of these same climate variables, but also with monthly field measurements of LAI, litterfall, and new leaf production in a dense forest near Santarem, Brazil.

measurements of LAI, litterfall, and new leaf production in a dense forest near Santarem, Brazil.

Methods

MODIS Data

I computed the enhanced vegetation index (EVI) at a spatial resolution of 500 m from the MCD43A4 (collection 5) MODIS Nadir Bidirectional Reflectance Distribution Function (BRDF) adjusted reflectance (NBAR). The NBAR data were standardized to a nadir view geometry and solar angle, and processed to limit the influence of cloud cover, thereby limiting the influence of seasonal variations in acquisition conditions (Schaaf et al. 2002). I further screened the NBAR reflectance quality by using the QA flags provided for the NBAR product and we generated a monthly and seasonal composite of “best quality” reflectance (only reflectance derived from full or magnitude inversion) to calculate the EVI. Because of the high number of observations influenced by cloud cover and atmospheric contamination during the wet seasons of 2000-2008, I focused our Basin-wide analysis on the average of the driest months of the year, July-September (referred to as dry season EVI; see appendix A), thus allowing direct comparisons with Saleska et al. (2007). If EVI in one of these three months was missing, the dry-season average EVI was based on the average of two other months. If EVI was missing in two months, the dry-season EVI was based on a single value. The NBAR EVI requires ~ 5-7 good looks every 16 days (which typically occurs only in the dry season), while for the standard EVI product a single good clear day every 16 days is sufficient. As a result, NBAR-EVI is a less noisy (temporally variable) data set. This procedure thereby assured the largest number of observations of the highest possible data quality.

Because I found that the choice of those months could potentially influence the spatial patterns of EVI from North to South of the Basin (see Appendix B) I did not focus our analysis on geographical gradients. Also, I included in all statistical analysis longitude and latitude as covariates (see statistical analysis for more details).

EVI Surrounding Meteorological Stations

For the comparison of EVI with in-situ climatic measurements, I averaged the EVI data over an area of 8 km x 8 km (256 pixels) surrounding each meteorological station. Following, I estimated canopy cover of the vegetation surrounding these meteorological stations as of 2005 (Hansen et al. 2003). This analysis included both low (e.g., <70%) and high (e.g., >70%) canopy cover. The former includes a mixture of vegetation types. In contrast, densely-forested areas included only cells with high canopy cover (≥ 70%).

Site-specific Analysis

The credibility of MODIS-EVI in capturing vegetation dynamics was tested in the Tapajos National Forest, Para, Brazil (2.897^{o}, 54.952^{o}W) (km-67) using data from both a 1-ha plot (a “control plot” of a rainfall exclusion experiment; details in (Brando et al. 2008, Nepstad et al. 2002)) and an eddy covariance flux tower (Hutyra et al. 2007). First, volumetric soil water content (VWC) was measured each month from 2000 to 2004 using a series of paired Time Domain Reflectrometry probes situated in five soil pits in the 1 ha plot (Nepstad et al. 2002). The VWC measurements were used to derive estimates of plant available water (PAW) for two interval depths: 0-2 m (PAW-2m); and 2-11 m (PAW-11m). Second, leaf area index (LAI) was measured monthly from January 2000 to December 2005 at 100 grid points systematically distributed in the 1 ha control-plot. We used two LiCor 2000 Plant Canopy Analyzers in differential mode (LI-COR, 1992) (Nepstad et al. 2002). Third, from January 2000 to December 2005, litterfall was

collected every 15 days using 100 screened traps (0.5 m^2 each) elevated 1 m from ground level (Brando et al. 2008) and located in the same grid points of LAI. Fourth, visual assessments of the presence of new foliage were conducted monthly between August 1999 and August 2004 for all individuals >= 10 cm in diameter at breast height in 1 ha plot (480 individuals). Here I present percent of individuals with new leaves at a given census. Finally, PAR was measured from 2002 to 2006 using an LiCor 190-SA at 63.6 m in height (Hutyra et al. 2007). Note that in this site: annual precipitation ranges from 1700-3000 mm with a mean of ~ 2000 mm; 2) during the dry season (July through December), rainfall rarely exceeds 75 mm mo^{-1}; soils are deeply weathered oxisol clays of the Haplustox group; and, the permanent water table at a similar site 12 km from the research plot was >100 m deep.

NBAR-EVI and EVI-Product

For the site-specific analysis, I used both the EVI derived from the NBAR product (500 m resolution) and the standard-EVI product (collection 5) composited each 16 days, with a spatial resolution of 250 m vs. 250 m. As noted earlier, the NBAR-EVI data limit the attenuating effects of the atmosphere and viewing conditions (Schaaf et al. 2002), but required temporal compositing to maximize data quality. I screened the NBAR reflectance quality using the QA flags provided for the NBAR product, generating a monthly and seasonal composite of “best quality” reflectance (Schaaf et al. 2002). The MODIS standard EVI product was also screened based on the MODIS product quality flags (e.g., reliability). No corrections for solar or viewing conditions are made in the standard EVI product. Thus, differences between the NBAR-EVI and standard EVI products could be related either to the BRDF model used to solve for surface reflectance, to procedures used to screen for cloud contamination and the normalization

for solar illumination angle, or to all of these factors. Moreover, I compared EVI through repeated measurements of individual pixels, thus corrections for the influences of viewing conditions and solar angle were potentially quite important.

Climate

Monthly data from ~280 meteorological stations (Nepstad et al. 2004) were used to derive dry and wet season averages for the Amazon (from 1995 to 2005). In the same locations where the meteorological stations were located, PAR was estimated using GOES observed cloud cover and a clear sky solar radiation model. I assessed seasonal averages of climatic variables through time for each meteorological station, using a linear mixture model that accounted for spatial and temporal autocorrelation (i.e., random effects of space and time) and a parameter to attenuate the effects of dry years (i.e., 1998 and 2005) (Bates and Sarkar 2006). Finally, the slopes of these regressions were tested for differences against the null model of zero change over time (Baayen 2008), which included only random effects. For each one of the 280 meteorological stations, I calculated PPT history, i.e., the average dry season precipitation based on data from 1996 through 2005.

Statistical Analysis of EVI and Climatic Variables

Basin-wide (mixed vegetation types)

A general linear model (*M1*) of EVI in mixed vegetation (i.e. not just densely forested) areas was comprised of three components: 1) the predictor variables VPD, PAR, PPT, canopy cover (CC), and the interaction of CC with the other covariates; 2) error terms assumed to be spatially autocorrelated according to an exponential spatial structure [see (Pinheiro et al. 2000.)]; and, 3) covariates of longitude and latitude, to capture the large scale spatial gradient of EVI. I fitted this model to the data for each

year of the study (2000-2005) and, therefore, do not account for inter-annual variability in mixed vegetation areas, which is complex because of its association land use change. It does allow for separate regression coefficients and autocorrelation coefficients for each year.

Densely forests areas

The general linear statistical models (*M2*) of EVI in forested areas were comprised of three components. First, covariates of PAR, VPD, and PPT (each term interacted with PPT history class), were included in order to assess the effects of climate on EVI in three different climatic regions: seasonally very dry regions (PPT history class: 0 mm to 65 mm); seasonally dry regions (PPT history class: 66 mm to 100 mm); and non-seasonal regions (PPT history class: > 100 mm). Second, longitude and latitude, were included as covariates to capture the large scale spatial gradient of EVI. Third, the error terms were assumed to have a autoregressive correlation structure of order 1 (Pinheiro et al. 2000) to account for temporal autocorrelation among observations from the same locations over several years. Note that for forested areas we did not find evidence of spatial autocorrelation in the residuals from the fitted model.

Hierarchical partitioning

In both mixed vegetation and densely forested areas, I used hierarchical partitioning (Murray and Conner 2009) as a complementary statistical method to evaluate each covariate's contribution to EVI. In this method, the variance in the response variable (EVI) shared by two predictors can be partitioned into the variance of EVI attributable to each predictor uniquely. For mixed vegetation areas, for each year of the study, I used hierarchical partitioning to evaluate model 1 (*M1*), but without a spatial structure. For densely forested areas, I evaluated a model that included all

climatic variables, the location of each meteorological station, longitude, latitude, and year; referred to throughout as a variation of *M2*. Because PPT was dependent on location of the meteorological station, I did not include this variable in the hierarchical partitioning analysis.

Relationship of the variability of EVI with PAW

I first calculated for each MODIS pixel the coefficient of variation of the EVI for the period 2000-2008, but retained only pixels with ≥ 70% of canopy cover and with data for 6 or more years. The Amazon Basin was then stratified by classes of PAW (0-0 m in depth): class 1: 470-985 mm; class 2: 986-1280 mm; class 3: 1281-1500 mm; class 4 1500-2100 mm, see Nepstad et al. (2004) for the calculation of PAW. Finally the coefficient of variation of the EVI was compared between the four PAW classes visually.

Results

Spatial-temporal Patterns of EVI

EVI varied spatially and temporally across the Amazon Basin during 2000-2008 (Fig. 4-1). Generally, EVI varied most where soil moisture availability (PAW) was the most variable. There was a strong gradient in mean annual EVI from the western to the central portion of the Basin, with associated gradients in the variability of EVI and in the estimated average annual PAW from 0 m to 10 m depth.

In areas with high (>70%) tree cover, roughly defining the area of intact forest across the Basin (Fig. 4-2), EVI was below average in 2000, 2001, 2004, and 2007; close to average in 2003 and 2008; and above average in 2005 and 2006. Pronounced shifts in the annual anomalies (deviations from 2000-2008 mean values) were observed over short time periods. For example, anomalies in 2002 were 151% higher than in 2001; in 2005 they were 168% higher than in 2004; and, in 2007 they were 257% lower

than 2006. Analysis of the spatial covariation of EVI and PAW revealed that inter-annual EVI variability in dense forests was slightly higher in drier areas, with gradually decreasing EVI variability as average PAW increased (Fig. 4-3).

Basin-wide Climate

The Amazon Basin experienced a decline in annual rainfall and an increase in PAR from 1995 through 2005. Based on data from ~280 meteorological stations distributed across the Amazon (Fig. 4-4), I found that annual wet-season PPT decreased at a rate of 5.31± 0.68 mm yr^{-1} (Fig. 4-4). Dry-season PPT also tended to decrease over this time period, but not significantly (-1.018 ± 0.92 mm yr^{-1}). In contrast, PAR increased over the period 1995-2005, primarily after 2002 (especially during the wet-season), but the rate was only statistically significant for the dry-season (15.8 ± 3.67 moles m^{-2} $month^{-1}$ yr^{-1}). I could not detect strong linear temporal pattern in VPD over the entire time period; on the other hand, it appears that VPD increased substantially after 2002 (Fig.4-4). For example, while the rate of increase of average VPD during 1995-2000 was modest (0.0029 kPa yr^{-1}), it increased to 0.43kPa yr^{-1} during 2002-2005. As a result of decreased PPT and increased VPD, modeled PAW from 0 to 10 m depth decreased significantly over the time period at a rate of 2.03 ± 0.22% during the wet season and 2.21 ± 0.11% $year^{-1}$ during the dry season [see also Nepstad et al. (2004)]. Similar patterns were observed for areas with high fraction of canopy cover (Table 4-1).

Table 4-1. Slopes of precipitation, photosynthetic active radiation (PAR), and vapor pressure deficit over time. All linear models between these climatic variables and time were fit using a linear mixed model with random effects of space and time, except for PAW. PAW was averaged over spaced and regressed over time.

	Meteorological stations surrounded by *all* fractions of forest cover		**Meteorological stations surrounded only by *high* fraction of forest cover**	
	Wet Season	Dry Season	Wet Season	Dry Season
Precipitation (mm)	-5.31 ± 0.68***	-0.35 ± 0.91	-7.79±1.62***	-1.35±1.13
PAR (moles m^{-2} mo^{-1})	10.38 ± 7.64	12.22 ± 4.51**	12.44±8.21	11.23±4.45**
VPD (kPa)	0.00 ± 0.00	0.00 ± 0.01	0.00±0.00	0.00±0.00
PAW (% of Max)	-2.03 ± 0.22***	-2.21 ± 0.11***	-	-

EVI and Climate Variables

Spatial analysis across the Amazon Basin

In areas with mixtures of vegetation types (e.g., pastures, cerrado, secondary and primary forests), it was predicted that EVI would decrease with (i) increasing VPD and (ii) decreasing canopy cover and PPT. Based on spatial analysis of EVI data from 256 cells (each 64 km^2) surrounding each meteorological station, these predictions were generally supported. There was a strong and significant interaction between canopy cover and VPD in 4 out of 6 years of the study (Table 4-2). Thus, EVI tended to decrease as VPD increased in areas of low canopy cover. Similarly, PPT interacted with canopy cover in 3 out of 6 years the study, but only marginally ($p<0.1$); as PPT decreased in areas of sparse canopy cover, EVI also decreased. In contrast, PAR showed a marginally significant interaction with canopy cover only in one year ($p = 0.054$). Thus only in 2004 did EVI increase as PAR increased in areas of high canopy cover. In addition to general linear models, I used hierarchical partitioning (Murray and Conner 2009) to estimate the relative importance of each predictor on EVI, accounting

for collinearity among predictors in a linear model (see methods). Based on this analysis, canopy cover, VPD and latitude explained, respectively, 55%, 17%, and 11% of the total variation associated with the full model (average R^2 of the full model, *M1*: ~56%; see methods). Overall these results indicate a strong effect of VPD and a weaker effect of PPT and PAR on EVI from 2000 to 2005. These results also suggest that spatial gradients, independent of variations in climate, had important effects on EVI.

Table 4-2. ANOVA table for all predictors of EVI in non-forested areas from a linear model (M1). Note that we ran one model for each year of the study.

	2000		2001		2002		2003		2004		2005	
	F	p	F	pl	F	p	F	p	F	p	F	p
Intercept	3741	<.001	4724	<.001	7069	<.001	1874	<.001	8012	<.001	3165	<.0001
Canopy Cover (CC)	66.481	<.001	83.257	<.001	125	<.001	96.3	<.001	123.0	<.001	138.7	<.0001
VPD	8.035	0.006	22.43	<.001	31	<.001	6.73	0.011	40.33	<.001	9.974	0.0021
PAR	0.882	0.350	0.028	0.868	3.7	0.055	0.93	0.336	0.773	0.3813	0	0.9935
PPT	6.834	0.010	7.060	0.009	2.6	0.106	2.21	0.136	0.01	0.9211	0.093	0.7604
Longitude	0.949	0.332	2.056	0.158	4.3	0.040	2.08	0.152	1.262	0.2637	6.376	0.013
Latitude	3.77	0.055	1.931	0.168	10.8	0.001	7.30	0.008	19.633	<.0001	5.551	0.0203
CC*VPD	0.863	0.355	2.034	0.157	7.8	0.006	4.00	0.048	11.975	0.0008	6.737	0.0108
CC*PAR	0.718	0.399	0.419	0.519	0.3	0.574	4.25	0.042	0.046	0.831	0.085	0.7715
CC*PPT	0.196	0.659	1.570	0.213	2.8	0.092	3.06	0.083	9.837	0.0022	0.113	0.738

Spatial-temporal analysis in densely forested areas

In densely forested areas (i.e., all cells with canopy cover ≥ 70%), there was no support for the hypothesis that inter-annual EVI variability was associated with temporal variation in PAR, VPD, or PPT across all classes of PPT history (Table 4-2). Rather, the only significant predictors of EVI were longitude (p=0.02) and PPT history alone (p=0.108) (Table 4-2). Using hierarchical partitioning analysis to assess the importance of each predictor of a linear model on EVI (*M2*; see methods), I found that spatial gradients accounted for most of the EVI variability. For example, of the 77% of the variation explained by the linear model, spatial variability alone accounted for 91% of this variation, whereas year, VPD, and PAR accounted for only 4.2%, 0.5%, 0.45%, respectively. Overall, these results show that, by considering the effects of spatial gradients and temporal autocorrelation in our analysis, no climatic variable could meaningfully explain the EVI inter-annual variability.

Table 4-3. ANOVA table for all predictors of EVI in dense forested areas from a general linear model (*M2*).

	F	p
Intercept	26359.68	<.0001
PPT History	2.253	0.1081
PAR	1.111	0.2933
VPD	0.276	0.6000
PPT	0.225	0.6359
Latitude	1.826	0.1783
Longitude	5.008	0.0265
PPT History*PAR	0.073	0.9300
PPT History*VPD	0.043	0.9577
PPT History*PPT	0.319	0.7274

Site-specific Analysis

At the intensively studied Tapajos site (near Santarem; 80% tree cover), I found that monthly EVI was highly seasonal and thus positively and strongly correlated with field measurements of the proportion of trees (≥ 10 cm in diameter at breast height) with new leaves (R^2=53%; p<0.01). EVI was also positively correlated with field measurements of PAR (R^2=35%; p<<0.01), but inversely correlated with PAW from 0 to 2 m depth (R^2=46%; p<0.01), which indicates no soil water constraints on photosynthesis (as 0-2m PAW decreased, EVI increased) (Figs. 4-5, 4-6). Hence, EVI was most sensitive to production of new leaves and associated light levels (the individual effects of PAR and leaf phenology on EVI could not be decoupled in our analysis). This interpretation is reinforced by the findings that field measured LAI varied little between seasons and was poorly correlated with EVI (R^2=17%, p=0.05) (Fig. 4-6). Although other environmental variables may also have affected EVI indirectly (for example, via lagged effects on vegetation processes), their direct relationships with EVI were not evident (Fig. 4-6).

In contrast to EVI derived from the MODIS corrected reflectance products (see methods), the MODIS “standard collection 5 product”, screened using standard quality control flags, was better correlated with correlated with these same measured seasonal environmental and biophysical variables (Fig. 4-7). These results indicate that the EVI product used for the analyses (produced from bi-directionally corrected reflectance data sets) was better correlated with field conditions than the standard MODIS EVI product, which could be a result of correction of viewing angle conditions, screening procedures for cloud cover, or both. While we cannot ensure the results at the Tapajos sites extend across the entire Amazon Basin, particularly because this site was not affected by

severe drought during the study period, confidence in our regional results was supported by these more local scale observations.

Discussion

Increases in solar radiation during dry periods may boost tropical forest productivity (Graham et al. 2003, Saleska et al. 2003, Wright et al. 1999), but prolonged and severe droughts ultimately limit this effect by inducing stomatal closure and even tree mortality (Brando et al. 2008, Nepstad et al. 2007). The thresholds at which drought starts to reduce productivity (as opposed to increasing it) are still not well known. While satellite-based vegetation indices allow insight into potential environmental thresholds (Huete et al. 2006, Myneni et al. 2007, Saleska et al. 2007, Xiao et al. 2005), they have provided an ambiguous measure of vegetation responses to drought in the Amazon Basin. Here, I demonstrate that spatial variations of an improved EVI metric, corrected for bi-directional reflectance variations and other potential attenuating influences (Schaaf et al. 2002), were associated with gradients of PAW and VPD. This indicates that EVI captured complex spatial patterns of photosynthetic responses to environmental variables across the Amazon. In particular, I show contrasting responses of EVI to the interaction between tree canopy cover and drought, over a wide range of environments (e.g., pastures, secondary forests, cerrados). These results reinforce findings from previous studies that demonstrated that where tree canopy cover is high, trees are better buffered against drought because of their deep root systems (Nepstad et al. 1994). Further, these results indicate that this buffering mechanism may not be restricted to the central Amazon (Huete et al. 2006).

In Tapajos's dense forest, even subtle changes in EVI captured complex seasonal ecosystem dynamics. In particular, the NBAR-EVI increased with the number of canopy

trees with new leaves, while LAI varied little between seasons. This finding show that leaf flushing (but also PAR) was an important driver of EVI and therefore of GPP (Doughty and Goulden 2008). The association between EVI and PAR was more apparent at Tapajos forest (R^2=35%) than in our Basin-wide analysis of densely forested areas, in which EVI was generally not responsive to any specific climatic variable. This finding raises the possibility that other mechanisms other than PAR could be driving the EVI inter-annual variability. I propose three possible mechanisms for this observation.

First, given the strong correlation between EVI and the number of trees with new leaves observed at Tapajos, it is reasonable to expect that leaf flushing could have played an important role on the Basin-wide, inter-annual variability in EVI. Whereas leaf flushing usually coincides with periods of increased radiation (Wright and van Schaik 1994), leaf bud break is not necessarily cued by radiation, but by gradual changes in daylength (Rivera et al. 2002). Once bud break occurs, however, leaf development is strongly controlled by water availability for cell expansion. Therefore, changes in tree water status modified by precipitation events (or even by leaf shedding) during the dry season of dry years is likely to synchronize bud development and, consequently, leaf flushing. Because inter-annual EVI variability in dense forests during the dry season was greatest in regions of lower PAW, I hypothesize that drought could increase EVI by synchronizing leaf flushing via its effects on leaf bud development and tree water status. This hypothesis could explain, in part, the high anomalies during dry years (e.g., 2005). I suggest that this is a potentially important area of research.

Second, the lack of a relationship between PAR and basin-wide EVI could be associated with long-term adaption for herbivory avoidance. It has been suggested that the timing of leaf flushing of tropical trees is the result of selective processes to coincide with periods of lowest insect activity, presumably during the peak of the dry season (Aide 1993). Based on this hypothesis, however, I could not explain the EVI inter-annual variability observed in this study.

Finally, the results presented here may be partly related to the sample size used in the spatial-temporal analysis. Although I used one of the best available data set, there were just 40 meteorological stations available for assessing significance in the densely forested parts of the Basin. As a result of this relatively small sample size, I could not further test the effects of PAR on the inter-annual variability of EVI nor the hypothesis of increased productivity (GPP) during dry periods of increased PAR.

I thus hypothesize that the apparently conflicting observations between Phillips et al. (2009) and Saleska et al. (2007) regarding the drought event of 2005 were related to several mechanisms operating simultaneously. GPP (expressed as EVI) appears to have increased due to the production of new leaves and increased PAR (Saleska et al. 2007), whereas aboveground net primary productivity (ANPP) measured in the field concurrently decreased (Phillips et al. 2009) because of higher tree mortality and increased respiration associated with lower PAW and high temperatures, respectively. Moreover, the allocation of non-structural carbohydrates to belowground processes may have increased, given that EVI (and possibly GPP) was higher and ANPP lower during the drought of 2005.

While it was observed important oscillations in weather over the Amazon from 1995 to 2005 (e.g., a 5.3 mm yr-1 reduction in PPT), these oscillations were not clearly related to EVI inter-annual variability in densely forested areas at the Basin scale. Thus, there is a need for additional analyses that couple field measurements with satellite observations in order to clarify how the Amazon region responds to drought, how those responses will be expressed in the future under increasing drought conditions, and to what extent those responses are captured in satellite observations of canopy photosynthesis.

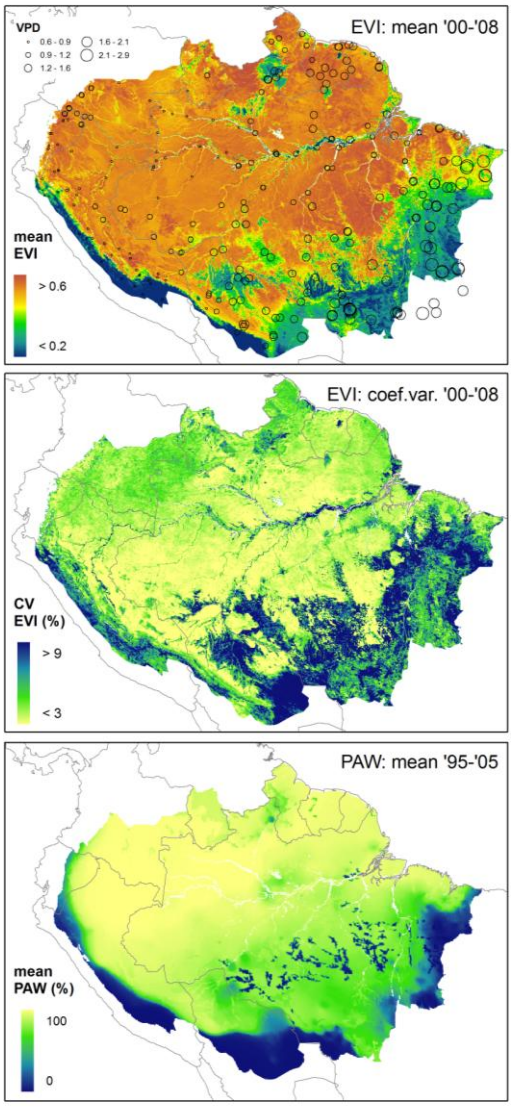

Figure 4-1. Upper panel: Average dry-season EVI across central South America for the period 2000-2008. Overlaid circles represent average vapor pressure deficit measured at 280 meteorological stations across the region for the period 1995-2005. Center panel: Coefficient of variation in annual EVI for the period 2000-2008.Lower panel: Average annual plant available water at 10m depth, expressed as a percentages of the maximum, for the period 1995-2005.

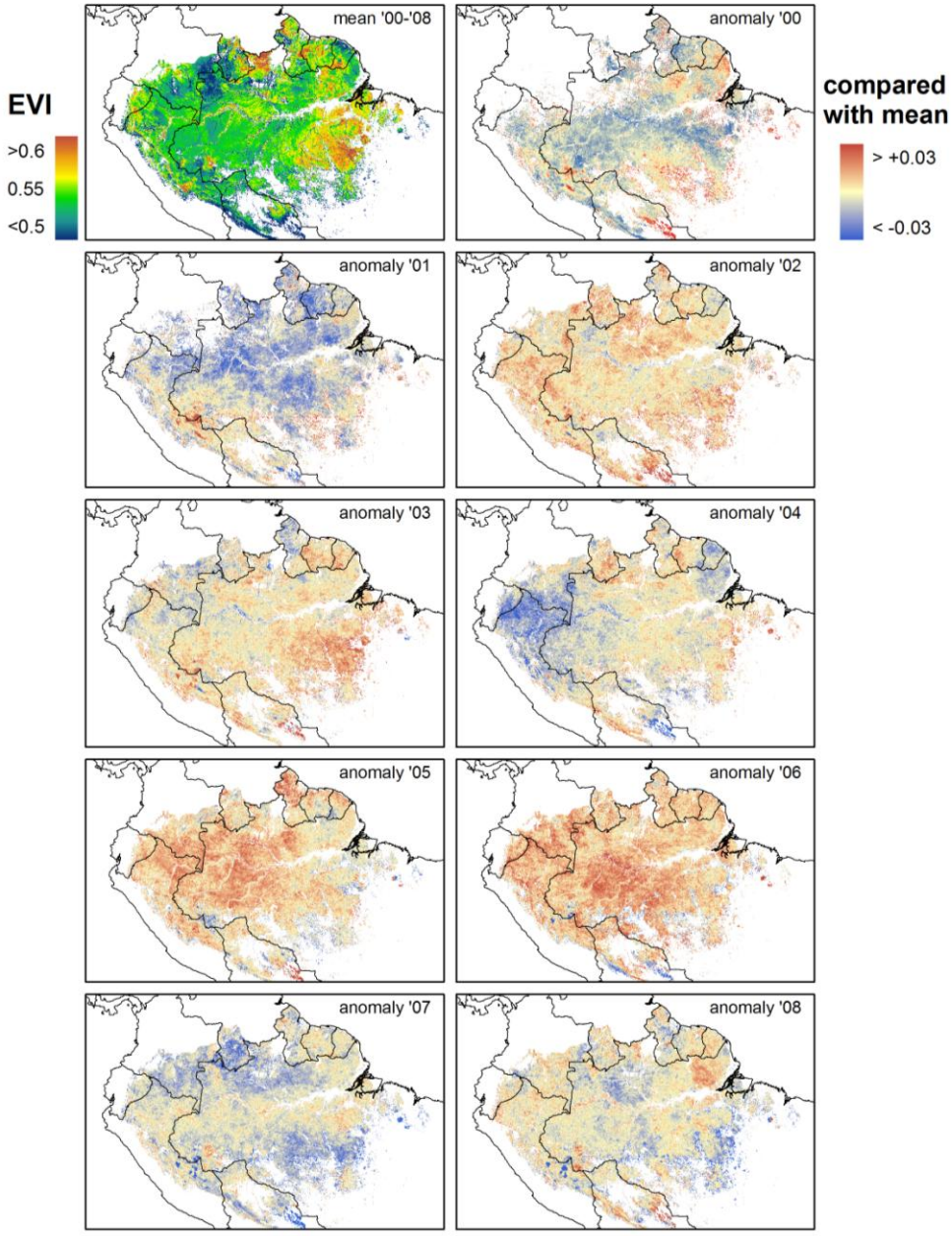

Figure 4-2. Spatial-temporal patterns of dry-season EVI across the Amazon for areas with high canopy cover (EVI > 0.4 and MODIS tree canopy cover product > 70%). The first panel shows average EVI from 2000-200 and the following panels show the EVI anomaly for each year, calculated as EVI_i - EVI_{mean}.

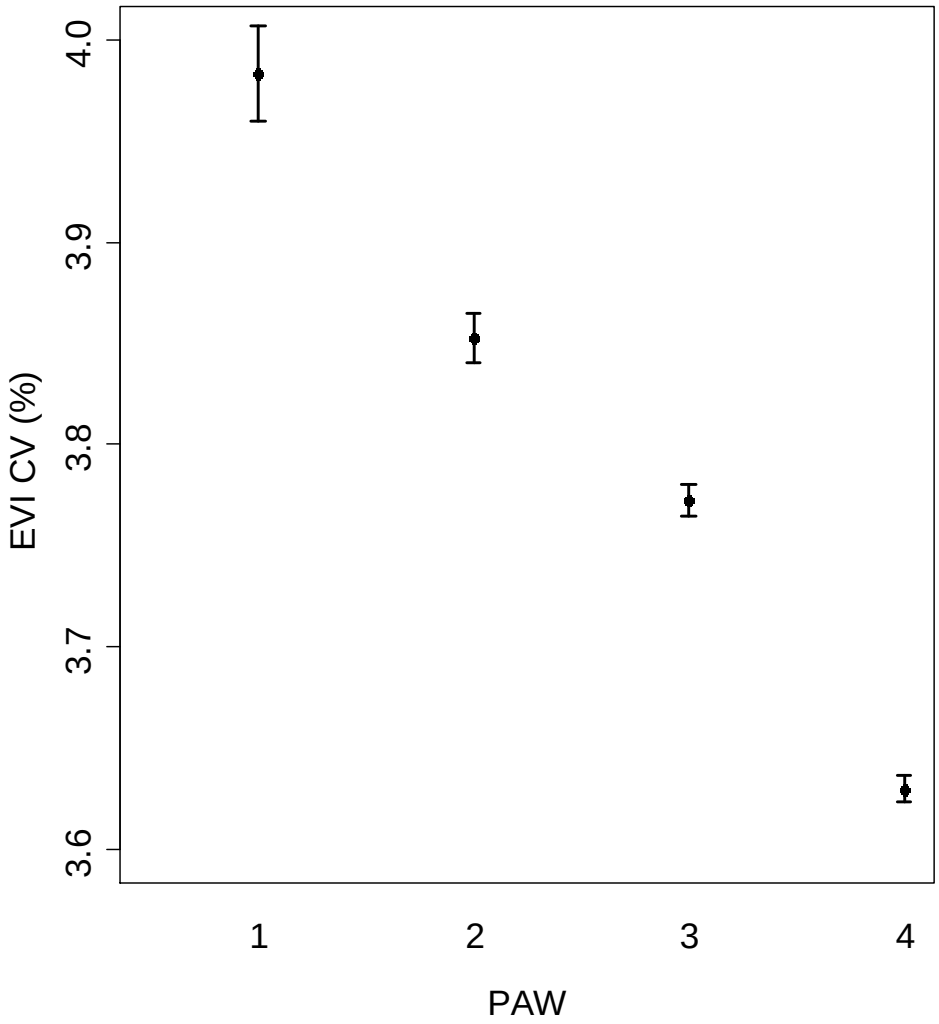

Figure 4-3. Average coefficient of variation of EVI for the entire Amazon, based on data at 500 x 500 m resolution (only for areas with canopy cover ≥ 70%).

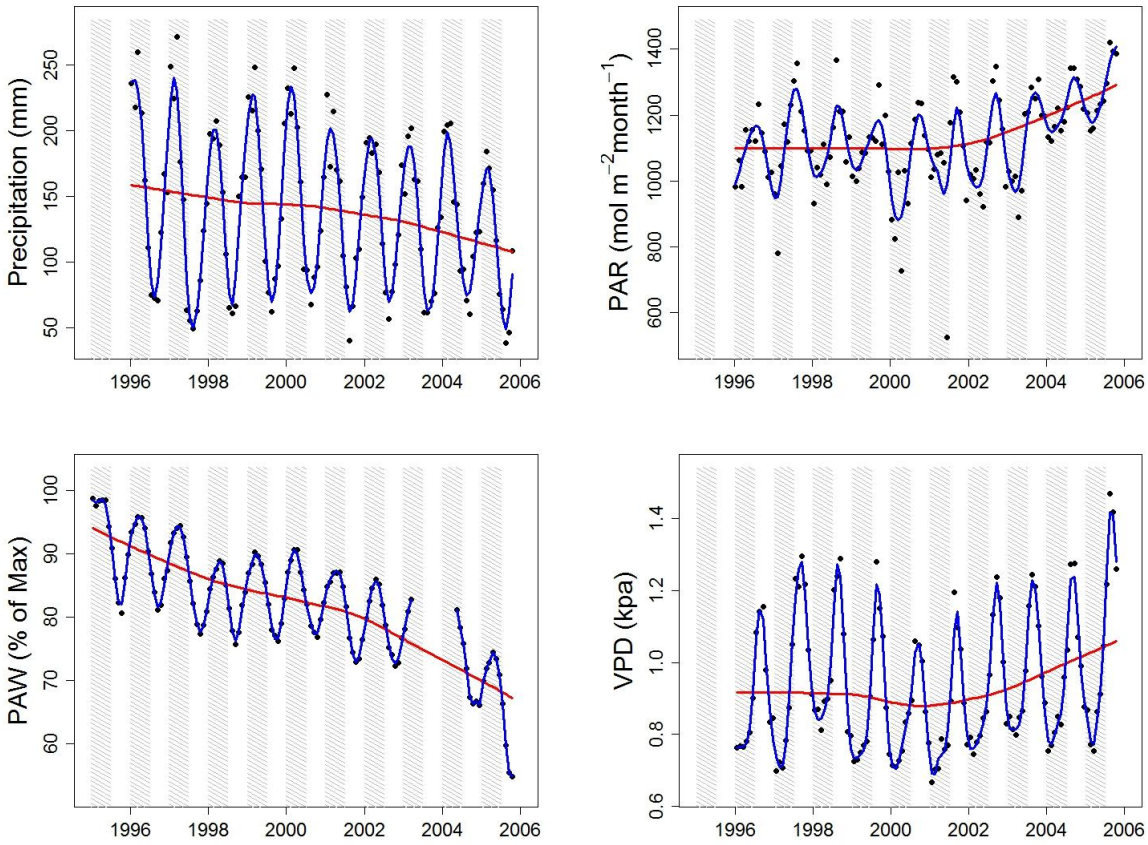

Figure 4-4. Monthly climate patterns over the Amazon region based on data from 280 meteorological stations distributed across the basin. (A) Monthly averages of Precipitation, (B) Monthly modeled photosynthetic active radiation (modeled PAR), (C) Modeled monthly plant available water at 10m depth (PAW), (D) Monthly vapor pressure deficit (VPD). Blue lines represent a smooth curve based on a loess method, and red lines represent a local regression model (spline).

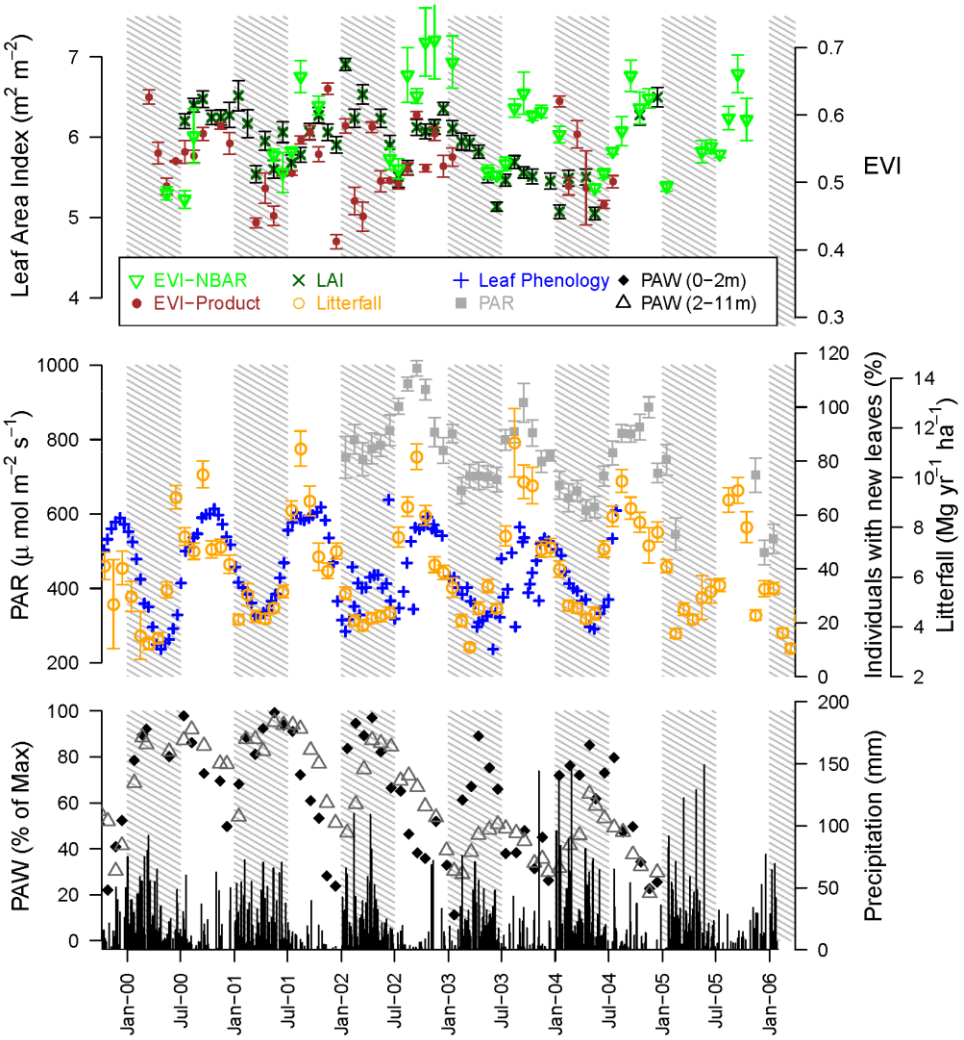

Figure 4-5. Temporal patterns of environmental and biophysical correlates of EVI. Upper panel: EVI derived from MODIS NBAR, EVI derived from the Collection 5 MODIS product screened to include only good or best quality control flags, and field-measured leaf area index (LAI) (see methods). Center panel: monthly photosynthetically active radiation (PAR), and bi-monthly litterfall and new leaf production (see methods). Lower panel: plant available water (% of maximum) at two depths (0-2m and 2-11m) and daily precipitation (mm).

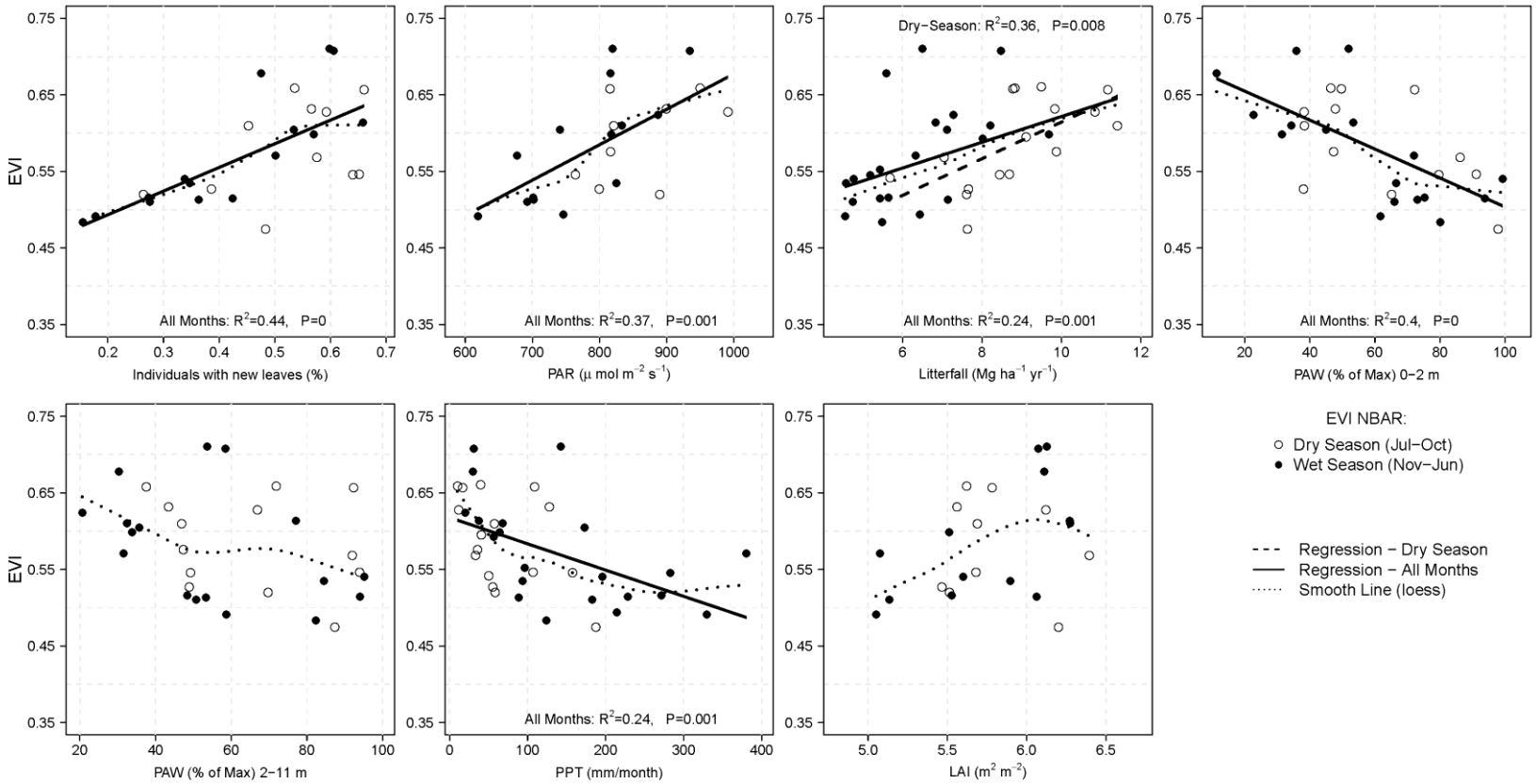

Figure 4-6. Site Specific analysis on the relationships between monthly EVI-NBAR and monthly field measurements of individuals with new leaves (%), PAR, litterfall, shallow (0-2m) and deep (2-11m) PAW, PPT, and LAI. The solid and dashed lines represent straight lines fitted using a standard linear regression models for all months and dry season; respectively. The dotted line represents a smooth line.

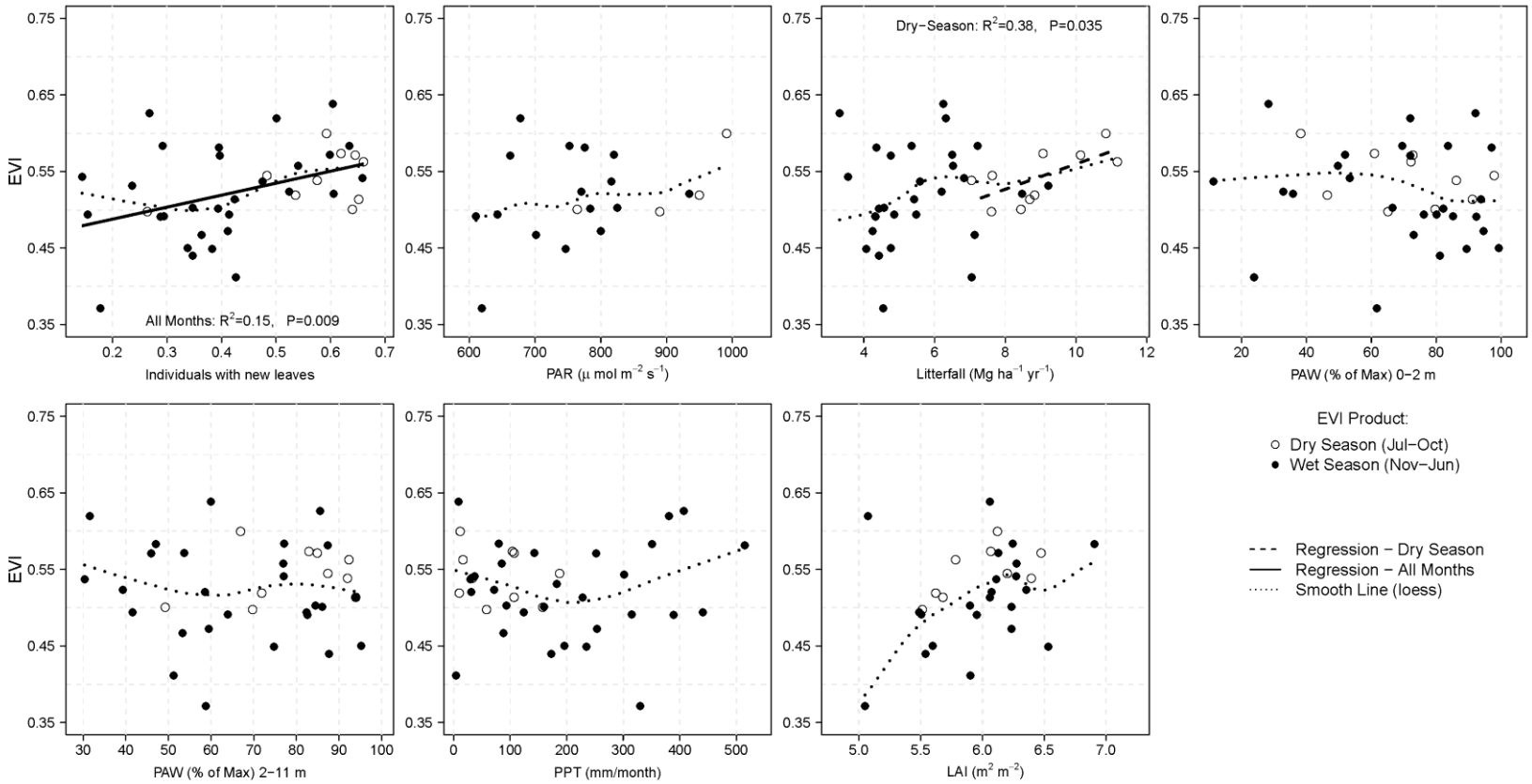

Figure 4-7. Site Specific analysis on the relationships between monthly EVI product and monthly field measurements of individuals with new leaves (%), PAR, litterfall, shallow (0-2m) and deep (2-11m) PAW, PPT, and LAI. The solid and dashed lines represents straight lines fitted using a standard linear regression models for all months and dry season; respectively. The dotted line represents a smooth line.

CHAPTER 5
POST-FIRE TREE MORTALITY IN A TROPICAL FOREST OF BRAZIL: THE ROLES OF BARK TRAITS, TREE SIZE, AND WOOD DENSITY

Introduction

The synergistic effects of droughts, forest degradation by logging, landscape fragmentation, and increased fire ignition have already rendered many Amazonian forests fire-prone (Alencar et al. 2006, 2004, Aragao et al. 2007, Aragao et al. 2008, Cochrane and Laurance 2008, Cochrane 2003, Nepstad et al. 2001, 2004, Nepstad et al. 2008). If current predictions of drier and warmer conditions (Cox et al. 2008, Cox et al. 2000) hold true, even large forested areas in Amazonia may become vulnerable to fire in the near future (Golding and Betts 2008). For example, 16 of 23 climate models predicted substantial reductions in precipitation by the mid 21st Century (Malhi et al. 2008). While this change is anticipated to have substantial effects on forest carbon storage and biodiversity (Barlow et al. 2002, Barlow and Peres 2008, 2006, Nepstad et al. 1999), there are few data available to evaluate the vulnerability of forest trees to fire.

One of the most obvious ways that understory forest fires affect tropical forests is by killing trees (Barlow et al. 2003, Cochrane and Laurance 2002, Pinard and Huffman 1997, Pinard et al. 1999, Uhl and Kauffman 1990). The characteristic low-intensity surface fires of closed canopy tropical wet and moist forest spread slowly through the understory and heat the vascular cambia of trees. When cambial cells die around the entire circumference of a tree's bole, it is expected to die (Michaletz and Johnson 2007). Based on this basic observation, a wide range of models have been proposed to measure the vulnerability of tropical trees –and hence tropical forests – to fire. The simplest (and so far most used) models assume that bark thickness is the most important trait in avoiding fire-induced cambium damage and, consequently, tree

mortality. Uhl and Kauffman (1990), for instance, studied a moist Eastern Amazonian forest and found that a simulated fire increased cambium temperatures to lethal levels of most trees with thin bark. Based on this finding, the authors speculated that the occurrence of surface fires would kill most standing trees. Pinard and Huffman (1997) used a similar approach to suggest that only individuals with bark > 18 mm thick would resist a fire in a dry forest of Bolivia.

Although back thickness has been shown to correlate well with post-fire tree mortality (Barlow et al. 2003), other traits that reduce the indirect (and negative) influences of fire on the physiology and structure of tree trunks could better represent the complex processes involved in post-fire tree mortality (Michaletz and Johnson 2007). For example, trees wounded during surface fires may experience wood decay ranging from severe to moderate depending on their capacity to compartmentalize wood decay, a process that is intrinsically associated with wood density (Romero and Bolker 2008). Likewise, simply by being large in diameter, trees may reduce the indirect effects of fire on tree mortality by being resistant to wind throw (Larjavaara and Muller-Landau 2010), less likely to be killed by branch and tree fall from other trees, and less likely to have their circumference heated during fires (Gutsell and Johnson 1996). Thus, large individuals may be more likely to survive surface fires than smaller trees with equally thick bark. Similarly, tall trees may disproportionally survive fires because their crowns are less likely to be damaged by fire.

Given the predictions of increasing fire frequencies in the tropics, it is important to elucidate the factors that render trees susceptible to fire-induced mortality. Here, I conducted two sets of related experiments to improve our understanding of the roles of

plant traits in avoiding tree mortality. I first evaluate which bark traits best predict rates of temperature change (R) of the vascular cambium during experimental bole heating. I use the exact solution of Newton's Law of cooling to calculate R (Appendix C for the reasoning behind the choice of Equation 3-1), a measure of how much conductive and convective heat is transferred through bark over time (the inverse of cambium insulation). My predictions are that: 1) bark thickness is inversely related to R and is the most important bark trait in preventing the cambium temperature from rising to lethal levels; 2) that R increases as a function of bark water content due to water's high conductivity; and, 3) that bark density is negatively associated with R, given that the greater the density, the lower diffusivity (Dickinson 2002; see Appendix C also).

While in the first set of analyses mentioned above I evaluate the important bark traits for cambium insulation, in the second set of analyses I test which plant traits best predict likelihoods of fire-induced tree mortality, including R, wood density, tree height, and diameter at breast height (dbh). I use data from a large-scale fire experiment located in the southern Amazon to test the following predictions: 1) increasing tree dbh and height decrease the likelihood of fire-induced tree mortality, not only because larger individuals tend to have thicker bark, but also because they have traits that reduce the indirect effects of fire; 2) decreasing R (higher cambium insulation) increases tree survivorship; and, 3) fire treatments lead to higher tree mortality close to the forest edge compared to the forest interior, given that fire intensity is expected to be higher at the edge relative to the interior (Cochrane and Laurance 2002).

Methods

General Approach and Site Description

The study was conducted in a transitional forest in the southern part of the Amazon Basin (13^{0}04'S, 52^{0}23') (Appendix D), where average annual precipitation is 1,800 mm and the dry season extends from May to September (Balch et al. 2008). To evaluate the importance of different bark traits in preventing fire-induced tree mortality, I conducted a series of field experiments. First, I heated the outer bark of trees with a propane torch to relate heat transfer rates (R; inversely related to cambium insulation, with units of ^{o}C second^{-1}) to bark traits. Second, I measured the bark thickness of 1,000 individuals representing 24 of the most common species in the study region to develop a predictive model of bark thickness as a function of tree diameter at breast height (dbh). Third, based on predicted bark thickness, I estimated R (referred as R_{hat}) for each tree growing in the area of a large-scale fire experiment. Fourth, I tested several statistical models of tree mortality as a function of R_{hat} under different experimental fire regimes. Finally, to test the importance of different plant traits in predicting fire-induced tree mortality, I compared the slope of models that included only R_{hat} with slopes from models that included tree height, dbh, or wood density (derived from the literature; Chave et al., 2006).

Modeling Cambium Insulation

During the dry season of 2008, cambium vulnerability to fire-induced damage was estimated as the rate of change (R; units of ^{o}C second^{-1}) in cambium temperature (CT) as a function of the air temperature adjacent to the outer bark, which was heated using a torch. I first removed a 5 cm x 5 cm sample of bark at 25 cm above the ground from each of 105 randomly sampled individuals, representing 18 species and ranging from

10-121 cm in dbh. These samples were taken to the lab for measurements of thickness (BT), density (ρb), and moisture content (BMC), following the procedures in Uhl and Kauffman (1990). Immediately following bark removal, a thermocouple was inserted between the inner bark and xylem (i.e., in the vascular cambium) and a second thermocouple was placed on the surface of the outer bark. The air adjacent to the outer bark of each tree was then heated using a propane torch coupled with a metal plate placed in front of the flame to prevent direct thermocouple contact. Temperatures in the vascular cambium and in the air adjacent to the outer bark were recorded every 10 seconds for 13 minutes, which allowed detection of changes in cambium temperatures in even thick-barked species. Using an asymptotic regression model (eq. 1; see also Appendix E), I estimated the rate of change (R in eq. 1) in CT as a function of cumulative air temperature at the outer bark, which integrates the colinear variables of time and air temperature adjacent to the outer bark into a single variable. To identify the most important predictor of R, I compared models with predictors of BT, BMC, and ρb using the Akaike Information Criterion (AIC, Burnham and Anderson, 2002) and hierarchical partitioning analysis. The latter method partitions the variance relative to R shared by two predictors into the variance of R attributable to each predictor uniquely (Murray and Conner 2009). Once the best model relating R and bark traits was selected, it was used to predict R for each individual in the fire experiment, referred to as R_{hat}. Note that the higher R_{hat}, the lower cambium insulation and the thinner the bark thickness.

$$CT = Asymptote + (CT_i - Asymptote)e^{CTFe^R} \quad (5\text{-}1)$$

Linking Tree Mortality and Cambium Insulation (R)

Data from a large-scale fire experiment was used to assess probabilities of fire-induced tree mortality as a function of R_{hat}. In this experiment (Fig. 5-1), three plots of 50 ha each were established in 2004 in Mato Grosso, Brazil (details in Balch et al. *submitted*): a control with no signs of recent fires; a plot that was experimentally burned twice (2004 and 2007; plot B2); and, a plot that was experimentally burned four times from 2004 to 2007 (plot B4). Within each of these plots, I conducted yearly mortality censuses for individuals 10-19 cm dbh (N=6 transects of 10 m x 500 m per plot) and 20-39 cm dbh (N= 6 transects of 20 m x 500 m per plot). All trees with dbh ≥ 40 cm were assessed annually for mortality in all 50 ha plots. In total, 6,570 individuals of 97 tree species were sampled for dbh (see Fig. 5-1). Height was measured for a subset of these, with 4,071 individuals sampled. Wood density was derived from the literature for 87 species (Chave et al. 2006). Note that the northern edge of the experimental area was adjacent to an open field (Appendix D).

Because some sampled trees were not charred during the experimental fires due to burn heterogeneity across years (details in Balch et al. 2008), they were grouped into the following categories, as summarized in Fig. 5-1:

Never charred and located in the control plot, in plot B2 (Charred 0x B2), or in plot B4 (Charred 0x B4). Note that mortality in the control was expected to be lower than in the burned plots even for trees not directly affected by the experimental fire (i.e., a strong treatment effect) due to the high number of falling trees in plots B2 and B4 and the associated changes in forest microclimate and canopy damage.

Charred once (either in 2004 or 2007) and located in plot B2 or charred once at any time between 2004 and 2007 and located in plot B4 (Charred 1x B4). Note that the fires of 2004 (Charred 04) and 2007 (Charred 07) apparently

differed in intensity (see Appendix E), justifying their separation into two distinct groups. In plot B4, however, this separation into groups was not possible because of the large number of fire treatments and the small sample size within each group for each species.

Charred twice and located either in plot B2 or in plot B4 (Charred 2x).

Charred three times and located in plot B4 (Charred 3x).

Charred four times and located in plot B4 (Charred 4x).

Given that BT could not be measured on all sampled individuals for logistical reasons and because the measurements could increase mortality rates, I developed predictive models of bark thickness (BT) for the 24 most common species in the region based on dbh of 1,000 trees sampled in an adjacent area to the fire experiment (see Appendix F). From BT, I then estimated a value for R for each individual of the 24 focal species in the fire experiment area (N=3,752).

Modeling Tree Mortality

Tree mortality and cambium insulation

To model the probability of tree mortality as a function of R_{hat} (and therefore assess the importance of R_{hat} in avoiding fire-induced mortality), I used logistic regression mixed models with fixed and random effects of R_{hat} and species, respectively. Because plot B2 was burned in 2004 and 2007, while plot B4 burned annually from 2004 to 2007, mortality assessments were carried out at different times among plots and over time. To deal with this complexity in the data set, I developed four models based on a subset of the trees located in the fire experiment (Fig. 5-1):

Model 1 included trees that were potentially affected by one low-intensity fire and were assessed for mortality after a period of one year following the experimental fire of 2004 (period: 2004-2005; plots *B1* and *B4*). Probability

of mortality was modeled as a function of R_{hat} interacting with five treatments [*Control*, *Charred 0x* (plot *B2* or *B4*), *Charred 04* (plot B2 or B4)].

Model 2 included trees that were potentially affected by one low-intensity fire and were assessed for mortality after a period of three years following the experimental fire of 2004 (period: 2004-2007; plot *B2*). Probability of mortality was modeled as a function of R_{hat} interacting with three treatments (*Control, Charred 0x, Charred 04*)

Model 3 included trees that were potentially affected by at least one moderate- to high-intensity fire and were assessed for mortality after a period of one year following the experimental fire of 2007 (period: 2007-2008; plot B2). Note that this group of trees included only those that were alive prior to the fires of 2007 and that were not charred by the fires of 2004. Probability of mortality was modeled as a function of R_{hat} interacting with four treatments (*Control, Charred 0x, Charred 07, Charred 2x*).

Model 4 included trees that were potentially affected by several fires and were assessed for mortality after a period ranging from 1 to 4 years following a given experimental fire (period: 2004-2008). Probability of mortality was modeled as a function of R_{hat} interacting with twelve treatments

To avoid bias due to spatial autocorrelation, I compared parameter estimates from the models with and without a spatial error structure (*glmer* function in R Bates and Maechler 2009; and *glmmPQL* function in R, Venables and Ripley 2002). Because the inclusion of the spatial structure did not change the results, I present here only the estimates derived from the *glmer* function (which is less likely to be biased Bolker et al. 2009). To account for the possible impact of proximity to an adjacent open field, the distance from the edge was included as a co-variate in all models for each individual. Given that R_{hat} was estimated from tree dbh, its association with mortality could simply be due to a demographic effect in which smaller individuals (with high R) die at higher rates than larger individuals, even in the absence of fire. To account for this potential demographic effect in models, the influence of R on mortality was evaluated based on

the slope of the regression for mortality in the fire treatments contrasted with the slope of the control. Therefore, if slopes for mortality in the control and fire treatments were equally steep, R was considered to have no effect on fire-induced tree mortality.

Other correlates of fire-induced tree mortality

To compare the influences of R_{hat}, plant size (height and dbh), and wood density on tree mortality, slopes of Model 4 were compared to the slopes of models that included each plant trait as a single covariate. More specifically, the relative importance of a given variable was based on the magnitude of the difference between slopes for mortality of the control and burned treatments. All covariates of mortality were standardized by two times the standard deviation of the entire population (Gelman and Hill, 2007), making it possible to compare the magnitude of slopes across models and treatments (note that slopes associated with R_{hat} are presented in absolute terms to facilitate comparison with slopes of other models). The potential effects of spatial autocorrelation were evaluated for all models but did not change the results (see section above on Modeling Mortality). Note also that covariates of mortality were not included in a single model because they were multi-collinear and had different sample sizes; when all covariates were included in the same model, the degrees of freedom were reduced substantially.

Results

Cambium Insulation (R)

Cambium temperatures (CT) were perhaps naively expected to increase steadily until they reached an asymptote at the torch temperature (i.e., temperature adjacent to the outer bark), but temperatures never exceeded 100°C because all the fire energy was absorbed in the process of boiling water (i.e., latent heat of vaporization, Fig. 5-2).

Consequently, the presence of moisture in the bark not only prevented CT from rising above 100°C, but also reduced the gradient in temperature (or introduced a step) between the air adjacent to the outer bark and the cambium. For instance, the air adjacent to the outer bark heated to 400°C for 10 minutes was expected to have created a differential in temperature with the vascular cambium of 400°C minus the initial cambium temperature (CT_i). The presence of water in the bark, however, constrained this differential to 100°C minus CT_i. Despite the constraint imposed by water, the amount of water in bark showed only a weak positive relationship with R (Fig. 5-2C). Bark thickness alone was the best predictor of R; as bark got thicker, the rates of change in temperature through the bark decreased exponentially (Fig. 5-3). Inclusion of ρb and BMC in predictive models of R was not justified (Table 5-1), as the model with only BT was the most parsimonious.

Table 5-1. - Model comparison using corrected Akaike Information Criteria (AICc) . In this table, we also report the number of parameters (K), the adjusted R^2, and the AICc weight for each model. BT, ρbT, BMC represent bark thickness, wood specific gravity, and moisture content, respectively.

Models	K	Adj. R^2	△AICc	Weight
BT + ρb + BMC	5	0.83	0.0	0.5
BT	3	0.83	1.3	0.3
BT + ρb	4	0.83	2.5	0.1
BT + BMC	4	0.83	2.8	0.1
BMC	3	0.14	146.5	0.0
ρb	3	0.03	156.7	0.0
Intercept	2	0.00	158.5	0.0

Cambium Insulation and Tree Mortality

The relationships between R_{hat} and tree mortality varied among years and treatments (Fig. 5-4). In the year following the low-intensity fire of 2004 (*Model 1*), mortality was weakly associated with R_{hat} (and hence BT) and was similar between the control and the burned plots (Fig. 5-4 and Appendix F; note that both standardized R_{hat} and the associated BT are presented in this figure). Three years following the 2004 fires (*Model 2*), survival in the control was higher than in the burned plots, but R_{hat} was still a poor predictor of mortality (Fig. 5-4 and appendix G). These results indicate that the fires of 2004 had minor effects on tree mortality compared to the control and that R was a good predictor of fire-induced tree mortality.

While fire-induced tree mortality was poorly associated with R_{hat} following a single low- to moderate-intensity fire, mortality was highly associated with R_{hat} during the year following the fire of 2007 (*Model 3*; which was followed by the fire of 2004): as R_{hat} increased, the probability of survival decreased (Fig. 5-4 and appendix H). This pattern was strong and significant for trees charred twice but also for non-charred trees, perhaps because smaller trees (with low cambium insulation) were more likely to be damaged by fire-induced branch and tree fall than large trees (with high cambium insulation) in the burned plots compared to the control. Hence, there was a strong treatment effect in which tree mortality in the control plot was substantially lower than mortality in the burned plots. However, there was a lack of relationship between R_{hat} and mortality for trees charred by the fires of 2007, suggesting that one year after a fire is perhaps too short an interval to evaluate fire-induced tree mortality. As expected, mortality in the control plot showed no relationship with cambium insulation.

When the effects on mortality of all of the 12 fires were included in a single model (*Model 4*), there was a positive relationship between tree mortality and R for trees charred once, twice, and three times (Fig. 5-4). In other words, charred trees showed strong, inverse relationships between mortality and cambium insulation for the period 2004-2008, but some new patterns emerged from this analysis. First, non-charred trees and trees charred only in 2004 suffered high mortality across the entire range of R, indicating a strong treatment effect of recurrent fires, but a minor effect of R for this group of trees, which could be a result of an increased number of falling trees in the burned plots killing non-charred trees. Second, trees that were charred 4 times showed a high probability of surviving (e.g., similar to the control) and showed no relationship with R_{hat}. This could be attributed to the fact that only the highly fire-resistant trees survived four fires (see Balch et al. submitted).

The inclusion of distance from the edge was highly significant in all models. This indicates that fire severity was higher at the forest edge adjacent to an open field than in the forest interior.

Other Correlates of Tree Mortality

Overall, trees with higher wood density and larger dbh showed lower probability of fire-induced mortality (Fig. 5-6), given that models with either wood density or dbh as a covariate had steeper slopes for the fire treatments compared to the control (Fig. 5-5). Further, the highest deviations from the control were observed for the fire treatments *Charred 1*, *2*, and *3x*. Tree height was strongly and negatively associated with mortality (Figs. 5-6), but mainly for non-charred trees and for trees in the control plot. In other words, likelihood of survival increased as a function of increasing tree height at similar rates between trees in the control and fire treatments. The exception to this pattern was

for trees burned during the fires of 2004 in plot *B2*, which had steeper slopes than trees in the control as a function of increasing height (Fig. 5-6). In absolute terms, R_{hat} and dbh were equally important in avoiding fire-induced tree mortality, while wood density and tree height (in particular) were apparently less important. Overall, it is difficult to separate the contribution of each variable to mortality, given that they are collinear and have different samples sizes.

Discussion

Cambium Insulation

The findings from the heating experiment support the widely-accepted notion that bark thickness is the single most important trait in insulating the vascular cambium and thus in preventing fire-induced cambium damage (Dickinson, 2002; Uhl and Kauffman, 1990; Pinard and Huffman, 1997; Michaletz and Johnson, 2007). Bark thickness alone accounted for 82% of the rate of change in cambium temperature (expressed as R) as a function of cumulative air temperature on the outer bark. Nevertheless, the presence of water in the bark also had substantial and potentially contrasting influences on R. On one hand, water in the bark constrained bark temperatures to an asymptote at 100˚C, even when the temperature of the air adjacent to the outer bark was much higher than 100˚C. This finding indicates that theoretical models of fire-induced cambial damage that do not account for latent heat of vaporization in the bark (e.g., Dickinson, 2002) could underestimate the differential in temperature between the fire and the cambium and, in turn, underestimate the time before fire-induced cambial damage occurs. On the other hand, the high conductivity of the water in the bark could increase bark diffusivity compared to dry bark tissues, thus increasing R (i.e., faster increases in CT during fires). In fact, it is suggested that the smaller the proportion of living tissues in the bark

(i.e., live inner vs. dead outer bark), the greater the cambium insulation, because dry, corky bark has numerous air spaces that provide better fire insulation (i.e., lower heat conductivity) than wet, dense phloem (Devet 1940 cited in Hare 1965). It is noteworthy that the opposite result for trees in a mixed conifer forest has been reported (van Mantgem and Schwartz 2003): the greater the proportion of bark composed by the phloem, the lower CT, presumably due to the high heat capacity of the phloem. Based on fig 2 in that study (p.346), nevertheless, it is reasonable to speculate that the latent heat of vaporization was the major factor influencing the rates of increase in CT for smaller trees (e.g., those with greater proportion of the bark composed by the phloem), as opposed to heat conductivity or heat capacity [see Reifsnyder et al. (1967) for a detailed discussion on the effects of BMC on heat capacity]. I suggest that the roles of bark water content are important and should be studied in greater depth.

Bark Correlates with Tree Mortality

Although BT appears to be the most important plant trait in preventing fire-induced cambial damage, its importance in preventing fire-induced tree mortality has not been widely tested for tropical forest trees and may be modulated by other traits. For example, during low intensity fires, heat is often distributed unevenly around the boles of trees, causing only partial damage to the cambium around a small proportion of the circumference of tree boles (Michaletz and Johnson, 2007). In such cases, plant traits that reduce the indirect (and negative) influences of fire on the physiology and structure of tree trunks may be even more important in avoiding tree mortality than BT alone, which provides cambium protection against the direct effects of fire. Here, I show that R_{hat} (and hence BT) was an important predictor of direct fire-induced tree mortality, particularly for moderate to high-intensity fires. Trees experiencing the fire of 2007

(which followed 1, 2, or 3 fires) were extremely fire-resistant for BT ≥ 21 mm (i.e., 75-100% probability of surviving) and fire-sensitive for BT ≤ 5.3 mm (0-25% probability of survivorship). This threshold is in the same range as that suggested by Pinard and Huffman (1997), who found that trees with BT ≥ 18 mm exhibited high resistance to understory forest fires.

Despite the generally strong relationship between tree mortality and bark thickness, I found no meaningful relationship between tree mortality and cambium insulation for trees charred only once in either the 2004 or 2007 fires. Furthermore, there were two common thin-barked species, *Aspidosperma excelsum* and *Sloanea escheri*, that exhibited high survivorship even when charred (Balch et al. *submitted*). These findings indicate that mechanisms associated with plant traits other than cambium insulation could also influence fire-induced tree mortality. For example, wood density has been shown to slow the progress of wood decay of damaged living trees (Romero and Bolker 2008), which should reduce the likelihood of mortality after cambium-exposing damage. Although our data suggest that wood density is important for post-fire survival, the evidence is not compelling. Similarly, I found that tree mortality decreased with increasing dbh. Although this relationship could result solely from the strong and positive relationship between BT and tree size, an alternate (or concurrent) explanation is that large trees are less likely to be killed by other falling trees and that the likelihood of the entire circumference being exposed to cambium-killing temperatures decreases with bole size (Gutsell and Johnson 1996). However, in this study I was unable to separate the individual effects of dbh from bark thickness on mortality. Finally, while tree height was apparently less important than other traits in

avoiding fire-induced mortality, height is expected to become more important during intense fires that have the potential to damage tree crowns.

Forest Resistance to Fire

Given the minor effect of the 2004 fires on post-fire tree mortality, it is reasonable to infer that this forest is relatively resistant to non-recurrent, low-intensity fires (as measured by fire-induced tree mortality in individuals with dbh ≥ 10 cm; see Balch et al. *submitted* for a discussion about smaller trees). This resistance may result from long-term tree adaptations to cope with fire in the region. Although I am unaware of formal estimates for fire return interval, transitional forests of Mato Grosso are flammable during most dry seasons due to elevated vapor pressure deficits (Balch et al. 2008; see also Blate 2005). Furthermore, they have been exposed to human-associated fire ignition for millennia, given the presence of indigenous groups in the region who make use of fire as a management tool (e.g., for hunting and agriculture). It is nevertheless apparent that the fire-resistance of this tropical forest was reduced substantially by recurrent fires, particularly near the forest edge adjacent to an open field. This edge effect is likely related to higher fire intensity caused by drier fuels, to higher density of small with low resistance to fire-induced cambium damage, or both. Also, changes in forest microclimate alone could lead to increased fire-induced tree mortality (Cochrane and Laurance 2002).

Predicted decreases in rainfall over portions of the tropics may cause extensive forest dieback in the next 50 to 100 years, particularly in the eastern Amazon (Cox et al. 2000; Malhi et al. 2008). Synergistic effects of recurrent fires and forest degradation, however, could drive this process much more rapidly (Nepstad et al. 2008). In predicting the rate of forest loss due to recurrent fires, it is evident that while cambial

insulation is an important determinant of fire-induced tree mortality, other plant traits also play important roles in avoiding fire-related death. Furthermore, the evidence that fire-related mortality occurs even when tree boles do not exhibit physical charring reminds us that fires influence several processes at the stand level. Examples of these processes may include proximate fire-induced branch or tree fall, fire damage to roots or leaves, or various indirect processes triggered by fire (e.g., disease, drought-related death). I conclude that in-depth assessments of fire-related mortality in tropical forests are needed for predicting the trajectories of Amazonian forests in the face of expected increases in fire associated with frontier expansion and episodic droughts related to climate change.

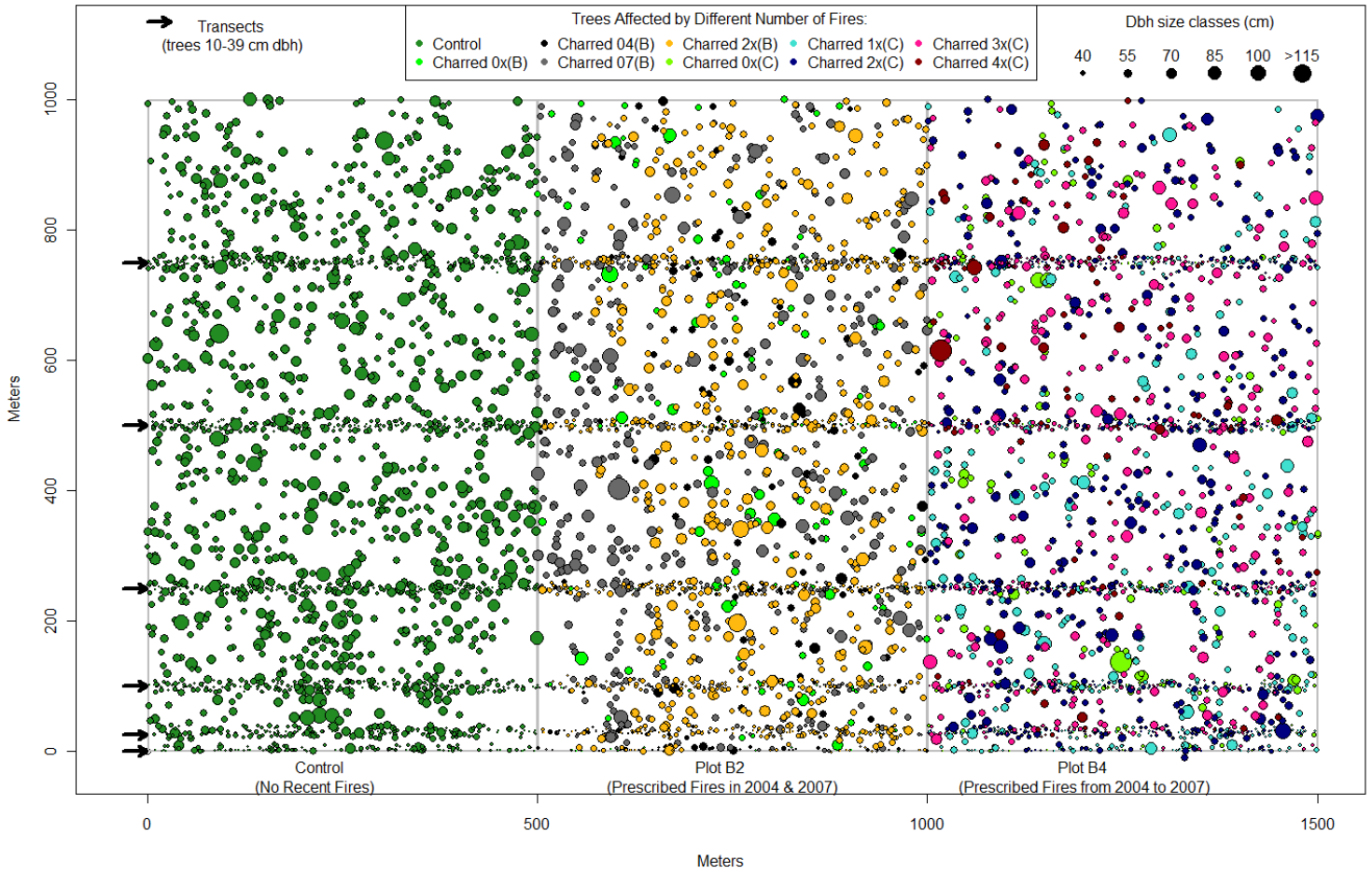

Figure 5-1. Map showing the spatial distribution of trees located in three 50 ha plots: plot A (Control); plot *B2* (burned in 2004 and 2007); and, plot *B4* (burned yearly between 2004 and 2007). Each color represents the number of times a given tree was charred. The size of symbols represents the dbh of each tree. Note that only trees ≥ 40 cm dbh were censused across the entire 150 ha. Trees < 40 cm were sampled along 6 transects (black arrows).

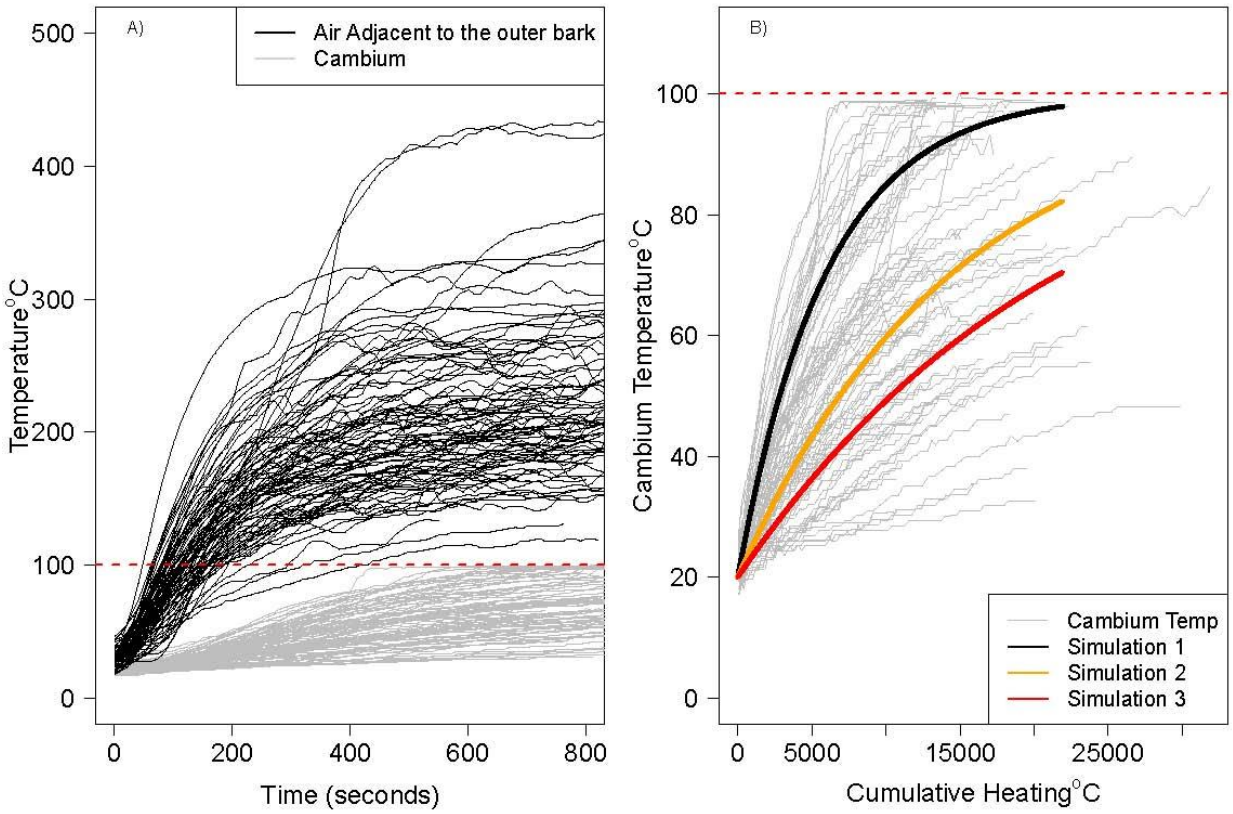

Figure 5-2. Overall results from the bark heating experiment: A) air temperature adjacent to the outer bark heated by a propane torch (black lines) and cambium temperature (gray lines) as a function of time; B) cambium temperature as a function of cumulative air temperature adjacent to the outer bark (*CTF*). The dashed red lines in both figures represent 100 ^{o}C. Simulations 1-3 represent three examples of R: lower quantile, median, and upper quantile.

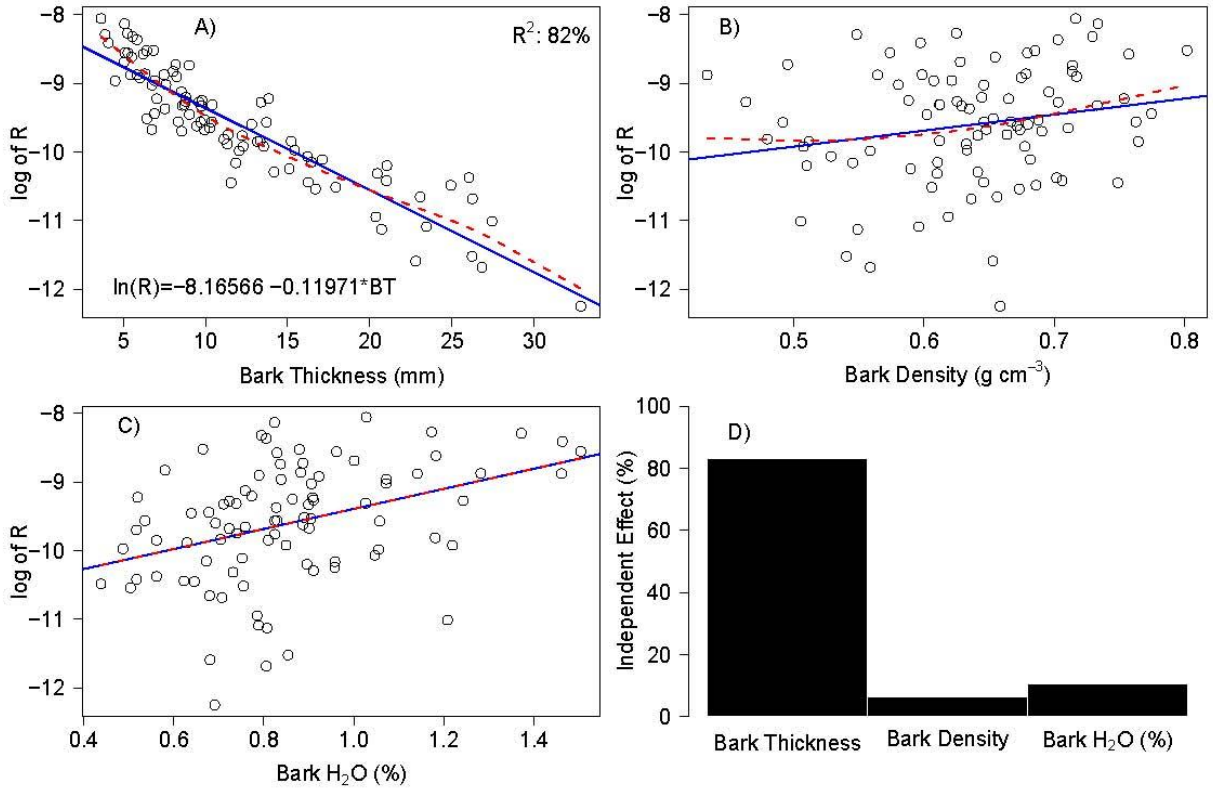

Figure 5-3. Relationships between rates of change in cumulative heating (*R)* and A) bark thickness, B) bark density, and C) bark moisture content. Figure D indicates the independent effect of each variable on *R*.

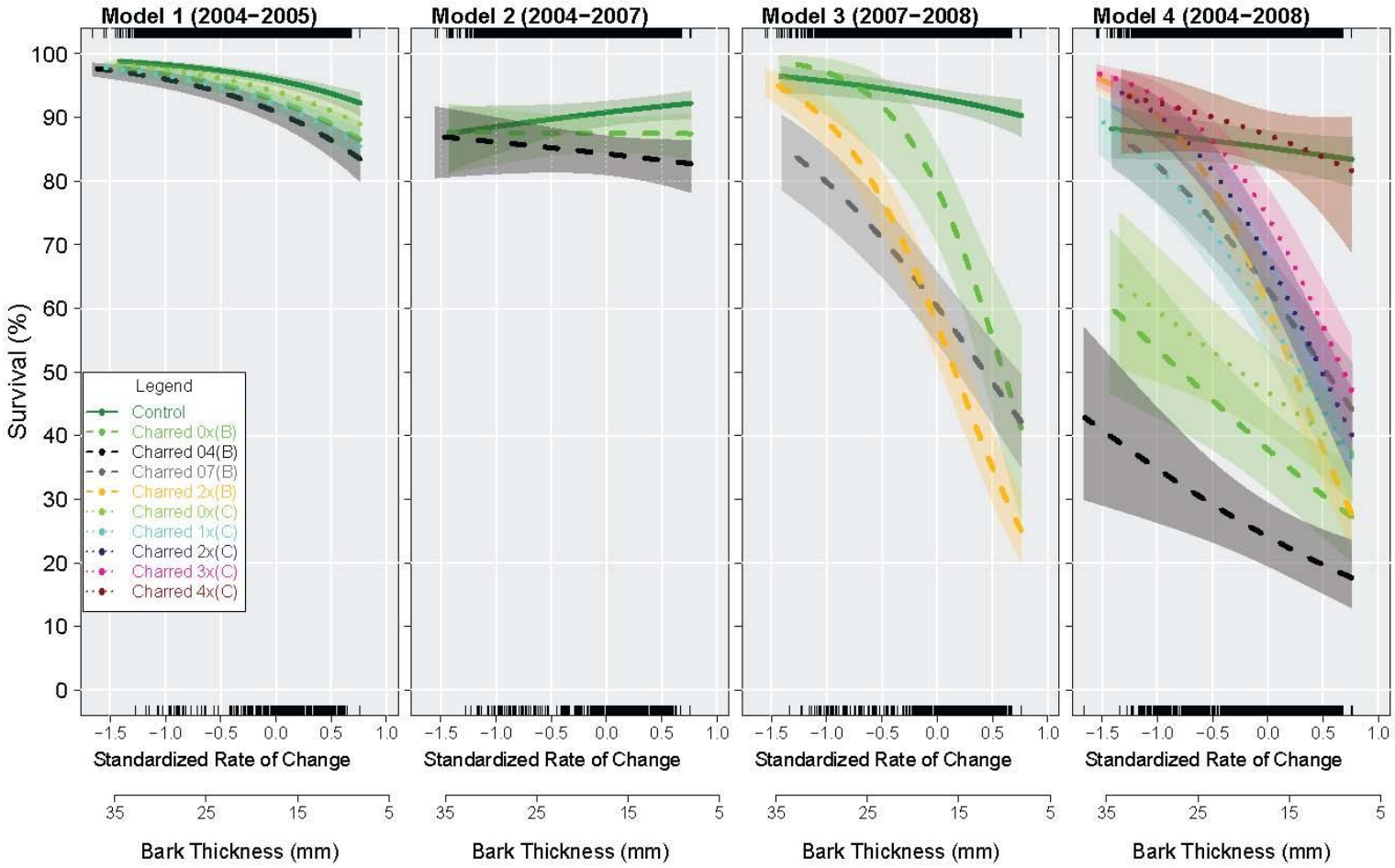

Figure 5-4. Survival probabilities of trees with dbh ≥ 10 cm dbh as a function of R_{hat}, a proxy of cambium insulation derived from the heating experiment. Each panel represents one logistic model (Models 1, 2, 3, and 4). Each color represents the number of times a given trees was charred in different treatments. The first x-axis represents the standardized rate of change (R_{hat}),while the second x-axis indicates the bark thickness associated with a given R_{hat} (note that R and bark thickness are inversely related).

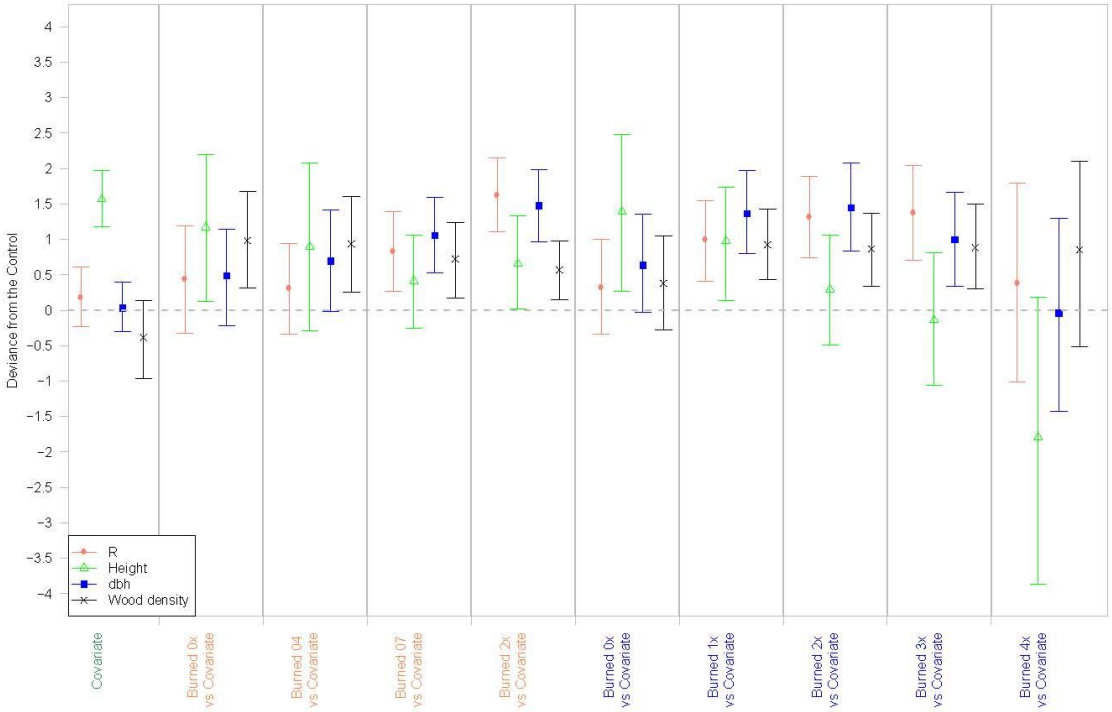

Figure 5-5. Relative influence of R_{hat}, tree height, dbh, and wood density on tree mortality for different fire treatments. On the x-axis, the control (A) is represented by green, B2 by orange, and B4 by blue. Note that the influence of each variable was inferred from on the magnitude of the difference between slopes of the control and fire treatments. Note also that all co-variates of mortality were standardized (centered and then divided by 2 times the standard deviation) and that R is presented in absolute terms for comparison with other plant traits.

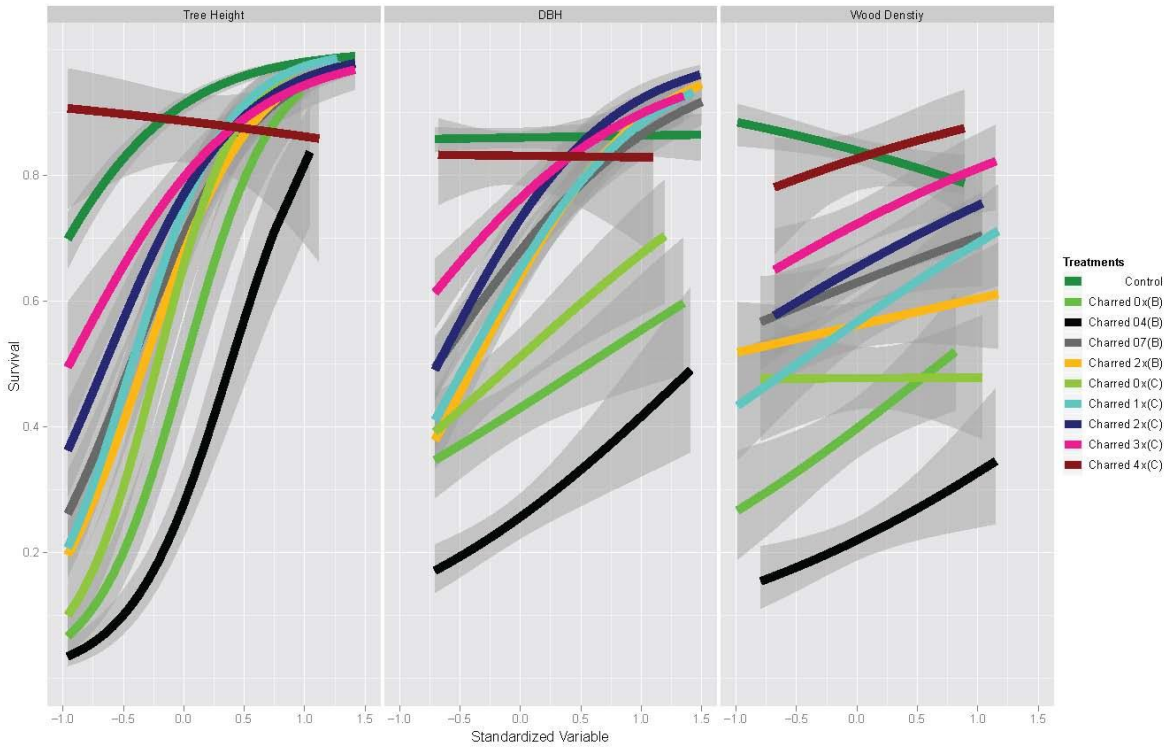

Figure 5-6. Probability of tree survival as a function of standardized tree height (left panel), dbh (middle panel), and wood density (right panel). Each color represents a different fire treatment.

CHAPTER 6
CONCLUSION

The synergistic effects of drought, forest degradation by logging, landscape fragmentation, and increased fire ignition already exert strong influences on the stability of tropical forests. In combination with climate change, they may cause large portions of tropical forests to suffer dieback events, with important implications for forest carbon stocks, product yields, and biodiversity. Yet, very little is known about the thresholds in environmental stresses beyond which regime shifts may occur. In my dissertation, I assessed the vulnerability of Amazonian forests to severe drought and fire events, with focus on the C cycle.

I first report on findings from a partial throughfall experiment located in a moist, eastern Amazonian forest. In particular, I show that wood increment, net primary productivity (NPP), and leaf area index (LAI) all declined in response to the drought treatment of 2-3 years. Following protracted water stress, substantial increases in mortality of large trees were observed, corresponding to sustained reductions in plant available water. The results from this experiment suggest that, if the general response of Amazonian forests to drought is similar to those recorded at the Tapajos Forest, a drier future climate is likely to have major consequences to carbon stocks of Amazonian forests (e.g., reductions of 25% of standing live biomass). This view receives support from findings of another throughfall exclusion experiment located in a moist, eastern Amazon forest (see Meir et al. 2009 for a review of these experiements), where rates of drought-induced tree mortality following 3-4 years of throughfall exclusion were reported within the ranges I found in my dissertation.

Whereas the throughfall experiments mentioned above provide new and important insights into drought-vegetation relations in Amazonia, they cover a relatively small area and may not represent the spatial variability of forests' susceptibility to drought across the Amazon. To deal with this limitation of field experiments, several studies took advantage of the 2005 drought (one of the most severe droughts over the past 100 years) to evaluate how forests respond drought over a greater spatial extent. Based on results from a network of permanent plots spread across the Amazon, Phillips et al. (2009) found that several forests were sensitive to the 2005 drought, with mortality increasing at rates that were high enough to reverse a trend in C accumulation of 0.45 PgC yr^{-1} to a -1.2-1.6 PgC annual source. The results in Phillip et al. (2009) appear to substantiate the notion that Amazonian forests are, overall, sensitive to severe, episodic droughts. Also, these results indicate that, if droughts become more intense and frequent in the future, large amounts of carbon will be released to the atmosphere.

Despite the apparently agreement among studies that Amazonian forests are drought-sensitive, there is still no agreement about the thresholds of drying of the basin that would cause regime shifts. In a controversial article, Samanta et al. (2010) claimed to debunk some conclusions from most recent IPCC report that portions of dense forests could "react drastically" to "slight reductions" in precipitation in the near future resulting from climate change. More specifically, Samanta et al. 2010 used satellite-based measurements of vegetation photosynthetic activity from MODIS to show that Amazonian vegetation remained relatively irresponsive to the drought encountered in 2005. These results contrast with previous studies that assessed forest responses to the drought of 2005; studies that showed that vegetation over Amazonia either became

more productive (Saleska et al. 2007) or experience elevated tree mortality (Phillips et al. 2009). Given these apparently conflicting results among different studies of the climate-productivity relationship, and the importance of these results for understanding the impacts of climate change on the terrestrial carbon cycle, there was clearly a need to properly quantify the mechanisms driving the variability of vegetation productivity of the world's tropical forests. Thus, in an effort to reconcile results from these field- and satellite-based studies, I conducted two experiments.

First, using a CARLUC process-based model, I estimated the effects of climate variability on total carbon stocks and fluxes of vegetation across the Basin and of forests where permanent plots from RAINFOR are located. I hypothesized that CARLUC simulations, which were driven by climate variability alone, would describe C accumulation over the Amazon from 1998 to 2004, but C losses during the 2005 drought (Phillips et al. 2009). While CARLUC simulated increases in C pools during the dry season from 1995 to 2004, followed by a reduction in 2005, the magnitude of the reduction reported in my dissertation was less pronounced than in Phillips et al. (2009). One possible explanation for this difference between studies is that the Tapajos Forest (where the mortality function in CARLUC was developed) was more drought resistance than RAINFOR forests on average.

Second, I conducted a study that combined analysis of climate data, field measurements of forest photosynthesis, and an improved satellite-based measure of forest photosynthetic activity (EVI). From this study, I show that none of the climatic variables tested (precipitation, vapor pressure deficit, photosynthetically active radiation) contributed to explaining inter-annual variability of EVI across the Amazon. Instead, I

found evidence that suggest that production of new leaves could play an important role in Basin-wide, inter-annual EVI variability, but not necessarily in changes in GPP or NPP. These results suggest that it is still unclear whether EVI can be employed as a tool to measure the vulnerability of tropical forests to drought. Also, they suggest that several mechanisms could operate simultaneously to explain the contrasting results between field-based studies and those that use satellite-based measurements to assess forests' vulnerability to drought. For example, GPP (expressed as EVI) appears to increase due to the production of new leaves and increased PAR during droughts, whereas aboveground net primary productivity (ANPP) measured in the field concurrently decreased because of higher tree mortality and increased respiration associated with lower PAW and higher temperatures. Moreover, the allocation of non-structural carbohydrates to belowground processes may have increased, given that GPP was higher and ANPP lower during the drought of 2005. It is also possible that MODIS cannot detect deaths of the large trees that store large amounts of carbon but that account for only a small portion of the canopy. This should be the topic of further research.

After evaluating the vulnerability of Amazonian forests to drought, I studied the mechanisms associated with fire-induced tree mortality in a tropical forest in the southern Amazon. Based on this study, I present two novel findings that improve our ability to characterize tropical forest vulnerability to fire. First, I found that the presence of water in the bark reduced the differential in temperature between the fire and vascular cambium due to boiling water in the bark. This result is important because it shows that theoretical models of fire-induced damage that do not account for the effects

of latent heat vaporization (boiling water) in the bark substantially underestimate the time before fire-induced cambial damage occurs. Second, I show that the experimental fires influenced mortality through several processes that were not directly related to cambium protection against fire-induced damage, suggesting that plant traits that reduce the negative and indirect effects of fire on post-fire tree mortality should also be considered in the assessments of tropical forests' vulnerability to fire.

In conclusion, I found evidence that droughts and fires exert strong influences on the terrestrial carbon cycling, but no evidences for imminent regime shifts in the region driven by climate change alone. However, human activities that reduce forest resistance to fire and in turn increase the likelihood of exotic grass invasions into forests may change these conclusions. Poor timber harvest practices, for example, can substantially increase canopy openness of tropical forests, which elevates forest flammability by i) promoting sunlight-induced drying of fuel loads and ii) increasing rates of fuel load accumulation on the forest floor. A thin canopy can also support the establishment of invasive C_4 grasses from forest-neighboring pastures, which can out-compete native vegetation and elevate forest flammability permanently, potentially causing a shift in stable state from tree to grass dominance. Because the two most common of the intensive land-use practices in the Amazon, cattle ranching and swidden agriculture, both use fire as a management tool, ignition sources for forest fires are common (Nepstad et al. et al. 2001). In an extreme scenario, these feedbacks among fire, vegetation, and climate can drive large portions of tropical forests to impoverished systems.

APPENDIX A
METEOROLOGICAL STATIONS

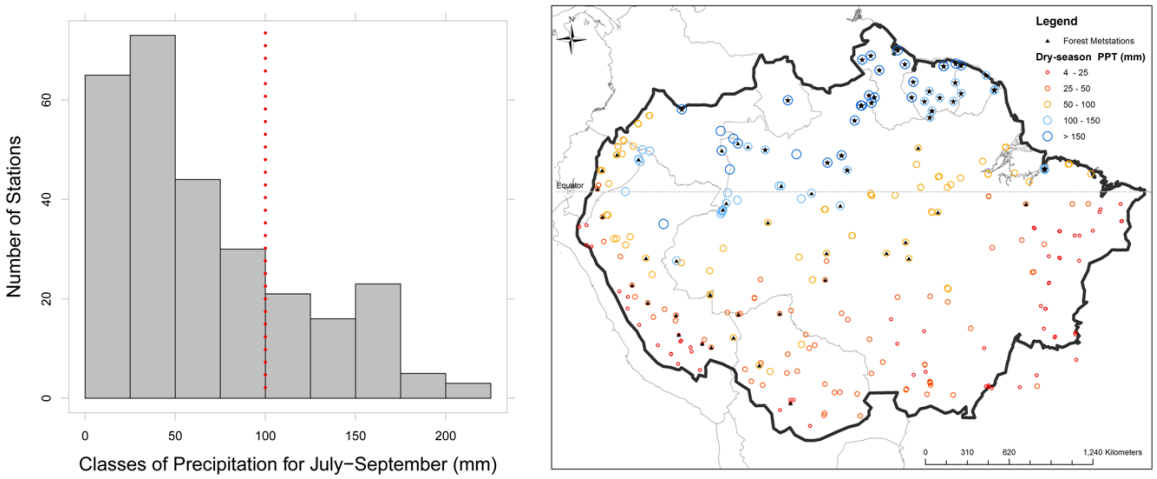

Figure A-1 - Upper panel: Number of meteorological stations per classes of precipitation (average between July and September); the dashed-red line separates the number of mestations with (left) and without (right) a dry season. Note that according to the standard definition of dry season as the average precipitation < 100 mm month-1, the period July-September chosen in this study captured the dry season in 76% of the meteorological stations (212 of 280). For the 68 remaining stations (24%), the average precipitation from July to September was not representative of the driest months of the year in 37 of them (13% of total) concentrated in the Northern Amazon (black stars).

APPENDIX B
VARIABILITY IN VEGETATION INDEX

Here I assessed whether the choice of months (July-Sept) could have influenced the spatial patterns of EVI (West-East and North-South), given the potential for lags in vegetation phenology (e.g., leaf flushing) across the wide ranges of latitude and longitude reported in this study. For instance, one could hypothesize that leaf flushing occurs predominantly in July-October in the East Amazon, October-November in the Central Amazon, and November/December in the Western Amazon; temporal-spatial patterns that could create trends of lower EVI from East to West of the Amazon.

Xiao et al. (2006) mapped the months with highest EVI (calculated from MODIS collection 5 reflectances) across the Amazon in 2002 (Fig. 5b in Xiao et al. 2006). If spatial patterns of EVI were closely associated with gradients in vegetation phenology, the results from Xiao et al. (2006) are likely to show a consistent shift in the month of highest EVI from West to East and/or South to North of the Amazon. Based on Fig.5*b* from that study, I detected no evidence of gradients in vegetation phenology that could explain the strong gradients found in our study.

Because Xiao et al. (2006) mapped peak EVI in only one year, I repeated their analysis using the GIMMS AVHRR NDVI data set from 1981 to 2008 (Figure A2a; upper panel) (Tucker et al. 2005). The GIMMS data generally confirmed the lack of a clear spatial pattern in the timing of peak EVI/NDVI in the Amazon with one exception: there was a potential gradient in the month with highest NDVI from South (earlier in the dry season) to North (later in the dry season/early in the wet season). To make sure that this potential gradient did not influence our conclusions, all statistical models between EVI and climatic variables, for both forest and non-forested areas (Figure A1b; lower

panel), included longitude and latitude as co-variates. While we do not exclude the possibility that the focus on the July-September period may have had some effect on the spatial patterns of EVI, we are confident that the gradients in NBAR-EVI from West to East were not merely an artifact of spatial phenological gradients. Also, the inclusion of latitude and longitude in the statistical models between EVI and climatic variables minimized any potential effect of the choice of month in our conclusions.

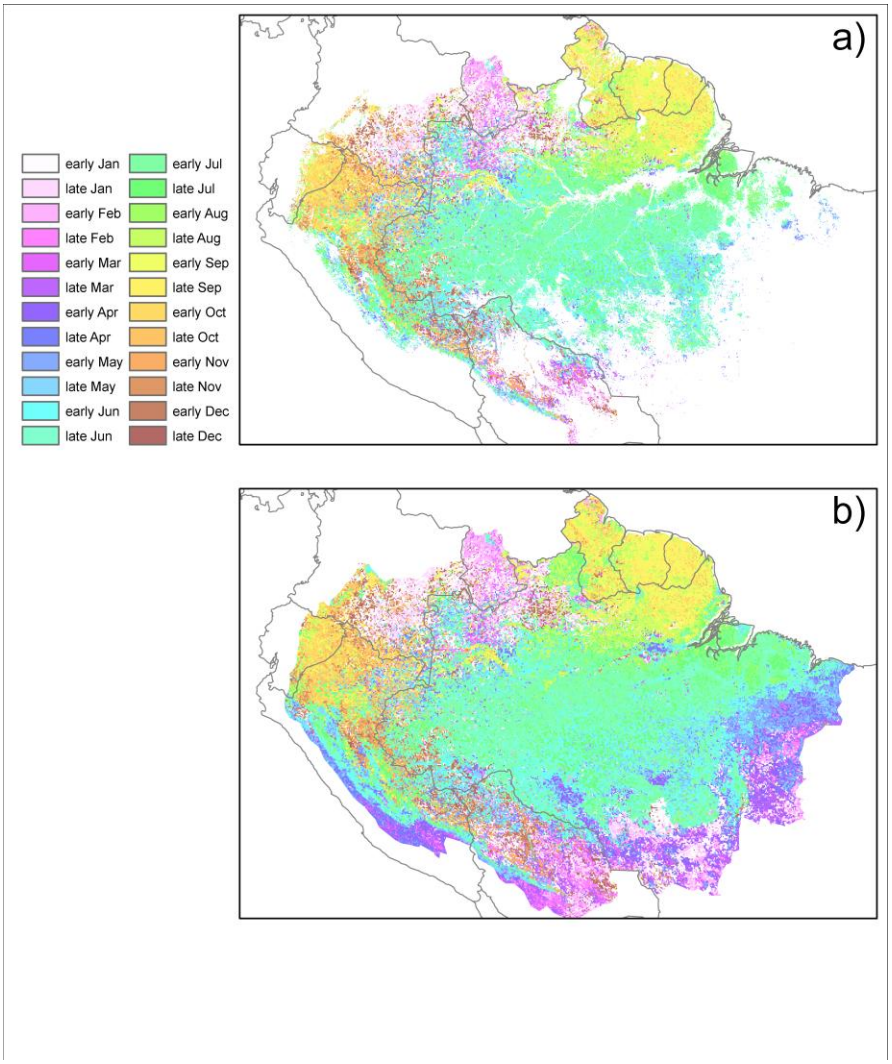

Figure A-2 - The month of peak NDVI as recorded in the GIMMS-NDVI dataset between 1981 and 2008 for areas of high canopy cover (A) and by a wide range fractions of canopy cover (B).

APPENDIX C
EQUATIONS ON HEAT TRANSFER

While the equation representing conductive heat transfer through bark (one-dimensional model; equation C1) can be useful for predicting the rates of change in cambium temperature (a proxy of cambium insulation) as a function of fire temperature, this equation requires information about diffusivity, which is very difficult to measure under field conditions and goes beyond of the scope of this work. Also, equation 1A requires a constant heat source, which is challenging under field conditions due to air movement during heating experiments. Thus, I decided to use Newton's Law of Cooling to calculate the rate of change in cambium temperature given a gradient in temperature (equation C2). In so doing, I could not separate the individual effects of conductivity and convection. Note that the exact solution of Newton's Law of Cooling (equation 1C) is an asymptotic model (i.e., the maximum temperature the cambium can reach is equal to the hot air temperature on the outer bark). However, I used basic theory of conductive heat transfer to drive my predictions (1, 2, and 3).

equation C1:

$$\frac{T_{camb}-T_{fire}}{T_{cambi}-T_{fire}} \sim erf\left(\frac{BT}{2\sqrt{(\alpha t)}}\right)$$

where:

T_{camb} = Cambium temperature (CT)

T_{fire} = Temperature of the flame

T_{cambi} = Initial temperature at the cambium

BT = Bark Thickness

α (diffusivity): heat conduction/(heat capacity x bark density)

t = time

Based on this relationship, the time for mortality at different temperatures (T_f) can be predicted for an individual:

time = constant*Bt^2

equation C2

$$\frac{dCT}{dt} = R(CT - T_f)$$

whree:

CT: Cambium temperature

R: Rate of change in temperature

T_f : Hot air temperature adjacent to the bark heated using a torch.

equation 1C (exact solution of equation C2):

$$CT = Asymptote + (CT_i - Asymptote)e^{-CFTeR}$$

Where:

Asymptote: Tf in equation 1B

CTF: cumulative air temperature adjacent to the bark

APPENDIX D
FIRE EXPERIMENT

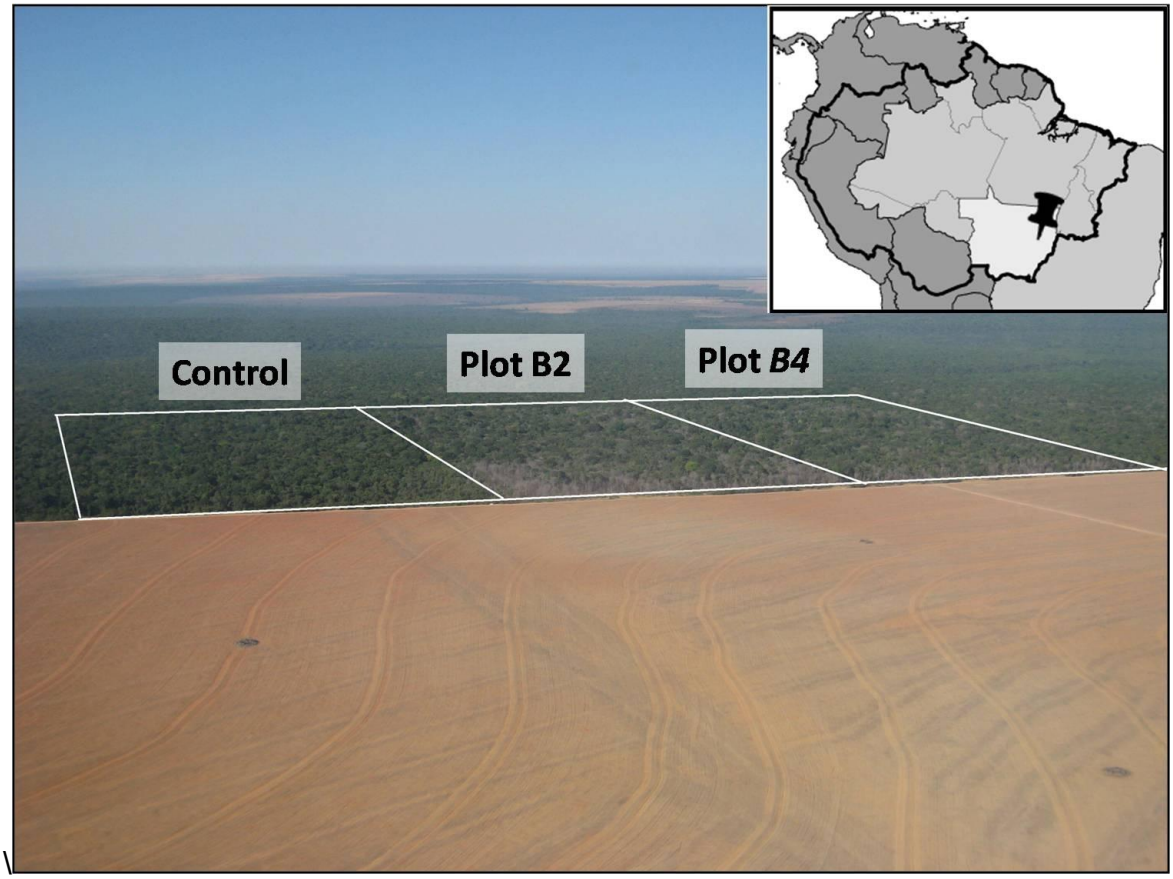

\

Figure A-3 - Aerial photo of the experimental fire. On the right corner of the figure I show the location of this experiment, Querencia, Mato Grosso State, Brazil.

APPENDIX E
FLAME HEIGHT

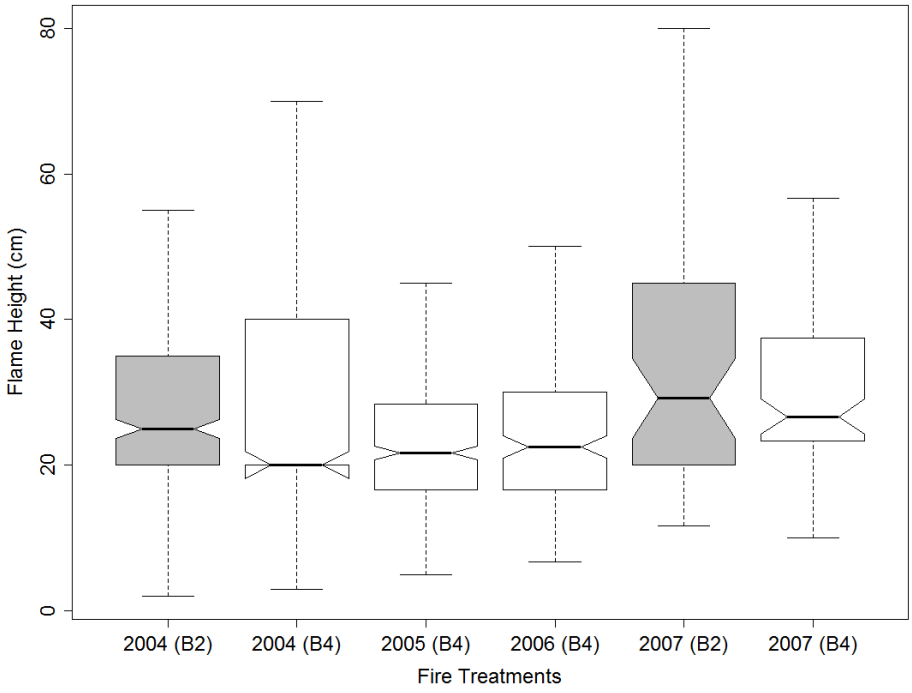

Figure A-4 - Box-plots for flame height in plot B2 (grey) and B4 from 2004 and 2007. Measurements were taken along the fire line and thus were spread across the experimental area in a pattern that depended on the fire behavior.

APPENDIX E
BARK THICKNESS AND TREE DBH

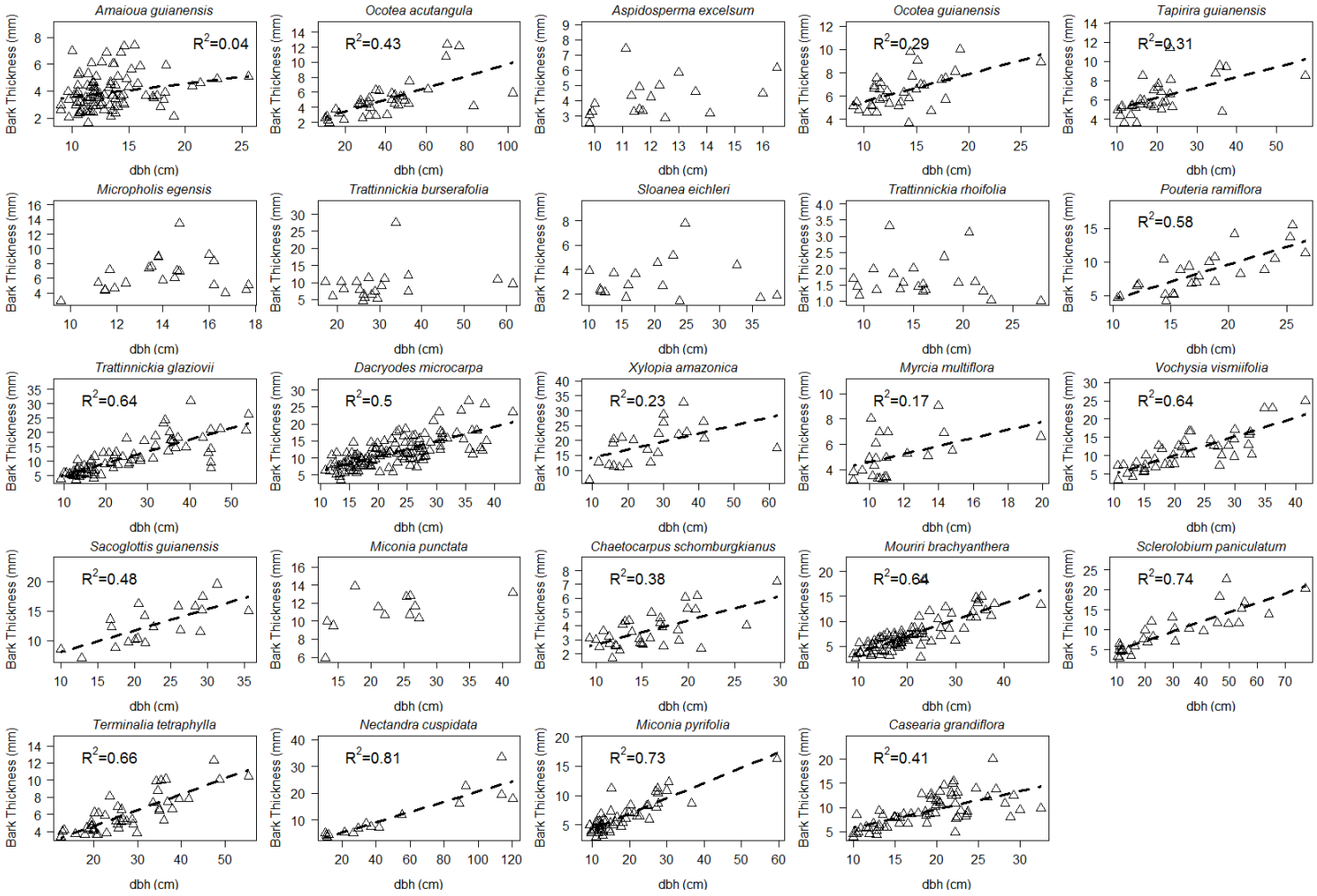

Figure A-5 - Relationships between dbh and bark thickness. Note that when there was no relationship between dbh and BT for a given species, predicted BT was based on the intercept of the model.

APPENDIX F
MODEL 1

Table F-1. Model 1. Period: 2004-2005 (plot *B2* and *B4*)

	Estimate	Std. Error	z value	Pr(>|z|)
Intercept	3.461	0.208	16.670	0.000
R	-0.615	0.373	-1.647	0.100
Charred.0x (B2)	-0.610	0.219	-2.791	0.005
Charred.04 (B3)	-0.812	0.184	-4.403	0.000
Charred.0x (B4)	-0.351	0.225	-1.560	0.119
Charred.04 (B4)	-0.597	0.196	-3.052	0.002
Edge Distance	0.655	0.142	4.604	0.000
R:Charred.0x (B2)	0.460	0.463	0.993	0.320
R:Charred.04 (B2)	-0.435	0.438	-0.991	0.322
R:Charred.0x (B4)	-0.364	0.503	-0.724	0.469
R:Charred.04 (B4)	-0.923	0.457	-2.017	0.044

APPENDIX G
MODEL 2

Table G-1. Model 2. Period: 2004-2007 (plot *B2*)

	Estimate	Std. Error	z value	Pr(>|z|)
Intercept	2.526	0.222	11.391	0.000
R	0.242	0.267	0.907	0.364
Charred.0x(B2)	-0.340	0.162	-2.103	0.035
Charred.04(B2)	-0.609	0.133	-4.594	0.000
Edge Distance	0.476	0.133	3.582	0.000
R:Charred.0x(B2)	-0.250	0.332	-0.755	0.450
R:Charred.04(B2)	-0.389	0.293	-1.327	0.185

APPENDIX H
MODEL 3

Table H-1. Model 3. Period: 2007-2008 (plot *B2*)

	Estimate	Std. Error	z value	Pr(>|z|)
Intercept	3.257	0.233	13.965	0.000
R	-0.494	0.338	-1.461	0.144
Charred.0x(B2)	-1.289	0.425	-3.035	0.002
Charred.07(B2)	-2.190	0.170	-12.885	0.000
Charred.2x(B2)	-2.308	0.154	-14.962	0.000
Edge Distance	1.303	0.138	9.462	0.000
R:Charred.0x(B2)	-1.703	1.007	-1.691	0.091
R:Charred.07(B2)	-0.468	0.372	-1.257	0.209
R:Charred.2x(B2)	-1.339	0.366	-3.656	0.000

LIST OF REFERENCES

Aide, T. M. 1993. Patterns of Leaf Development and Herbivory in a Tropical Understory Community. Ecology 74:455-466.

Alencar, A., D. Nepstad, and M. C. Diaz. 2006. Forest understory fire in the Brazilian Amazon in ENSO and non-ENSO years: area burned and committed carbon emissions. Earth Interactions 10:1–17.

Alencar, A. A., L. A. Solórzano, and D. C. Nepstad. 2004. Modeling forest understory fires in an eastern Amazonian landscape. Ecological Applications 14:139–149.

Aragao, L. E. O. C., Y. Malhi, R. M. Roman-Cuesta, S. Saatchi, L. O. Anderson, and Y. E. Shimabukuro. 2007. Spatial patterns and fire response of recent Amazonian droughts. Geophysical Research Letters 34:-. doi: Artn L07701 Doi 10.1029/2006gl028946.

Aragao, L., Y. Malhi, N. Barbier, A. Lima, Y. Shimabukuro, L. Anderson, and S. Saatchi. 2008. Interactions between rainfall, deforestation and fires during recent years in the Brazilian Amazonia. Philosophical Transactions of the Royal Society B: Biological Sciences 363:1779-1785.

Baayen, H. 2008. Analyzing linguistic data: A practical introduction to statistics using R. Cambridge University Press.

Baker, T. R., O. L. Phillips, Y. Malhi, S. Almeida, L. Arroyo, A. Di Fiore, T. Erwin, N. Higuchi, T. J. Killeen, S. G. Laurance, W. F. Laurance, S. L. Lewis, A. Monteagudo, D. A. Neill, P. N. Vargas, N. C. A. Pitman, J. N. M. Silva, and R. V. Martinez. 2004a. Increasing biomass in Amazonian forest plots. Philos. Trans. R. Soc. Lond. Ser. B-Biol. Sci. 359:353-365.

Baker, T. R., O. L. Phillips, Y. Malhi, S. Almeida, L. Arroyo, A. Di Fiore, T. Erwin, N. Higuchi, T. J. Killeen, S. G. Laurance, W. F. Laurance, S. L. Lewis, A. Monteagudo, D. A. Neill, P. Núñez Vargas, N. C. A. Pitman, J. N. M. Silva, and R. Vásquez Martínez. 2004b. Increasing biomass in Amazonian forest plots. Philosophical Transactions of the Royal Society B: Biological Sciences 359:353-365. doi: 10.1098/rstb.2003.1422.

Balch, J., D. Nepstad, P. Brando, L. Curran, O. Portela, O. de Carvalho, and P. Lefebvre. 2008. Negative fire feedback in a transitional forest of southeastern Amazonia. Global Change Biology 14:2276-2287.

Barlow, J., T. Haugaasen, and C. A. Peres. 2002. Effects of ground fires on understorey bird assemblages in Amazonian forests. Biological Conservation 105:157–169.

Barlow, J., B. O. Lagan, and C. A. Peres. 2003. Morphological correlates of fire-induced tree mortality in a central Amazonian forest. Journal of Tropical Ecology 19:291–299.

Barlow, J., and C. A. Peres. 2008. Fire-mediated dieback and compositional cascade in an Amazonian forest. Philosophical Transactions of the Royal Society B: Biological Sciences 363:1787.

Barlow, J., and C. A. Peres. 2006. Effects of single and recurrent wildfires on fruit production and large vertebrate abundance in a central Amazonian forest. Biodiversity and Conservation 15:985-1012.

Bates, D., and M. Maechler. 2009. lme4: Linear mixed-effects models using S4 classes. R package version 0.999375–31.

Bates, D., and D. Sarkar. 2006. lme4: Linear mixed-effects models using S4 classes. URL http://CRAN. R-project. org, R package version 0.99875-8.

Betts, R. A., P. M. Cox, M. Collins, P. P. Harris, C. Huntingford, and C. D. Jones. 2004. The role of ecosystem-atmosphere interactions in simulated Amazonian precipitation decrease and forest dieback under global climate warming. Theoretical and Applied Climatology 78. doi: 10.1007/s00704-004-0050-y.

Betts, R., M. Sanderson, and S. Woodward. 2008. Effects of large-scale Amazon forest degradation on climate and air quality through fluxes of carbon dioxide, water, energy, mineral dust and isoprene. Philosophical Transactions of the Royal Society B: Biological Sciences 363:1873-1880.

Blate, G. M. 2005. Modest trade-offs between timber management and fire susceptibility of a Bolivian semi-deciduous forest. Ecological Applications 15:1649–1663.

Bolker, B. M., M. E. Brooks, C. J. Clark, S. W. Geange, J. R. Poulsen, M. H. Stevens, and J. S. White. 2009. Generalized linear mixed models: a practical guide for ecology and evolution. Trends in Ecology & Evolution 24:127–135.

Bonan, G. B. 2008. Forests and climate change: forcings, feedbacks, and the climate benefits of forests. Science 320:1444.

Brando, P. M., D. C. Nepstad, E. A. Davidson, S. E. Trumbore, D. Ray, and P. Camargo. 2008b. Drought effects on litterfall, wood production and belowground carbon cycling in an Amazon forest: results of a throughfall reduction experiment. Philosophical Transactions of the Royal Society B: Biological Sciences 363:1839-1848.

Burnham, K. P., and D. R. Anderson. 2002. Model selection and multimodel inference: a practical information-theoretic approach. Springer Verlag.

Chambers, J. Q., J. Santos, R. J. Ribeiro, and N. Higuchi. 2001. Tree damage, allometric relationships, and above-ground net primary production in central Amazon forest. Forest Ecology and Management 152:73–84.

Chapin III, F. S., E. Schulze, and H. A. Mooney. 1990. The ecology and economics of storage in plants. Annual Review of Ecology and Systematics 21:423–447.

Chave, J., H. C. Muller-Landau, T. R. Baker, T. A. Easdale, H. Steege, and C. O. Webb. 2006. Regional and phylogenetic variation of wood density across 2456 neotropical tree species. Ecological Applications 16:2356–2367.

Christensen, J. H., B. Hewitson, A. Busuioc, A. Chen, X. Gao, I. Held, R. Jones, R. K. Kolli, W. T. Kwon, R. Laprise, and others. 2007. Climate change 2007: the physical science basis. Contribution of Working Group I to the Fourth Assessment Report of the Intergovernmental Panel on Climate Change. Cambridge University Press Cambridge, New York.

Clark, D. A. 2002. Are tropical forests an important carbon sink? Reanalysis of the long-term plot data. Ecological Applications 12:3–7.

Clark, D. A., and D. B. Clark. 1994. Climate-induced annual variation in canopy tree growth in a Costa Rican tropical rain forest. Journal of Ecology 82:865–872.

Clark, D. A., S. Brown, D. W. Kicklighter, J. Q. Chambers, J. R. Thomlinson, and J. Ni. 2001. Measuring net primary production in forests: concepts and field methods. Ecological Applications 11:356-370.

Cochrane, M. A., and W. F. Laurance. 2002. Fire as a large-scale edge effect in Amazonian forests. Journal of Tropical Ecology 18:311–325.

Cochrane, M. A., and W. F. Laurance. 2008. Synergisms among fire, land use, and climate change in the Amazon. AMBIO: A Journal of the Human Environment 37:522–527.

Cochrane, M. A. 2003. Fire science for rainforests. Nature 421:913-919.

Cochrane, M. A., and W. F. Laurance. 2002. Fire as a large-scale edge effect in Amazonian forests. Journal of Tropical Ecology 18. doi: 10.1017/S0266467402002237.

Condit, R., S. Aguilar, A. Hernandez, R. Perez, S. Lao, G. Angehr, S. P. Hubbell, and R. B. Foster. 2004. Tropical forest dynamics across a rainfall gradient and the impact of an El Nino dry season. Journal of Tropical Ecology 20:51–72.

Condit, R., S. P. Hubbell, and R. B. Foster. 1995. Mortality rates of 205 neotropical tree and shrub species and the impact of a severe drought. Ecological Monographs:419–439.

Costa, M. H., and J. A. Foley. 2000b. Combined effects of deforestation and doubled atmospheric CO2 concentrations on the climate of Amazonia. Journal of Climate 13:18-34.

Cox, P. M., R. A. Betts, M. Collins, P. P. Harris, C. Huntingford, and C. D. Jones. 2004. Amazonian forest dieback under climate-carbon cycle projections for the 21st century. Theoretical and Applied Climatology 78. doi: 10.1007/s00704-004-0049-4.

Cox, P. M., P. P. Harris, C. Huntingford, R. A. Betts, M. Collins, C. D. Jones, T. E. Jupp, J. A. Marengo, and C. A. Nobre. 2008. Increasing risk of Amazonian drought due to decreasing aerosol pollution. Nature 453:212-215.

Cox, P. M., R. A. Betts, C. D. Jones, S. A. Spall, and I. J. Totterdell. 2000. Acceleration of global warming due to carbon-cycle feedbacks in a coupled climate model. Nature 408:184-187. doi: 10.1038/35041539.

Cramer, W., A. Bondeau, F. I. Woodward, I. C. Prentice, R. A. Betts, V. Brovkin, P. M. Cox, V. Fisher, J. A. Foley, and A. D. Friend. 2001. Global response of terrestrial ecosystem structure and function to CO2 and climate change: results from six dynamic global vegetation models. Global Change Biology 7:357-373.

Davidson, E. A., F. Y. Ishida, and D. C. Nepstad. 2004. Effects of an experimental drought on soil emissions of carbon dioxide, methane, nitrous oxide, and nitric oxide in a moist tropical forest. Global Change Biology 10:718–730.

Davidson, E. A., L. V. Verchot, J. H. Cattânio, I. L. Ackerman, and J. E. M. Carvalho. 2000. Effects of soil water content on soil respiration in forests and cattle pastures of eastern Amazonia. Biogeochemistry 48:53–69.

Davidson, E. A., I. A. Janssens, and Y. Luo. 2006. On the variability of respiration in terrestrial ecosystems: moving beyond Q10. Global Change Biology 12:154-164.

Dickinson, M. & Johnson, E. (2001) Fire effects on trees. In: *Forest fires: behavior and ecological effects, Academic Press,* **2001**, 477-521

Doughty, C. E., and M. L. Goulden. 2008. Seasonal patterns of tropical forest leaf area index and CO2 exchange. J Geophys Res 113.

Fisher, R. A., M. Williams, A. L. da Costa, Y. Malhi, R. F. da Costa, S. Almeida, and P. Meir. 2007. The response of an Eastern Amazonian rain forest to drought stress: results and modelling analyses from a throughfall exclusion experiment. Global Change Biology 13:2361-2378.

Fisher, R., M. Williams, R. Lobo Do Vale, A. Lola Da Costa, and P. Meir. 2006. Evidence from Amazonian forests is consistent with isohydric control of leaf water potential. Plant, cell and environment(Print) 29:151-165.

Foley, J. A., S. Levis, I. C. Prentice, D. Pollard, and S. L. Thompson. 1998. Coupling dynamic models of climate and vegetation. Glob. Change Biol. 4:561-579.

Foley, J. A., I. C. Prentice, N. Ramankutty, S. Levis, D. Pollard, S. Sitch, and A. Haxeltine. 1996. An integrated biosphere model of land surface processes, terrestrial carbon balance, and vegetation dynamics. Glob. Biogeochem. Cycle 10:603-628.

Gerwing, J. J., and D. L. Farias. 2000. Integrating liana abundance and forest stature into an estimate of total aboveground biomass for an eastern Amazonian forest. Journal of tropical ecology 16:327–335.

Gloor, M., O. L. Phillips, J. J. Lloyd, S. L. Lewis, Y. Malhi, T. R. Baker, G. López-González, J. Peacock, S. Almeida, A. C. de OLIVEIRA, and others. 2009. Does the disturbance hypothesis explain the biomass increase in basin-wide Amazon forest plot data? Global Change Biology 15:2418–2430.

Golding, N., and R. Betts. 2008. Fire risk in Amazonia due to climate change in the HadCM3 climate model: Potential interactions with deforestation. Global Biogeochemical Cycles 22.

Grace, J., J. Lloyd, J. McIntyre, A. C. Miranda, P. Meir, H. S. Miranda, C. Nobre, J. Moncrieff, J. Massheder, and Y. Malhi. 1995. Carbon dioxide uptake by an undisturbed tropical rain forest in southwest Amazonia, 1992 to 1993. Science 270:778.

Graham, E. A., S. S. Mulkey, K. Kitajima, N. G. Phillips, and S. J. Wright. 2003b. Cloud cover limits net CO2 uptake and growth of a rainforest tree during tropical rainy seasons. Proceedings of the National Academy of Sciences 100:572-576.

Gutsell, S. L., and E. A. Johnson. 1996. How fire scars are formed: coupling a disturbance process to its ecological effect. Canadian Journal of Forest Research 26:166–174.

Hansen, M. C., R. S. DeFries, J. R. G. Townshend, M. Carroll, C. Dimiceli, and R. A. Sohlberg. 2003. Global percent tree cover at a spatial resolution of 500 meters: First results of the MODIS vegetation continuous fields algorithm. Earth Interactions 7:1–15.

Hare, R. C. 1965. Contribution of bark to fire resistance of southern trees. Journal of Forestry 63:248–251.

Hashimoto, H, F. Melton, F, K. Ichii, K, C. Milesi, C, W. Wang, W, and R. R. Nemani, R. 2009. Evaluating the impacts of climate and elevated carbon dioxide on tropical rainforests of the western Amazon basin using ecosystem models and satellite data. Global Change Biology.

Hirsch, A. I., W. S. Little, R. A. Houghton, N. A. Scott, and J. D. White. 2004. The net carbon flux due to deforestation and forest re-growth in the Brazilian Amazon: analysis using a process-based model. Global Change Biology 10:908-924. doi: 10.1111/j.1529-8817.2003.00765.x.

Houghton, R. A. 2005. Aboveground Forest Biomass and the Global Carbon Balance. Global Change Biology 11:945-958. doi: 10.1111/j.1365-2486.2005.00955.x.

Huete, A., K. Didan, T. Miura, E. P. Rodriguez, X. Gao, L. G. Ferreira, and others. 2002. Overview of the radiometric and biophysical performance of the MODIS vegetation indices. Remote Sensing of Environment 83:195–213.

Huete, A. R., K. Didan, Y. E. Shimabukuro, P. Ratana, S. R. Saleska, L. R. Hutyra, W. Yang, R. R. Nemani, and R. Myneni. 2006a. Amazon rainforests green-up with sunlight in dry season. Geophysical Research Letters 33.

Huntingford, C., R. A. Fisher, L. Mercado, B. B. Booth, S. Sitch, P. P. Harris, P. M. Cox, C. D. Jones, R. A. Betts, Y. Malhi, G. R. Harris, M. Collins, and P. Moorcroft. 2008. Towards quantifying uncertainty in predictions of Amazon 'dieback'. Philosophical Transactions of the Royal Society B: Biological Sciences 363:1857-1864.

Hurlbert, S. H. 1984. Pseudoreplication and the design of ecological field experiments. Ecological monographs 54:187–211.

Hutyra, L. R., J. W. Munger, S. R. Saleska, E. Gottlieb, B. C. Daube, A. L. Dunn, D. F. Amaral, P. B. De Camargo, and S. C. Wofsy. 2007. Seasonal controls on the exchange of carbon and water in an Amazonian rain forest. J. Geophys. Res 112.

Jipp, P. H., D. C. Nepstad, D. K. Cassel, and C. Reis de Carvalho. 1998. Deep soil moisture storage and transpiration in forests and pastures of seasonally-dry Amazonia. Climatic Change 39:395–412.

Landsberg, J. J., and R. H. Waring. 1997. A generalised model of forest productivity using simplified concepts of radiation-use efficiency, carbon balance and partitioning. Forest Ecology and Management 95:209–228.

Larjavaara, M., and H. C. Muller-Landau. 2010. Rethinking the value of high wood density. Functional Ecology.

Li, W., R. Fu, and R. E. Dickinson. 2006. Rainfall and its seasonality over the Amazon in the 21st century as assessed by the coupled models for the IPCC AR4. Journal of Geophysical Research 111:D02111.

Lloyd, J., and G. D. Farquhar. 2008. Effects of rising temperatures and [CO2] on the physiology of tropical forest trees. Philosophical Transactions of the Royal Society B: Biological Sciences 363:1811-1817.

Malhi, Y., E. Luiz, D. Aragao, C. Huntingford, R. Fisher, P. Zelazowski, S. Sitch, C. McSweeney, and P. Meir. 2008a. Exploring the likelihood and mechanism of a climate-change-induced dieback of the Amazon rainforest. Proceedings of the National Academy of Sciences.

Malhi, Y., J. T. Roberts, R. A. Betts, T. J. Killeen, W. Li, and C. A. Nobre. 2008b. Climate change, deforestation, and the fate of the Amazon. Science 319:169.

Malhi, Y., L. E. O. C. Aragão, D. Galbraith, C. Huntingford, R. Fisher, P. Zelazowski, S. Sitch, C. McSweeney, and P. Meir. 2009. Special Feature: Exploring the likelihood and mechanism of a climate-change-induced dieback of the Amazon rainforest. Proceedings of the National Academy of Sciences of the United States of America. doi: 10.1073/pnas.0804619106.

van Mantgem, P., and M. Schwartz. 2003. Bark heat resistance of small trees in Californian mixed conifer forests: testing some model assumptions. Forest Ecology and Management 178:341–352.

Marengo, J. A., C. A. Nobre, J. Tomasella, M. F. Cardoso, and M. D. Oyama. 2008a. Hydro-climatic and ecological behaviour of the drought of Amazonia in 2005. Philosophical Transactions of the Royal Society B: Biological Sciences 363:1773-1778.

Marengo, J. A., C. A. Nobre, J. Tomasella, M. D. Oyama, G. Sampaio de Oliveira, R. de Oliveira, H. Camargo, L. M. Alves, and I. F. Brown. 2008c. The Drought of Amazonia in 2005. Journal of Climate 21:495. doi: 10.1175/2007JCLI1600.1.

Mayle, F. E., and M. J. Power. 2008. Impact of a drier Early–Mid-Holocene climate upon Amazonian forests. Philosophical Transactions of the Royal Society B: Biological Sciences 363:1829-1838.

Meir, P., P. Brando, D. Nepstad, Vasconcelos, S, A. Costa, E. A. Davidson, S. Almeida, R. A. Fisher, E. Sotta, D. Zarin, and G. Cardinot. 2009. The Effects of Drought on Amazonian rain forests. In: Large-Scale Biosphere-Atmosphere Project in Amazonia: A synthesis

Michaletz, S., and E. Johnson. 2007. How forest fires kill trees: A review of the fundamental biophysical processes. Scandinavian Journal of Forest Research 22:500-515. doi: 10.1080/02827580701803544.

Murray, K., and M. M. Conner. 2009. Methods to quantify variable importance: implications for the analysis of noisy ecological data. Ecology 90:348–355.

Myneni, R. B., W. Yang, R. R. Nemani, A. R. Huete, R. E. Dickinson, Y. Knyazikhin, K. Didan, R. Fu, R. I. Negrón Juárez, and S. S. Saatchi. 2007a. Large seasonal swings in leaf area of Amazon rainforests. Proceedings of the National Academy of Sciences 104:4820.

Nakagawa, M., K. Tanaka, T. Nakashizuka, T. Ohkubo, T. Kato, T. Maeda, K. Sato, H. Miguchi, H. Nagamasu, K. Ogino, and others. 2000a. Impact of severe drought associated with the 1997–1998 El Nino in a tropical forest in Sarawak. Journal of Tropical Ecology 16:355–367.

Nepstad, D., G. Carvalho, A. Cristina Barros, A. Alencar, J. Paulo Capobianco, J. Bishop, P. Moutinho, P. Lefebvre, U. Lopes Silva, and E. Prins. 2001. Road paving, fire regime feedbacks, and the future of Amazon forests. Forest Ecology and Management 154:395–407.

Nepstad, D., P. Lefebvre, U. Lopes da Silva, J. Tomasella, P. Schlesinger, L. Solorzano, P. Moutinho, D. Ray, and J. Guerreira Benito. 2004a. Amazon drought and its implications for forest flammability and tree growth: a basin-wide analysis. Global Change Biology 10:704-717.

Nepstad, D. C., C. R. de Carvalho, E. A. Davidson, P. H. Jipp, P. A. Lefebvre, G. H. Negreiros, E. D. da Silva, T. A. Stone, S. E. Trumbore, and S. Vieira. 1994. The role of deep roots in the hydrological and carbon cycles of Amazonian forests and pastures.

Nepstad, D. C., I. M. Tohver, D. Ray, P. Moutinho, and G. Cardinot. 2007a. Mortality of large trees and lianas following experimental drought in an Amazon forest. Ecology 88:2259–2269.

Nepstad, D. C., P. Moutinho, M. B. Dias-Filho, E. Davidson, G. Cardinot, D. Markewitz, R. Figueiredo, N. Vianna, J. Chambers, and D. Ray. 2002a. The effects of partial throughfall exclusion on canopy processes, aboveground production, and biogeochemistry of an Amazon forest. Journal of Geophysical Research 107:8085.

Nepstad, D. C., C. M. Stickler, B. S. Filho, and F. Merry. 2008. Interactions among Amazon land use, forests and climate: prospects for a near-term forest tipping point. Philosophical Transactions of the Royal Society B: Biological Sciences 363:1737-1746.

Nepstad, D. C., A. Verissimo, A. Alencar, C. Nobre, E. Lima, P. Lefebvre, P. Schlesinger, C. Potter, P. Moutinho, and E. Mendoza. 1999. Large-scale impoverishment of Amazonian forests by logging and® re. Nature 398:505-508.

Nobre, C. A., P. J. Sellers, and J. Shukla. 1991a. Amazonian deforestation and regional climate change. Journal of Climate 4:957-988.

Oliveira, R. S., T. E. Dawson, S. S. O. Burgess, and D. C. Nepstad. 2005. Hydraulic redistribution in three Amazonian trees. Oecologia 145:354-363. doi: 10.1007/s00442-005-0108-2.

Phillips, O. L., Y. Malhi, N. Higuchi, W. F. Laurance, P. V. Núñez, R. M. Vásquez, S. G. Laurance, L. V. Ferreira, M. Stern, and S. Brown. 1998b. Changes in the carbon balance of tropical forests: evidence from long-term plots. Science 282:439.

Phillips, O. L., L. E. O. C. Aragao, S. L. Lewis, J. B. Fisher, J. Lloyd, G. Lopez-Gonzalez, Y. Malhi, A. Monteagudo, J. Peacock, C. A. Quesada, G. van der Heijden, S. Almeida, I. Amaral, L. Arroyo, G. Aymard, T. R. Baker, O. Banki, L. Blanc, D. Bonal, P. Brando, J. Chave, A. C. A. de Oliveira, N. D. Cardozo, C. I. Czimczik, T. R. Feldpausch, M. A. Freitas, E. Gloor, N. Higuchi, E. Jimenez, G. Lloyd, P. Meir, C. Mendoza, A. Morel, D. A. Neill, D. Nepstad, S. Patino, M. C. Penuela, A. Prieto, F. Ramirez, M. Schwarz, J. Silva, M. Silveira, A. S. Thomas, H. T. Steege, J. Stropp, R. Vasquez, P. Zelazowski, E. A. Davila, S. Andelman, A. Andrade, K. Chao, T. Erwin, A. Di Fiore, E. H. C., H. Keeling, T. J. Killeen, W. F. Laurance, A. P. Cruz, N. C. A. Pitman, P. N. Vargas, H. Ramirez-Angulo, A. Rudas, R. Salamao, N. Silva, J. Terborgh, and A. Torres-Lezama. 2009. Drought Sensitivity of the Amazon Rainforest. Science 323:1344-1347. doi: 10.1126/science.1164033.

Pinard, M. A., and J. Huffman. 1997. Fire resistance and bark properties of trees in a seasonally dry forest in eastern Bolivia. Journal of Tropical Ecology:727–740.

Pinard, M. A., F. E. Putz, and J. C. Licona. 1999. Tree mortality and vine proliferation following a wildfire in a subhumid tropical forest in eastern Bolivia. Forest Ecology and Management 116:247–252.

Pinheiro, J., D. Bates, S. DebRoy, and D. Sarkar. (2000). the R Core team (2008), nlme: Linear and Nonlinear Mixed Effects Models. R package version:3–1.

Potter, C., E. Davidson, D. Nepstad, and C. R. de Carvalho. 2001. Ecosystem modeling and dynamic effects of deforestation on trace gas fluxes in Amazon tropical forests. For. Ecol. Manage. 152:97-117.

Poulter, B., U. Heyder, and W. Cramer. 2009. Modeling the Sensitivity of the Seasonal Cycle of GPP to Dynamic LAI and Soil Depths in Tropical Rainforests. Ecosystems 12:517-533. doi: 10.1007/s10021-009-9238-4.

Reifsnyder, W. E., L. P. Herrington, and K. W. Spalt. 1967. Thermophysical properties of bark of shortleaf, longleaf, and red pine. Yale University School of Forestry Bulletin 70:1–40.

Rivera, G., S. Elliott, L. Caldas, G. Nicolossi, V. Coradin, and R. Borchert. 2002. Increasing day-length induces spring flushing of tropical dry forest trees in the absence of rain. Trees - Structure and Function 16:445-456. doi: 10.1007/s00468-002-0185-3.

Romero, C., and B. M. Bolker. 2008. Effects of stem anatomical and structural traits on responses to stem damage: an experimental study in the Bolivian Amazon. Canadian Journal of Forest Research 38:611–618.

Saatchi, S. S., R. A. HOUGHTON, R. Alvala, J. V. Soares, and Y. YU. 2007. Distribution of aboveground live biomass in the Amazon basin. Glob. Change Biol. 13:816-837.

Saldarriaga, J. G., D. C. West, M. L. Tharp, and C. Uhl. 1988. Long-term chronosequence of forest succession in the upper Rio Negro of Colombia and Venezuela. The Journal of Ecology:938–958.

Saleska, S. R., K. Didan, A. R. Huete, and H. R. da Rocha. 2007b. Amazon forests green-up during 2005 drought. Science 318:612-612. doi: DOI 10.1126/science.1146663.

Saleska, S. R., S. D. Miller, D. M. Matross, M. L. Goulden, S. C. Wofsy, H. R. da Rocha, P. B. De Camargo, P. Crill, B. C. Daube, and H. C. de Freitas. 2003b. Carbon in Amazon forests: unexpected seasonal fluxes and disturbance-induced losses. American Association for the Advancement of Science.

Samanta, A., S. Ganguly, H. Hashimoto, S. Devadiga, E. Vermote, Y. Knyazikhin, R. R. Nemani, and R. B. Myneni. 2010. Amazon forests did not green-up during the 2005 drought. Geophysical Research Letters 37:L05401.

Schaaf, C. B., F. Gao, A. H. Strahler, W. Lucht, X. Li, T. Tsang, N. C. Strugnell, X. Zhang, Y. Jin, and J. P. Muller. 2002. First operational BRDF, albedo nadir reflectance products from MODIS. Remote Sensing of Environment 83:135-148.

Tian, H., J. M. Melillo, D. W. Kicklighter, A. D. McGuire, J. V. K. Helfrich, B. Moore, and C. J. Vorosmarty. 1998. Effect of interannual climate variability on carbon storage in Amazonian ecosystems. Nature 396:664-667. doi: 10.1038/25328.

Tomasella, J., and M. G. Hodnett. 1998. Estimating soil water retention characteristics from limited data in Brazilian Amazonia. Soil science 163:190.

Trumbore, S., E. S. Da Costa, D. C. Nepstad, B. De Camargo, L. A. Martinelli, D. Ray, T. Restom, and W. Silver. 2006. Dynamics of fine root carbon in Amazonian tropical ecosystems and the contribution of roots to soil respiration. Global Change Biology 12:217-229.

Tucker, C. J., J. E. Pinzón, M. E. Brown, D. A. Slayback, E. W. Pak, R. Mahoney, E. F. Vermote, and N. El Saleous. 2005. An extended AVHRR 8-km NDVI dataset compatible with MODIS and SPOT vegetation NDVI data. International Journal of Remote Sensing 26:4485–4498.

Uhl, C., and J. B. Kauffman. 1990. Deforestation, fire susceptibility, and potential tree responses to fire in the eastern Amazon. Ecology:437-449.

Van Nieuwstadt, M. G. L., and D. Sheil. 2005a. Drought, fire and tree survival in a Borneo rain forest, East Kalimantan, Indonesia. JOURNAL OF ECOLOGY 93:191-201. doi: 10.1111/j.1365-2745.2004.00954.x.

Venables, W. N., and B. D. Ripley. 2002. Modern applied statistics with S. Springer verlag.
Werth, D., and R. Avissar. 2002. The local and global effects of Amazon deforestation. J. Geophys. Res 107.

Williamson, G. B., W. F. Laurance, A. A. Oliveira, P. Delamonica, C. Gascon, T. E. Lovejoy, and L. Pohl. 2000. Amazonian Tree Mortality during the 1997 El Nino Drought. Conservation Biology 14:1538.

Wright, S. J., and C. P. van Schaik. 1994. Light and the phenology of tropical trees. The American Naturalist 143:192–199.

Wright, S. J., C. Carrasco, O. Calderón, and S. Paton. 1999. The El Nino Southern Oscillation, variable fruit production, and famine in a tropical forest. Ecology 80:1632-1647.

Xiao, X., Q. Zhang, S. Saleska, L. Hutyra, P. De Camargo, S. Wofsy, S. Frolking, S. Boles, M. Keller, and B. Moore. 2005. Satellite-based modeling of gross primary production in a seasonally moist tropical evergreen forest. Remote Sensing of Environment 94:105-122.

Xiao, X. M., S. Hagen, Q. Y. Zhang, M. Keller, and B. Moore. 2006. Detecting leaf phenology of seasonally moist tropical forests in South America with multi-temporal MODIS images. Remote Sensing of Environment 103:465-473. doi: 10.1016/j.rse.2006.04.013.

Zeng, N., J. Yoon, J. A. Marengo, A. Subramaniam, C. A. Nobre, A. Mariotti, and J. D. Neelin. 2008. Causes and impacts of the 2005 Amazon drought. Environmental Research Letters 3:014002.

BIOGRAPHICAL SKETCH

Paulo Brando was born in the town of Assis, five hundred kilometers from the most populated state capital in Brazil, Sao Paulo. Early in his career, he decided to work on topics related to conservation in Amazonia. With this goal in mind, he joined the University of Sao Paulo to study forestry in 1999. After three years in college learning more about pulp production than conservation, he was fortunate to join the Forest Institute for a 2-year internship on restoration of savannas (cerrados). After developing some skills as an ecologist during this internship, Paulo had the opportunity to study at McGill University, Canada, where he was exposed to a vibrant scientific community working on future scenarios for the Amazon. Excited by this approach, he contacted a Brazilian institution, IPAM (Amazon Environmental Research Institute), to find out about the possibilities of conducting similar research upon his return to Brazil. Two weeks following this first contact with IPAM, Paulo arrived in Santarem, Para State, where he spent the following three and half years studying the effects of droughts on the carbon and water cycling of tropical forests. During this period he worked closely with local community members, from whom he learned more about conservation than he had in school or anywhere else. Paulo left Santarem in 2006 to join the Ph.D. program at the University of Florida. In the near future, Paulo hopes for a career in which he can continue to explore the vulnerability of tropical forests to repeated disturbances and prolonged degradation. He intends to continue to inform the public and policy-makers about potentially dangerous future trends of Amazonian forests in response to large-scale deforestation, forest fires, and climate change. Perhaps more importantly, Paulo Brando aims to develop an interdisciplinary career that will allow him to develop workable approaches to large-scale conservation.